THESIS

PARTICLE TRACKING USING DYNAMIC WATER LEVEL DATA

Submitted by

Yuan Gao

Department of Civil and Environmental Engineering

In partial fulfillment of the requirements

For the Degree of Master of Science

Colorado State University

Fort Collins, Colorado

Spring 2017

Master's Committee:

Advisor: Thomas Sale

Michael Ronayne
Jens Blotevogel

ABSTRACT

PARTICLE TRACKING USING DYNAMIC WATER LEVEL DATA

Movement of fluid particles about historic subsurface releases and through well fields is often governed by dynamic subsurface water levels. Factors influencing temporal changes in water levels include changes in river stage, tidal fluctuation, seasonal transpiration from trees and pumping of wells. Motivations for tracking the movement of fluid particles include tracking the fate of subsurface contaminants and resolving the fate of water stored in subsurface aquifers.

This research provides novel methods for predicting the movement of subsurface particles relying on dynamic water level data derived from continuously recording pressure transducers or an analytic solution based on a Theis superposition model that predicts water levels about dynamically operated wells in well fields. For particle tracking at field sites without pumping conditions, firstly, the dynamic water level data obtained from sites in Kansas City, Missouri; Pueblo, Colorado; and Honolulu, Hawaii are employed. The basic idea is to use water-level data from at least three wells to solve for the plane of the water table and obtain the hydraulic gradient in the *x* and *y* directions. Secondly, based on the Darcy's equation, the position of a particle is moved in the *x* and *y* directions at each time step. Finally, by connecting all the positions of particle together, the path line of particle flowed in the subsurface can be obtained. Homogeneous, isotropic and homogeneous, anisotropic conditions with retardation were considered for particle tracking at the three sites in this research. Also, consideration is given to natural degradation of contaminants in the subsurface. By assuming the degradation of contaminants at each site follows first order kinetics, the distance the contaminants can flow

within the minimum concentration requirement and the time when the concentration of contaminants arrived at the minimum concentration requirement can be obtained.

Based on the results from this research, river stage, seasonal transpiration and precipitation, and tidal fluctuation at three sites all have great influences on local groundwater flow. The great changes of water-level in short periods caused by seasonal recharge and discharge and seasonal transpiration and precipitation make the hydraulic gradient changed greatly, subsequently make the direction of groundwater flow altered. For the site near a harbor, tidal fluctuations make the groundwater level changed, which correspondingly have the hydraulic gradient and direction of groundwater flow changed.

Initial review of water-level in rose chart indicates a range of groundwater flow direction and gradient with time. This indicates a wide range of temporally changing flow directions and gradients. Surprisingly, despite temporal variation in flow directions, the net groundwater flow at all field sites is largely constant in one direction. From the results of particle tracking and rose charts, groundwater flow mainly follows the direction of the hydraulic gradients with large magnitudes in rose charts, but does not follow every direction of hydraulic gradient in the rose chart. The explanation for this phenomena is the main direction of groundwater flow is driven by hydraulic gradient with large magnitude, because the time interval for each groundwater flow driven by each hydraulic gradient is the same, according to the Darcy's equation, hydraulic gradient in the direction with small magnitude cannot drive particles flow long enough to make particles flow away from the main direction.

Moreover, this research uses dynamic pumping well data to test how particles move under dynamic pumping conditions in well fields. Based on superposition of the Theis solution in both space and time, this research uses an analytical solution to resolve how fluid particles

move about wells under dynamic pumping conditions. The results from particle tracking under dynamic pumping conditions in this research provide: firstly, a relatively uniform capture zone in the well field. Secondly, even under continuous pumping and injection conditions, groundwater will not flow far away from the well. Thirdly, particle tracking provides groundwater positions and delineates the position of storage water under dynamic pumping and injection condition.

ACKNOWLEDGEMENTS

I would like to thank all of my committee members. I am especially grateful to Dr. Thomas Sale, who gave me the opportunity as his graduate student to study groundwater research at CSU. He provided me with his precious time and substantial knowledge to help me develop my academic life.

I would like to show my deep gratitude to Dr. Michael Ronayne for his time investment and passionate input to my study and research. His help considerably enlightened my research methods.

I would like to thank Dr. Jens Blotevogel, who gave me valuable perspective in processing my research.

I would also like to thank TRC solutions and Pat Hughes for providing the data to make this research possible. I am thankful to Emily Stockwell for helping me understanding theoretical knowledge and providing water level data.

Additionally, I would like to express my great appreciation of my family and friends for their tremendous support, patience, and companionship in helping me to complete this process.

TABLE OF CONTENTS

CHAPTER 1 – INTRODUCTION

1.1 Motivation

Groundwater is a primary source of water for human consumption, agriculture, and industry. As the world's population has risen, use of groundwater has increased. Also, industrialization has led to widespread contamination of groundwater by a diverse suite of organic and inorganic compounds. Although many contaminants are attenuated in the subsurface, residual chemicals can persist in the subsurface for a long period. Subsurface contamination can pose great harm to human health and the environment. Some public water supply well fields are located at sites that were historically impacted by releases. Consideration of capture zones in well fields under both pumping and injection stresses is also an important issue.

Efficient methods are needed to track the flow of contaminants in the subsurface. Particle tracking is commonly used to define the pathlines of solute particles under purely advective transport (Jackson, 2002). Particle-tracking schemes have been formally incorporated into solute transport models to account for the advective component of transport (Pollock, 1988). The basic idea is to follow the movement of infinitely small imaginary particles placed in a flow field using either analytical or numerical methods (Lu, 1994). Particle tracking has been widely used in the numerical modeling of groundwater flow to track contaminant paths (e.g., Yidana, 2011 and Shamsuddin et al., 2014). Cunningham et al. (1994) described the information on the regional groundwater flow field as "inferred from particle pathlines". Maskey et al. (2002) presented the use of different global optimization (GO) algorithms to determine the optimized combination of pumping rates and well locations for the removal of a contaminant plume using particle tracking.

Two modeling codes, MODFLOW and MODPATH, are commonly used for groundwater flow and particle tracking. Moutsopoulos et al. (2008) presented backward particle-tracking methods to delineate groundwater protection zones, which is an effective and powerful tool. Robinson et al. (2010) established a new numerical technique called "the convolution-based particle tracking (CBPT) method", which was developed to simulate resident or flux-averaged solute concentrations in groundwater models. The method is valid for steady-state flow and linear transport processes such as sorption with a linear sorption isotherm and first-order decay. Yidana (2011) used particle tracking to define flow paths of the recharge in some aquifers in Ghana, and the particle tracking simulation identified travel times in the specific years from recharge areas to discharge areas along the flow paths. Further, the conventional approach to groundwater protection is based on the concept of the wellhead protection area (WHPA) (Frind et al., 2006). A wellhead-protection area, as defined by U.S. EPA, is "*the surface and subsurface area surrounding a water well or a well field, supplying a public water system, through which contaminants are reasonably likely to move toward and reach such water well or well field.*" (Bair et al., 1991). A WHPA may comprise all or part of the capture zone from which the well draws its water (Frind et al., 2006).

This research explores a novel and more percise method to track particles, so that provide an efficient tool for predicting the movement of subsurface contaminants by tracking particles. To date, limited attention has been given to particle tracking given dynamic water level data. Although numerical models are widely employed described in the last paragraph, there are still limitations to use numerical models to track particles. For complicated buondray conditions, numerical models are the first choice to resolve particle tracking, even though they give people the proximate answers. But compare to numerical models, specially for some simple boundary

conditions, continuous water data from field sites can generate more precise results for particle tracking. The advantage of using continuous water data from field sites is this method can resolve particles tracking in a simpler and more efficient way under simple boundary conditions. Furthermore, for numerical models, temporal and spatial discretizations maybe insufficient to accurately track particles under dynamic pumping condition about dynamically operated wells in well fields. But analytical solutions can generate more precise results of particle tracking under this conditions. And the advantage of using analytical solutions is that they provide a continuous solutions in space and time for particle tracking under pumping conditions.

There are two general approaches employed in this research, continuous water-level data from field sites and analytical solutions. For continuous water level data from field sites, hydraulic head is obtained through continuous measurement of water levels in wells using pressure transducers. Planer water surfaces can be defined using water data from three or more monitoring wells at fixed points in time. Progress of a particle through time is achieved using a succession of steady-state solution applied over short time increments. For analytical solutions, dynamic water levels can also be obtained using analytical solutions for dynamic pumping conditions.

1.2 Research Objectives

The first objective of this research is to use continuous water level data at three sites to resolve groundwater flow under dynamic conditions. The sites are located near a river with a seasonal water-level change of up to 40 ft, at a shallow desert aquifer (where seasonal transpiration affects groundwater flow), and adjacent to a harbor (where tides control water levels). For each site, particle tracking is conducted assuming A) homogeneous, isotropic conditions without reactions, B) homogeneous, anisotropic conditions with retardation and

without reactions, and C) by assuming that the degradation of contaminants in the subsurface follows the first-order kinetics. The path lines and distance of particle flow within the required minimum concentration under homogeneous and anisotropic conditions with retardation can be obtained.

The second objective of this research is to use an analytical model developed from a Theis superposition model (Davis, 2013) that can calculate head under dynamic pumping and injection conditions to evaluate particle tracking under dynamic pumping conditions. Incremental time steps are used to resolve particle-flow path lines. Consideration is given to the prediction of flow under the influence of pumping and injection conditions. Over all, this research advances simple methods for predicting the movement of subsurface contaminants given dynamic water levels at sites where historical releases have occurred and in dynamic well fields with dynamic water levels.

In this research, the parameters assumed at each site and the well field are not necessarily truly representative of site condition. However, this will not influence the objective of this research. The overall objective of this research is to demonstrate methods to use continuous water level data from field sites and analytical solutuions to resolve particle tracking under dynamic conditions and about dynamically operated wells in well fields. And the most important goal in this research is to demonstrate the methods can be used to resolve the particle tracking issues but not rigorously making predictions about processes at sites.

1.3 Organization and Content

This thesis is divided into four parts. The hydrogeology of the study sites are presented in Chapter 2. Computational methods are presented in Chapter 3. Results are described in Chapter 4. Lastly, conclusions and recommendations for future work are presented in Chapter 5.

CHAPTER 2 - HYDROGEOLOGICAL DESCRIPTION AND SITE DATA

Dynamic water-level data from four field sites with different geologic conditions were selected to demonstrate novel methods for tracking fluid particles under dynamic water level conditions. The sites are located in Kansas City, Missouri, Pueblo, Colorado, Honolulu, Hawaii, and Castle Rock, Colorado. The following section provides an introduction to hydrogeologic conditions and water-level data at each site.

2.1 Hydrogeological Description

2.1.1 Kansas City, Missouri

The first site is a petroleum fuel terminal located in Kansas City, Missouri. The primary sources of information are site investigation and monitoring reports developed by TRC Solutions, Inc. The site is located near the Missouri River. Following TRC (2012), Current site includes above-ground storage tanks, several maintenance and operation buildings. Released petroleum products at this site were sufficient in magnitude to have products reached and accumulated at the water table. Benzene is considered to be the primary contaminant of concern in the study area.

Figure 2.1: The terminal in Kansas City, MO.

From TRC (2012), the area surrounding the terminal is underlain by alluvial sediments deposited by Missouri River, and these deposits may exceed 100 feet in thickness. The main soil type within the uppermost 10 to 15 feet includes silt, clay, and silty fine sand. Moreover, underlying this uppermost soil layer, the main two soil types are fine sand and silty sand, which have 5 or more feet in thickness.

Well locations and continuous water level data were both provided by TRC staff. TRC used four wells to obtain water-level data at the terminal (Figure 2.2). The water level data were collected from June 29, 2009 to July 31, 2015, which are shown in Figure 2.3. The time step for each water level data collection is 1 day. Water levels in the Missouri River near the site dynamically changed through the six-year period recording (Figure 2.4). The biggest variation in river stage is up to 40 feet. From Figure 2.4, six peaks of water level occurred in the Missouri River from Jun 29, 2009 to Jul 31, 2015. However, in Figure 2.3 the peaks of water level are not identical to that of Figure 2.4. The reason for the missing peaks is due to missing data of water-

level from the wells at the terminal. In order to calculate the particle position, the model of this research requires water-level data from at least four wells. This research omitted the data that from four wells in the same measured time is unavailable. Therefore, the data from June 29, 2009 to July 31, 2015 are not continuous. The data omitted in this research are data from: February 6, 2009 to June 28, 2009, March 12, 2010 to November 30, 2010, August 20, 2011 to April 19, 2012, June 7, 2013 to July 2, 2013, November 24, 2013 to April 9, 2014. The omissions are marked on Figure 2.3 except the short periods (February 6, 2009 to June 28, 2009, and June 7, 2013 to July 2, 2013).

Figure 2.2: Water-level monitoring locations at the terminal in Kansas City, MO.

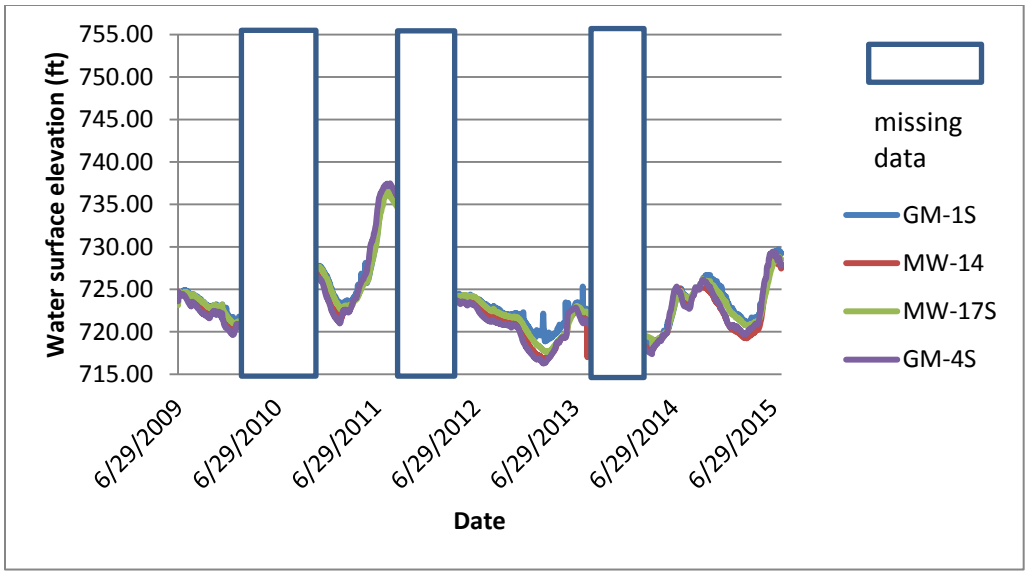

Figure 2.3: Water-level data from four wells at the terminal in Kansas City, MO.

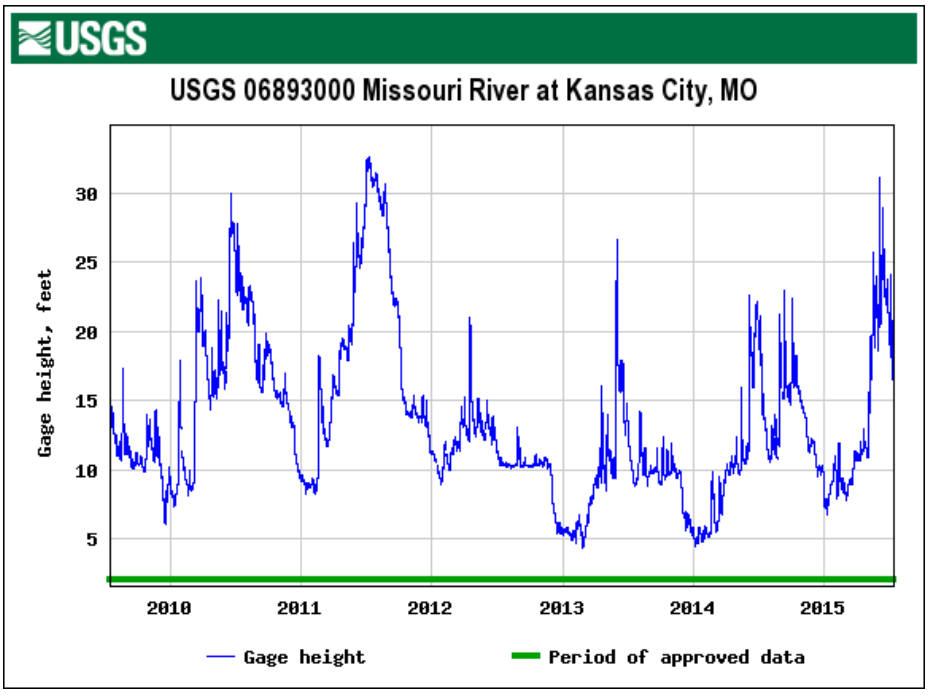

Figure 2.4: Missouri River stage at Kansas City, MO from July 15, 2009 to July 15, 2015. Data are provided by USGS National Water Information System.

Figure 2.5 was generated using the Mathcad 15® code presented in Appendix A. The rose chart shows groundwater gradient ranging from east-southeast to west-northwest. Hydraulic gradients are varied at almost every direction with different magnitudes, and the hydraulic

gradients with greater magnitudes are mainly distributed in the southeast to northwest direction. Building on description presented in (TRC, 2012), the hydraulic conductivity of the saturated zone was estimated at 0.0033 ft/sec, porosity was 0.25, and bulk density was 1.987 kg/L. The time step used for computation of particle tracking at this site is the same with that of water level data collection, which is 1 day. For homogeneous and anisotropic conditions with retardation, values of hydraulic conductivity were assumed to be $K_x = 0.0033$ ft/sec in the *x* direction, and $K_y = 0.00164$ ft/sec in the *y* direction. The partition coefficient $K_{oc}$of benzene is 59 ml/gm (USGS report, 2005), and the weight fraction of organic carbon f_{oc} is assumed to be 0.01. The first order rate constant for benzene degradation *k* is 0.0036/day (Rifai and Newell, 1998).

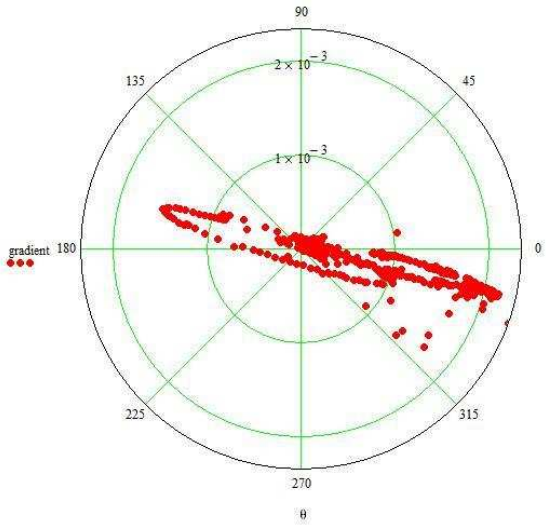

Figure 2.5: Rose chart for hydraulic gradients vs. angles at the terminal in Kansas City, MO.

2.1.2 Pueblo, Colorado

The second site is Pueblo Chemical Depot (PCD) located approximately 15 miles east of Pueblo, Colorado (see Figure 2.6). Primary sources of information are site investigation and monitoring reports presented in Sale et al. (2010). From Sale et al. (2010), PCD was built to serve as an ammunition and material storage and shipping center. And PCD stored chemical munitions in the late 1990s.

Figure 2.6: Location of Pueblo Chemical Depot near Pueblo, CO (Sale et al., 2010).

From Sale et al. (2010), releases from PCD made plumes discharged into the Arkansas River alluvium. There were still several contaminants remained in the soil in the subsurface at this site after source excavation. Hexahydro-1,3,5-trinitro-1,3,5-triazine (RDX) is the primary contaminant of concern in this study. Groundwater occurred at about 8 to10 feet below ground surface. The main soil type underlain by 10 to 15 feet at this site is sand.

Well locations and continuous water-level data are described in Sale et al., 2010. Five wells were employed to measure water-level data at the site (Figure 2.7). Water-level data were collected over the period from March 1, 2006 to September 16, 2008. The time step for each water level data collection is 1 day; however, some data are absent during this period (November 14, 2007 to April 22, 2008, August 29, 2006 to October 10, 2006). The method to address the missing data at this site is skipping the time period. The data are presented in Figure 2.8. A.S.L in Figure 2.8 is defined as the above ground level. Precipitation and transpiration of the vegetations contribute to the water-level changes in this area. From the beginning of fall to the

summer, precipitation forces the water surface elevation to rise. On the other hand, transpiration contributes to the water-surface-elevation decline from the end of the spring to the summer (Figure 2.8).

Figure 2.9 presents a rose chart for the site. The rose chart shows groundwater gradient ranging from east-northeast to west-southwest. Hydraulic gradients are varied at almost every direction with different magnitudes, and the hydraulic gradients with greater magnitudes are mainly distributed in the northeast to southwest direction. During brief periods, hydraulic gradient direction shifts to the northwest.

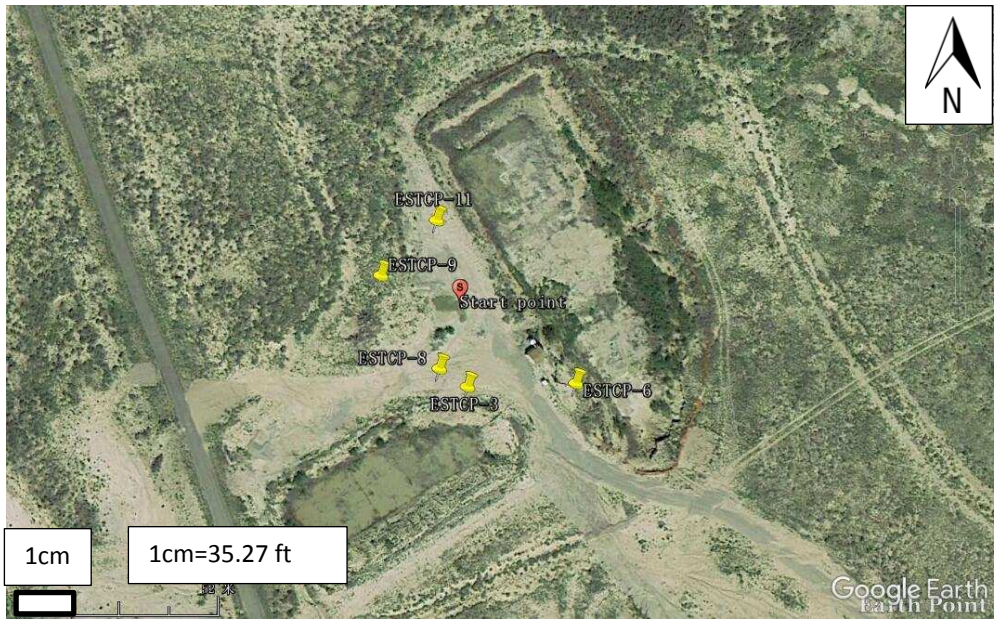

Figure 2.7: Well locations at PCD, CO.

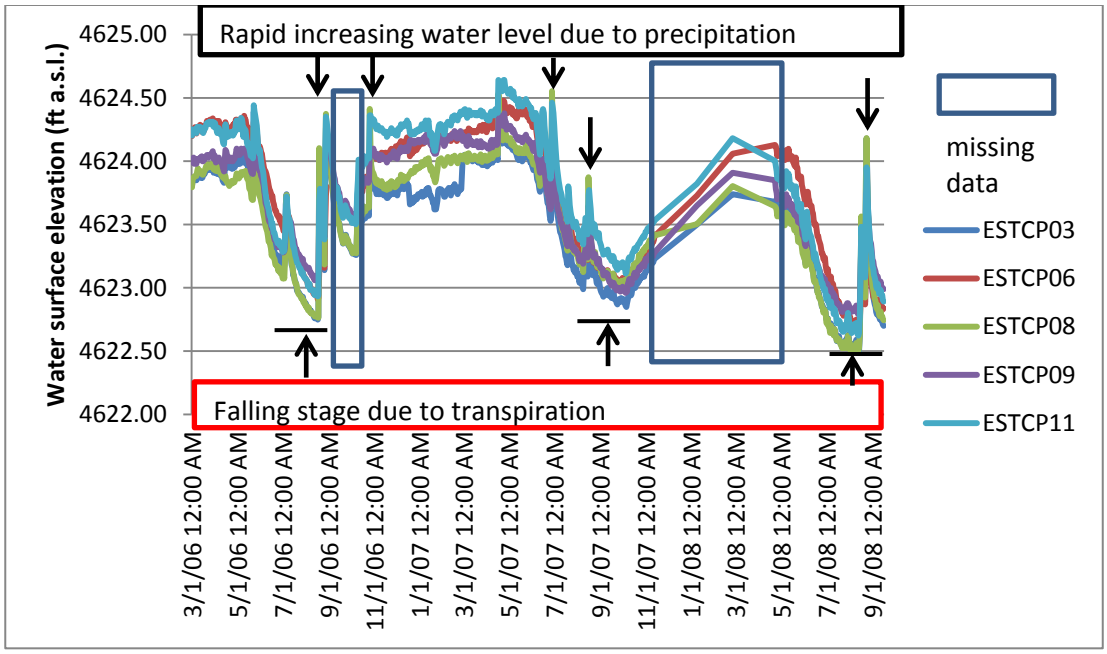

Figure 2.8: Water-level data in five wells at PCD, CO.

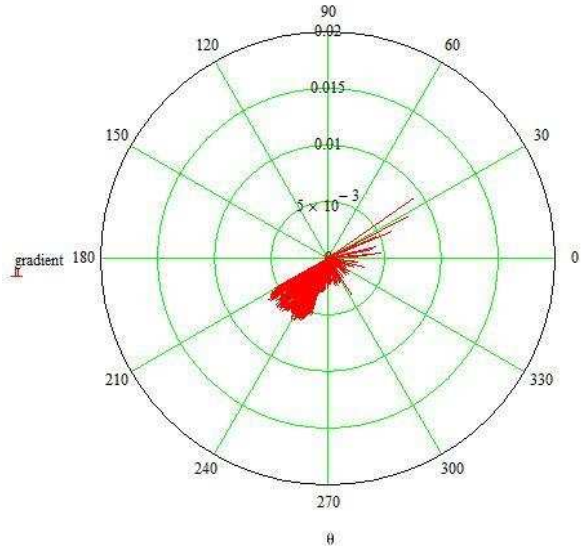

Figure 2.9: Rose chart for hydraulic gradients vs. angles at PCD, CO.

Based on the geologic information in this site, for homogeneous and isotropic conditions, the hydraulic gradient was set at $K = 0.00033$ ft/sec, porosity was $\varphi = 0.25$, and bulk density $\rho_b = 1.987$ kg/L. The time step used for computation of particle tracking at this site is the same with that of water level data collection, which is 1 day. For homogeneous and anisotropic

conditions with retardation, hydraulic conductivity in the *x* direction was $K_x = 0.00033$ ft/sec, in the *y* direction $K_y = 0.000164$ ft/sec. This value is accordant with the results estimated by the column study data and estimates of hydraulic conductivity for sands in Sale (2012), which shows that for two kinds of soil types at this site, the average hydraulic conductivities are 0.00049 ft/sec and 0.00011 ft/sec (Sale et al., 2010). And the partition coefficient K_{oc} of RDX is 63 ml/gm (U.S. Department of Health and Human Services, 1995), the weight fraction of organic carbon f_{oc} is assumed to be 0.01. The first order degradation rate constant of RDX k is 0.063/day (U.S. Department of Health and Human Services, 1995).

2.1.3 Honolulu, Hawaii

The third site is located adjacent to a tidal harbor in Honolulu, Hawaii (Figure 2.10). The main soil type in the subsurface of this region is silt/dense coral sands (Mahler et al., 2011). Well locations and continuous water level data were provided by Pat Hughes, Chevron. Five wells were selected to measure water levels at the site (Figure 2.10). The time steps for each water and LNAPL level data collected are both 360 seconds.The primary contaminant of concern for this site is benzene.

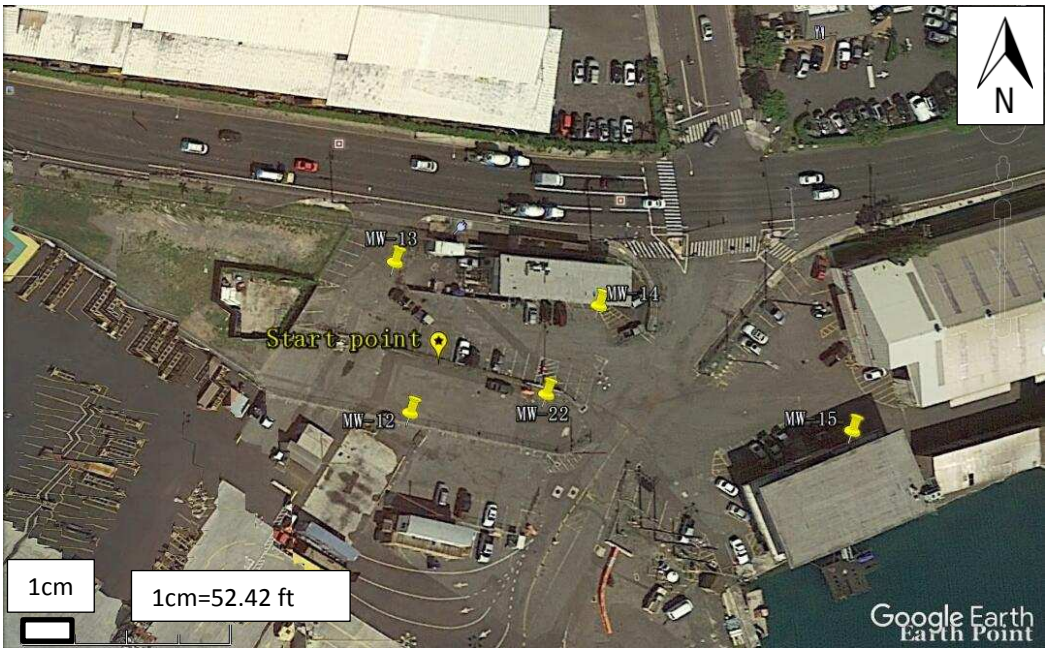

Figure 2.10: Well locations at the Honolulu harbor site.

Chevron Corporation invested great effort into resolving water-table elevations and product thicknesses through the time period from 2007 to 2011. The tides adjacent to the harbor are largely lunar-influenced, which correspondingly affect the flow of groundwater and other fluid in the subsurface of this area (Figure 2.11). Figure 2.11 shows the predicted ocean water levels influenced by lunar activity. MLLW in the Figure 2.11means mean lower low water, which is the average height of the lowest tide recorded at a tide station each day during the recoring period (Tidal Datums, tidesandcurrents.noaa.gov). MSL in the Figure 2.12 to 2.21 is defined as the mean sea level. The elevations of air/oil (A/O) interface and oil/water (O/W) interface influenced by the tides are shown in Figures 2.12 to 2.16. Both air/oil (A/O) and oil/water (O/W) interfaces follow tidal fluctuations which are illustrated in Figure 2.12. Further, because water levels influenced by the tides, the thickness of NAPL is also affected (Figures 2.17 to 2.21).

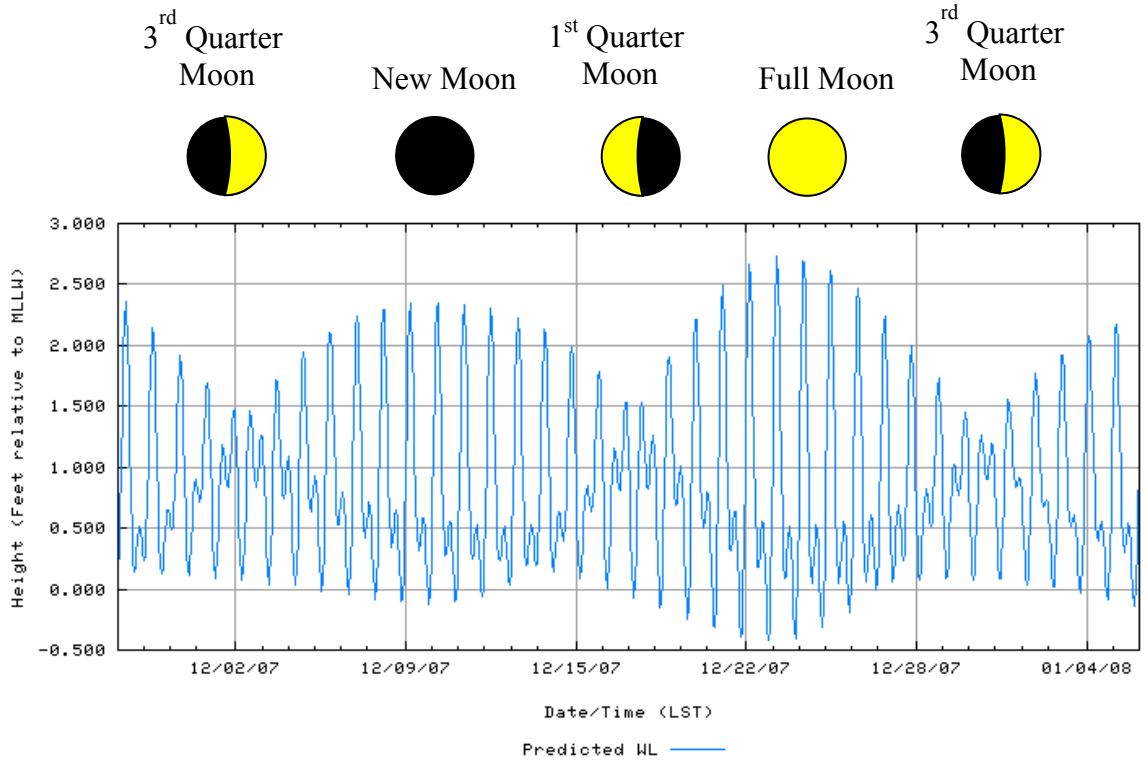

Figure 2.11: Tides influenced by the Moon. (Chevron Corporation)

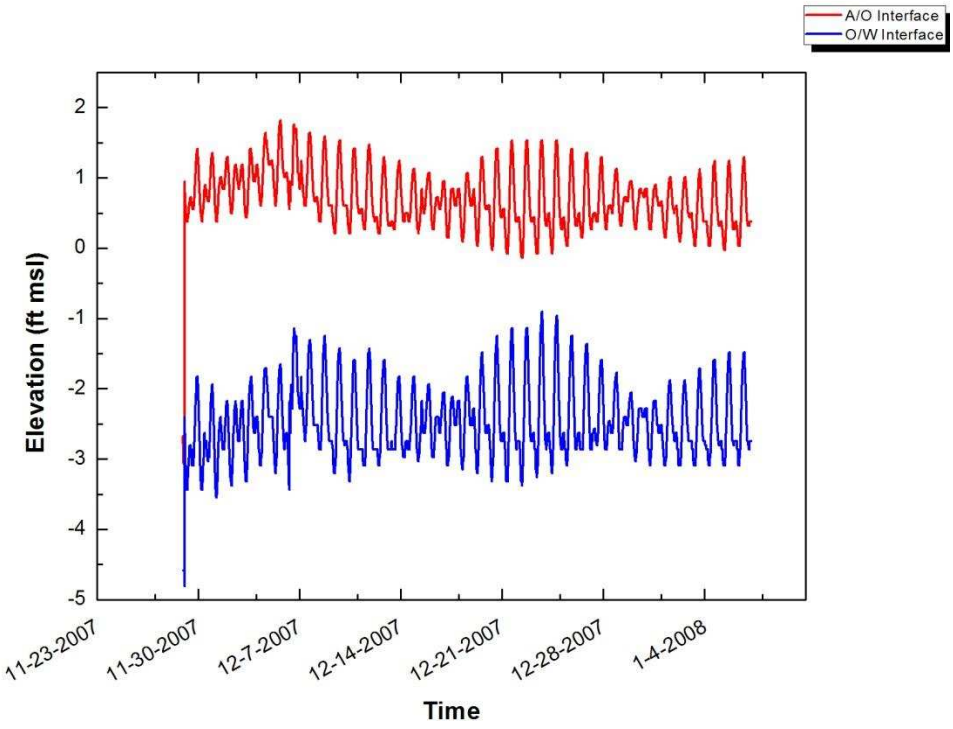

Figure 2.12: A/O interface vs. O/W interface in well MW-12 at Honolulu, HI.

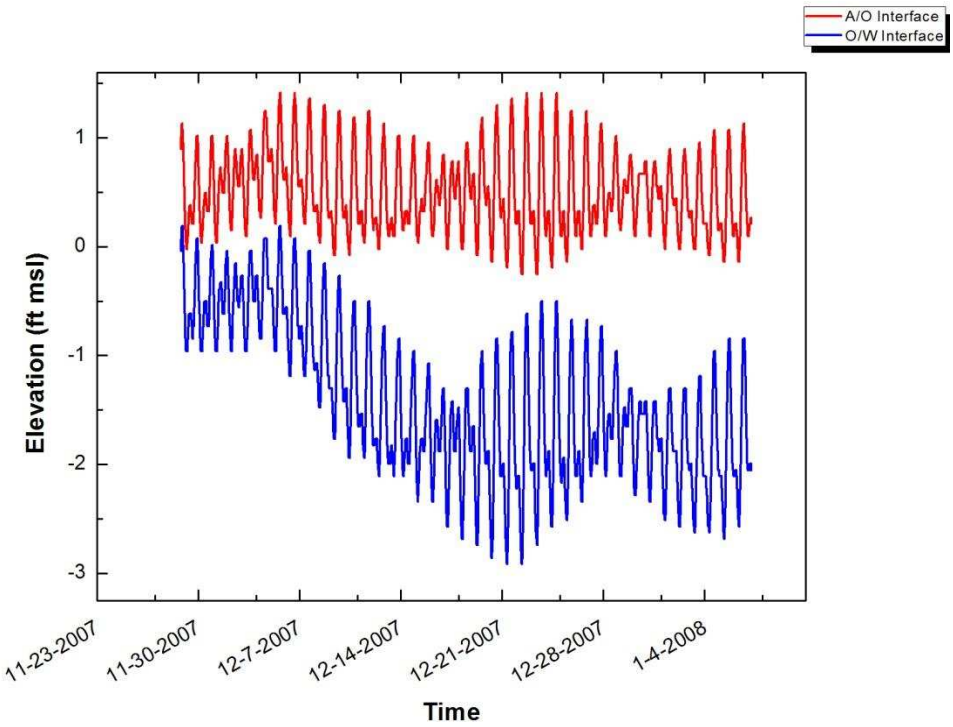

Figure 2.13: A/O interface vs. O/W interface in well MW-13 at Honolulu, HI.

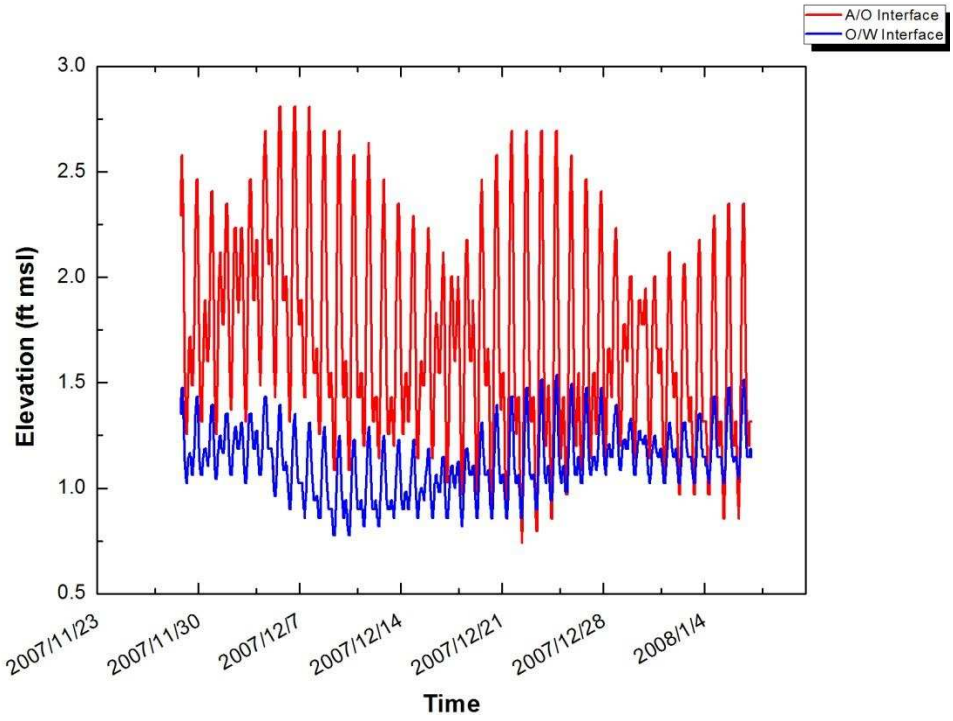

Figure 2.14: A/O interface vs. O/W interface in well MW-14 at Honolulu, HI.

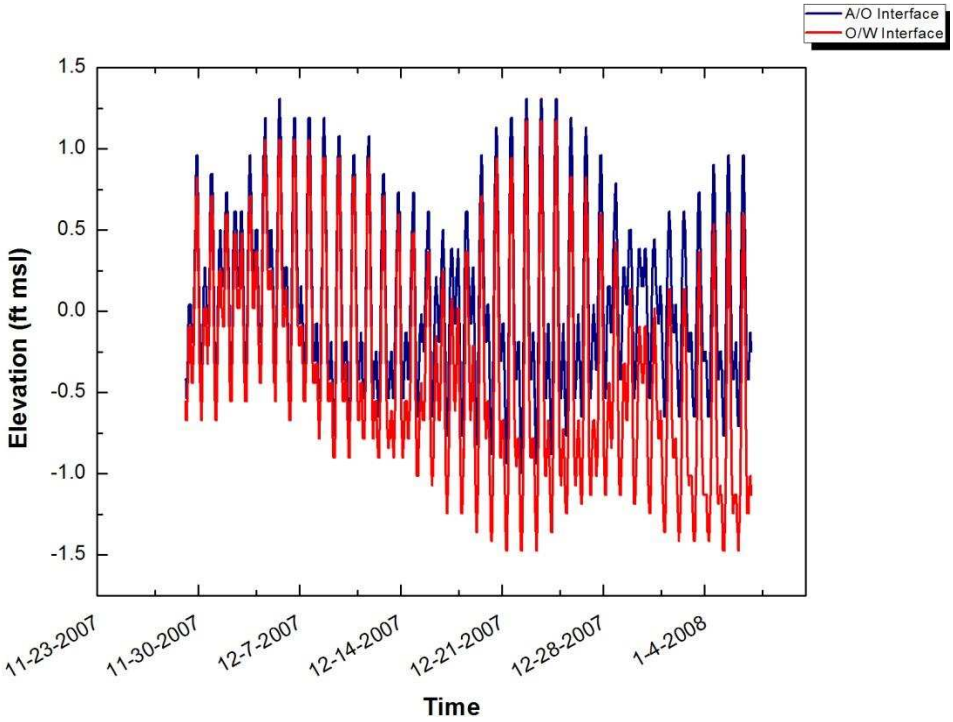

Figure 2.15: A/O interface vs. O/W interface in well MW-15 at Honolulu, HI.

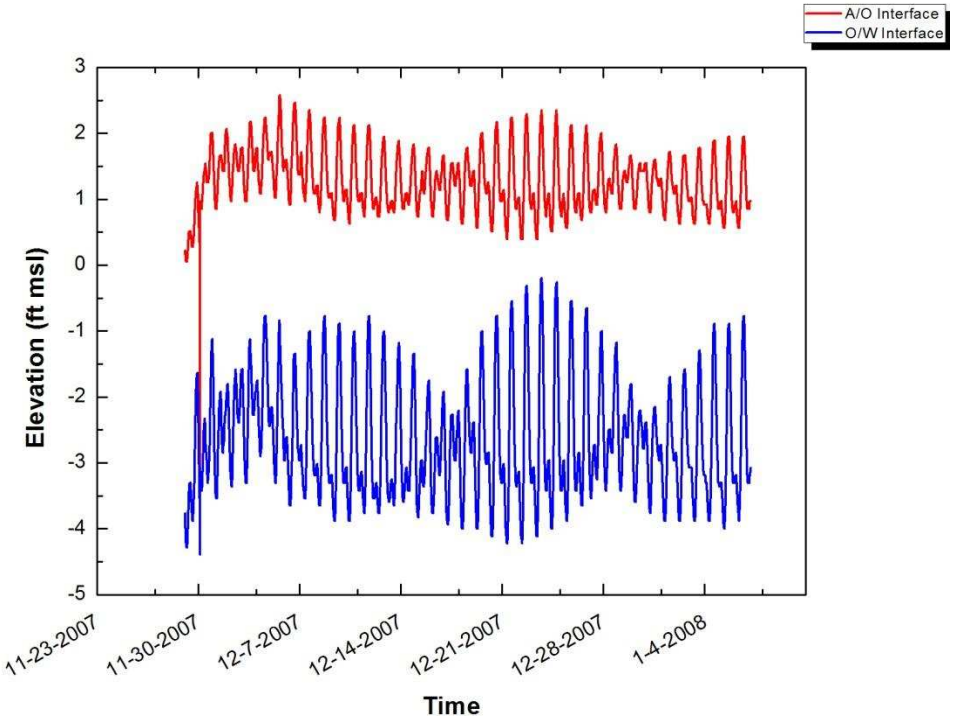

Figure 2.16: A/O interface vs. O/W interface in well MW-22 at Honolulu, HI.

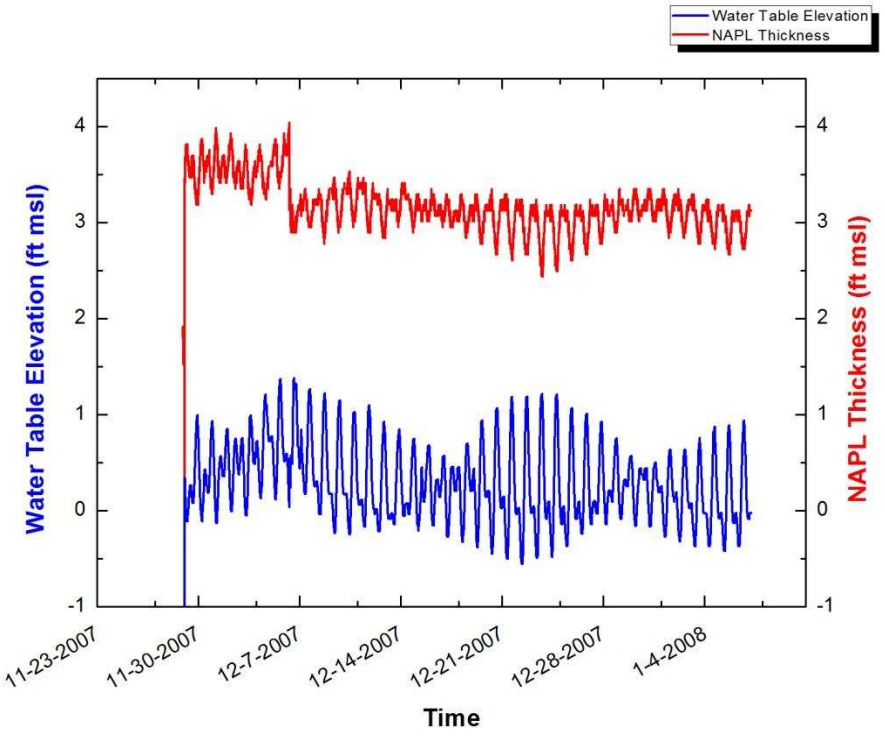

Figure 2.17: LNAPL thickness vs. water table elevation in well MW-12 at Honolulu, HI.

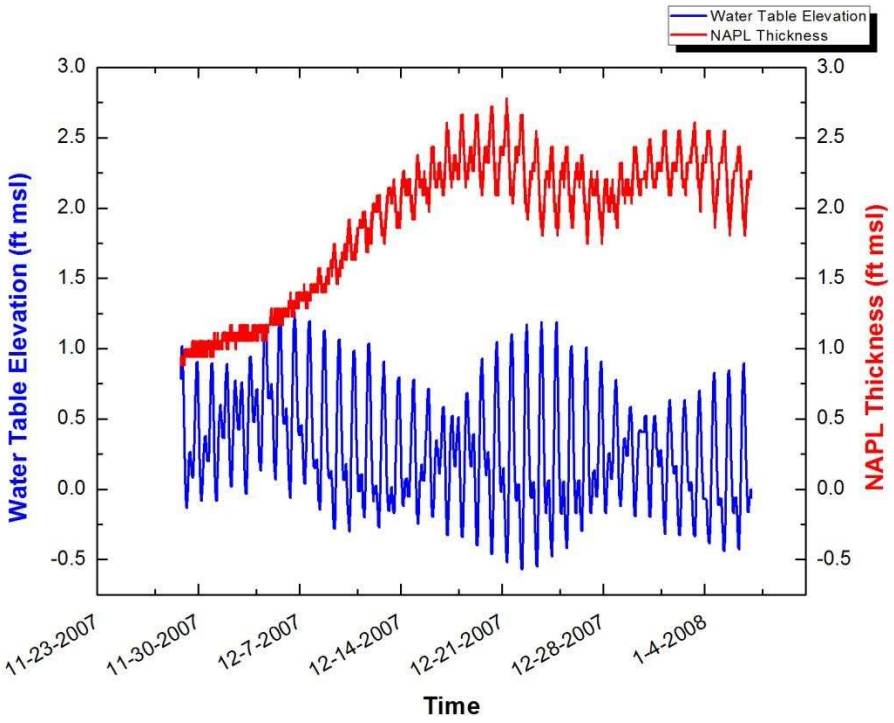

Figure 2.18: LNAPL thickness vs. water table elevation in well MW-13 at Honolulu, HI.

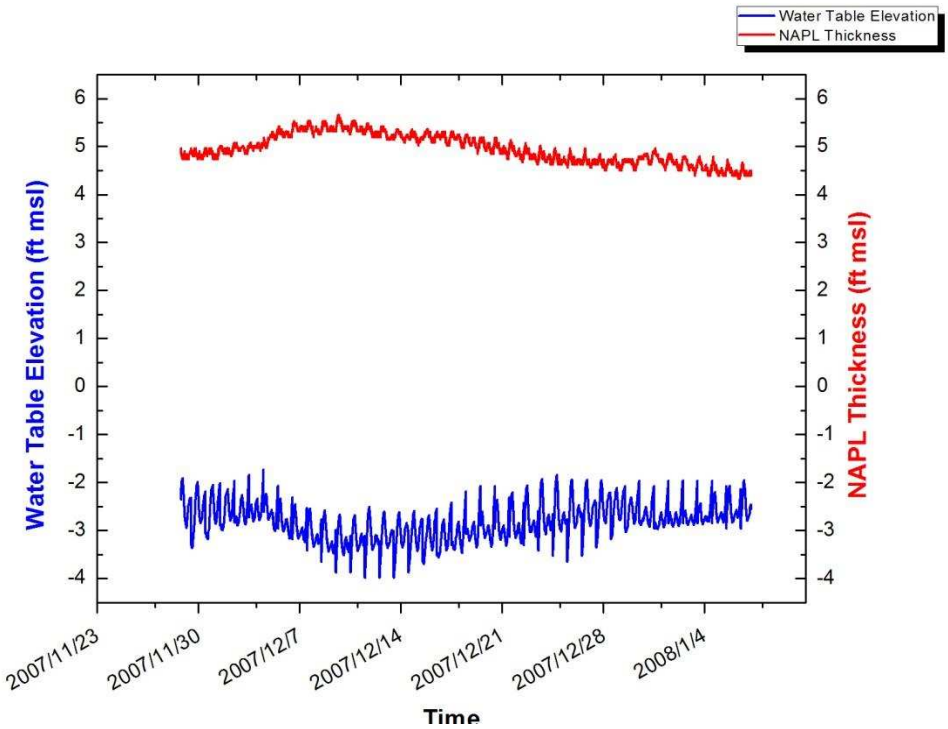

Figure 2.19: LNAPL thickness vs. water table elevation in well MW-14 at Honolulu, HI.

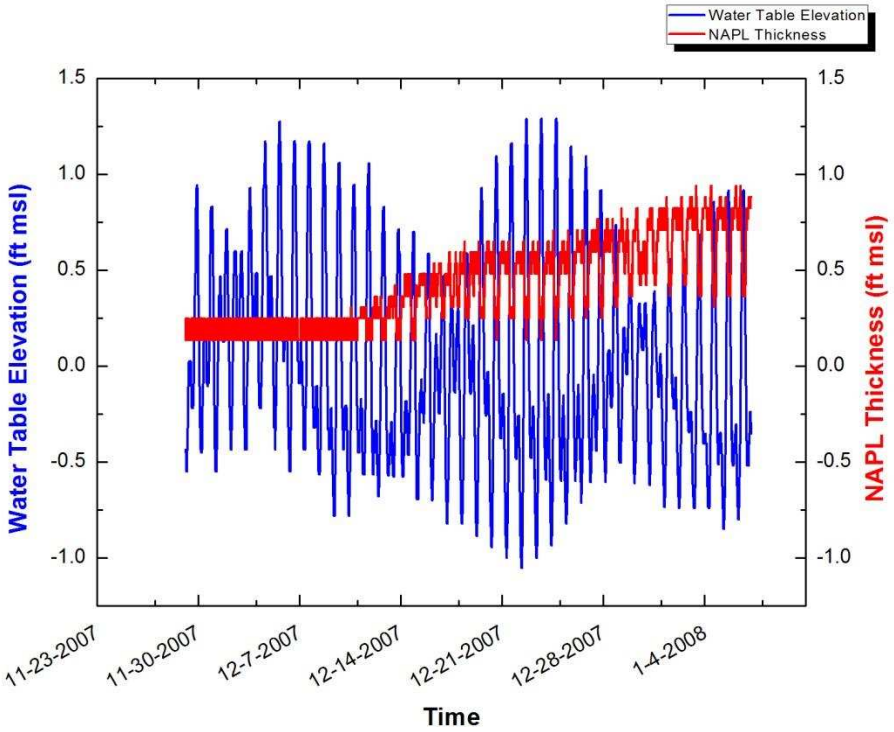

Figure 2.20: LNAPL thickness vs. water table elevation in well MW-15 at Honolulu, HI.

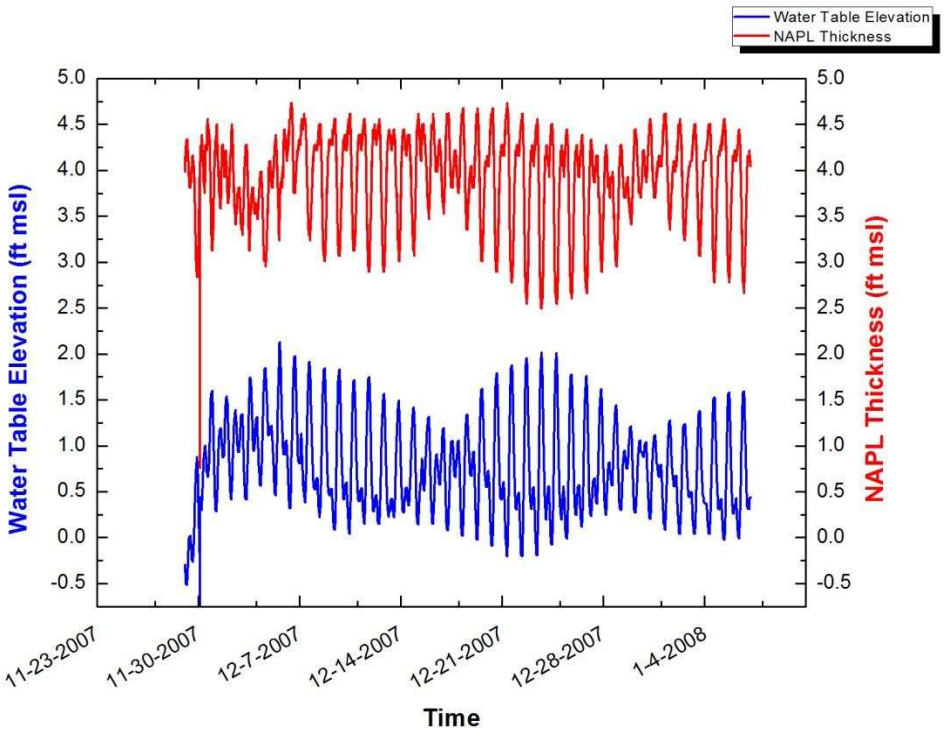

Figure 2.21: LNAPL thickness vs. water table elevation in well MW-22 at Honolulu, HI.

The rose charts in Figure 2.22 show hydraulic gradients of groundwater (left) and gradients of LNAPL (right) varied with different magnitudes in almost every direction in the southwest part of rose charts. The main directions of hydraulic gradient and LNAPL gradient are concentrated in the northwest to southeast and southwest. And the magnitude of hydraulic gradient and LNAPL gradient in the northwest to southeast direction are smaller to the magnitude of hydraulic gradient and LNAPL gradient in the southwest direction. Based on local geologic conditions, for homogeneous and isotropic conditions, the hydraulic conductivity of water K_w is assumed to be 3.28×10^{-6} ft/sec for coral sands. Based on the density, an assumed relative permeability and viscosity of the two fluids (water and LNAPL), the conductivity of LNAPL is calculated to be 4.39×10^{-7} ft/sec (see in Chapter 3). Porosity φ is 0.25, and bulk density ρ_b is 1.987 kg/L. The time steps used for computation of particle tracking at this site for groundwater and LNAPL are the same with that of water and LNAPL level data collection,

which are 360 seconds. For homogeneous and anisotropic conditions with retardation, hydraulic conductivity of water in the *x* direction $K_x = 3.28\times10^{-6}$ ft/sec, and $K_y = 1.64\times10^{-6}$ ft/sec in the *y* direction. And the conductivity of LNAPL in the *x* direction is $K_x = 4.39\times10^{-7}$ ft/sec, and $K_y = 2.19\times10^{-7}$ ft/sec in the *y* direction.

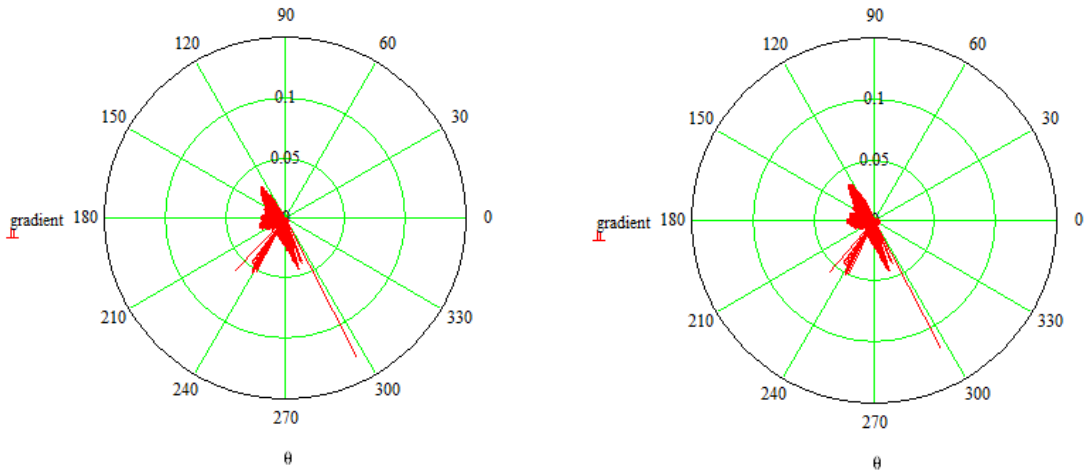

Figure 2.22: Rose charts for the hydraulic gradients (left) and gradients of LNAPL (right) vs. angles in the field site of Honolulu, HI.

2.1.4 Castle Rock, CO

Denver Basin groundwater is the primary water source for the Town of Castle Rock, Colorado (Sale et al., 2009). The Denver Basin aquifer system is a group of confined, deep-bedrock sandstones located east of the Colorado Front Range (Figure 2.23; Robson and Banta, 1995). This field site is situated along the western flank of the Denver Basin aquifer system and is one of many towns included in the Front Range urban corridor (Davis, 2013). There are four main well fields in Castle Rock, shown in Figure 2.24. Data from the Meadows Pumping Center were used for analysis in this study. Well locations of the Meadows Pumping Center are shown in Figure 2.25.

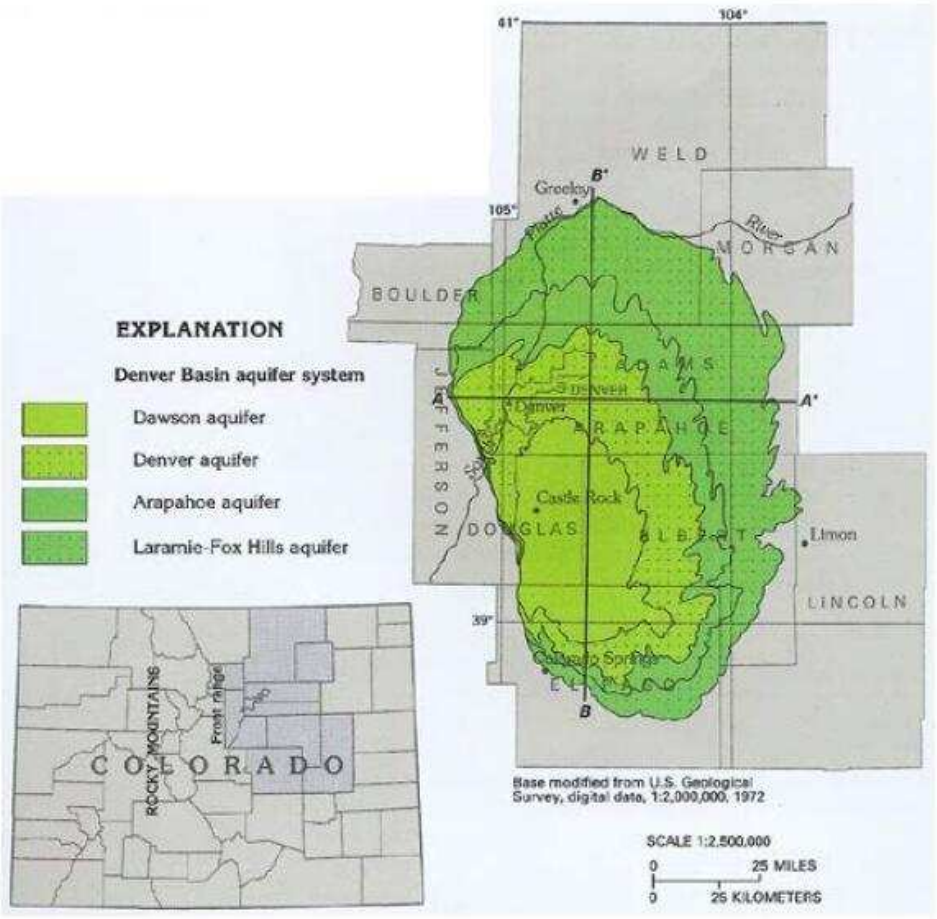

Figure 2.23: Location map for the Denver Basin (Robson and Banta, 1995).

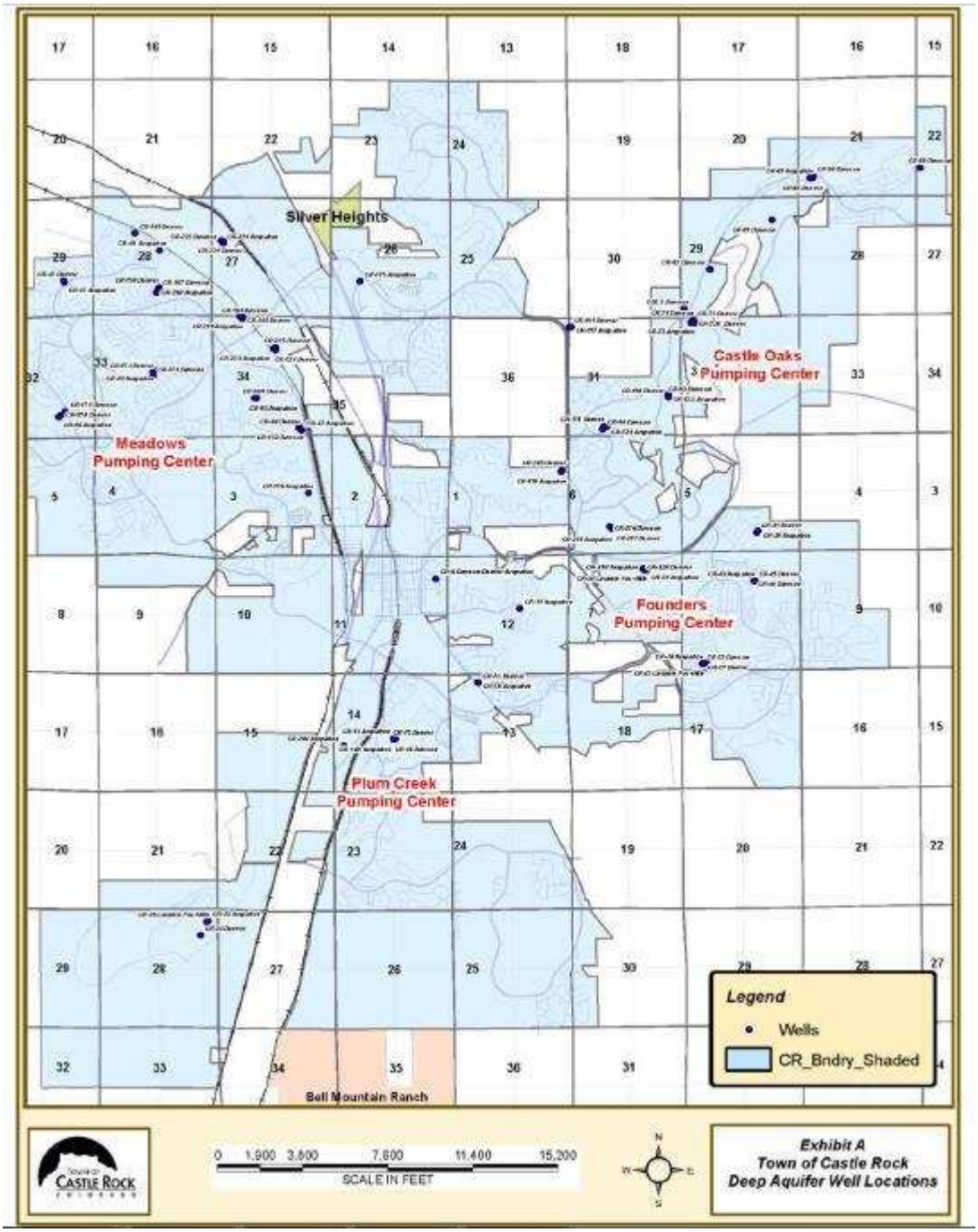

Figure 2.24: Castle Rock well locations. Provided by the Castle Rock Utilities Department.

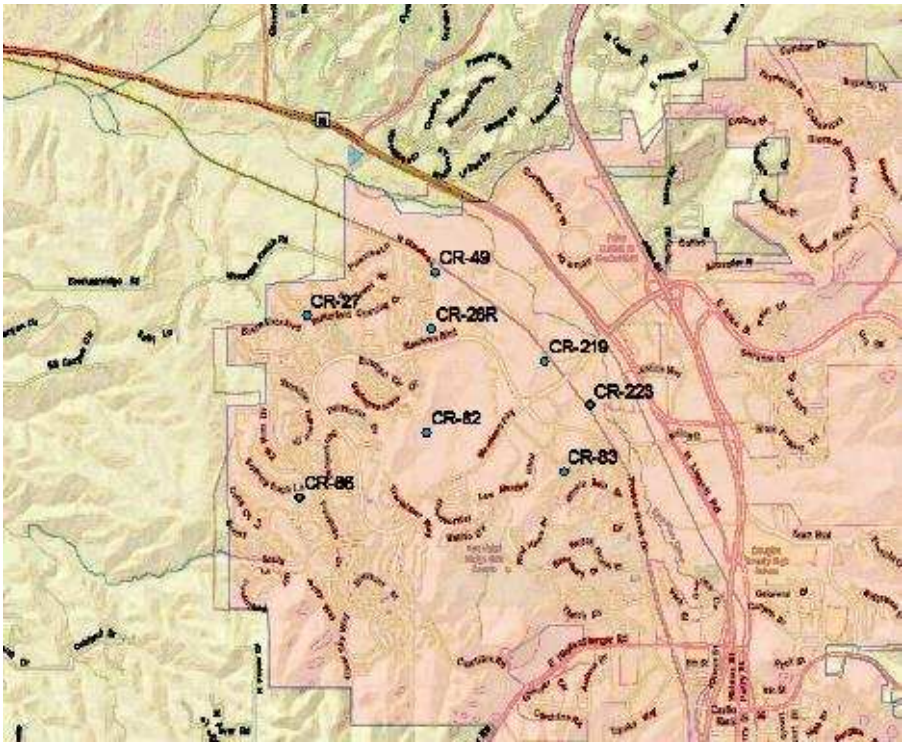

Figure 2.25: Wells locations at the Meadows Pumping Center in Castle Rock, CO.

Transmissivity of the aquifer in the Meadows Pumping Center is 4000 gal/day/ft (Davis, 2013), storativity is 0.00005 (Davis, 2013), porosity is assumed to be 0.25, and aquifer thickness is assumed to be 32.8 ft. There are eight wells operated at the Meadows Pumping Center. Pumps in the eight wells at the Meadows Pumping Center cycled on and off from 2007 to 2011, as shown in Figure 2.26. Correspondingly, water levels in these eight wells continuously changed over this period, as shown in Figure 2.27 (a-h). The time interval for each pumping rate and water level data collected is 1 day.

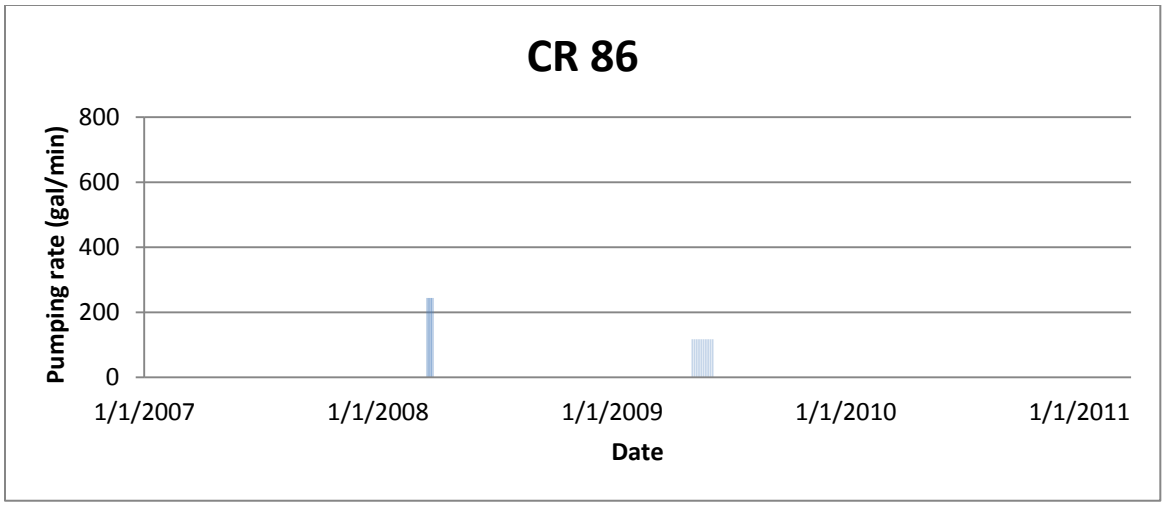
CR 86
Pumping rate (gal/min)
800
600
400
200
0
1/1/2007
1/1/2008
1/1/2009
1/1/2010
1/1/2011
Date

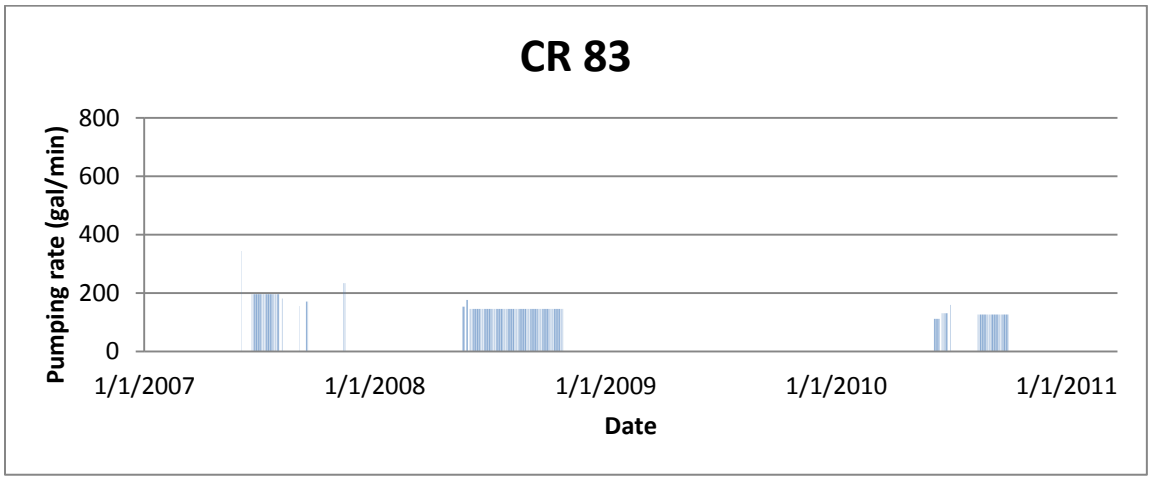
CR 83
Pumping rate (gal/min)
800
600
400
200
0
1/1/2007
1/1/2008
1/1/2009
1/1/2010
1/1/2011
Date

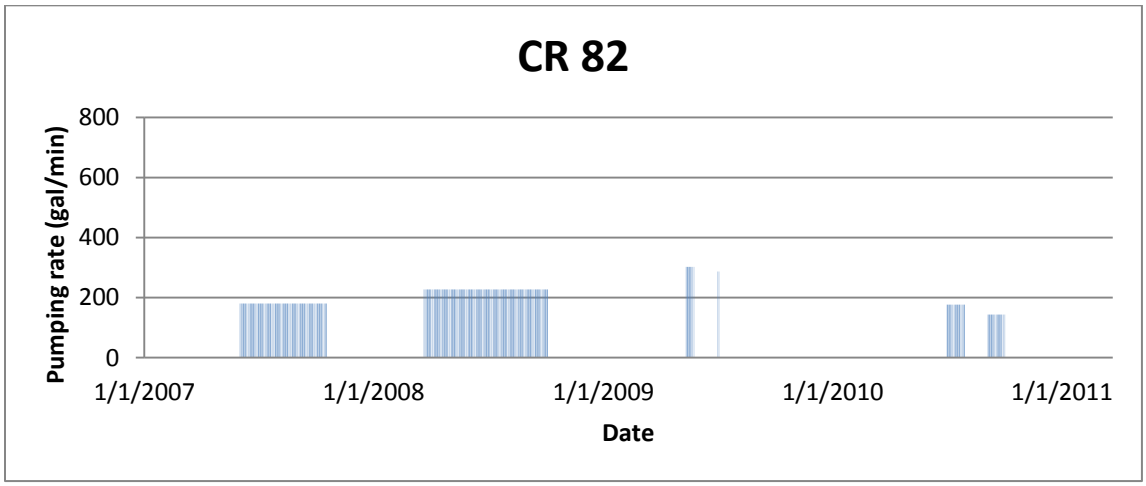
CR 82
Pumping rate (gal/min)
800
600
400
200
0
1/1/2007
1/1/2008
1/1/2009
1/1/2010
1/1/2011
Date

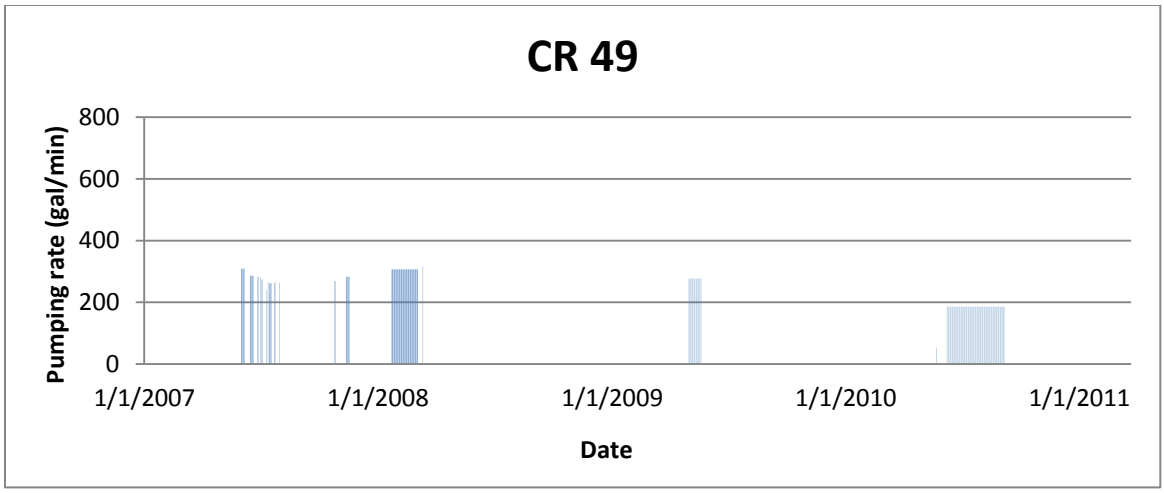
CR 49
Pumping rate (gal/min)
800
600
400
200
0
1/1/2007
1/1/2008
1/1/2009
1/1/2010
1/1/2011
Date

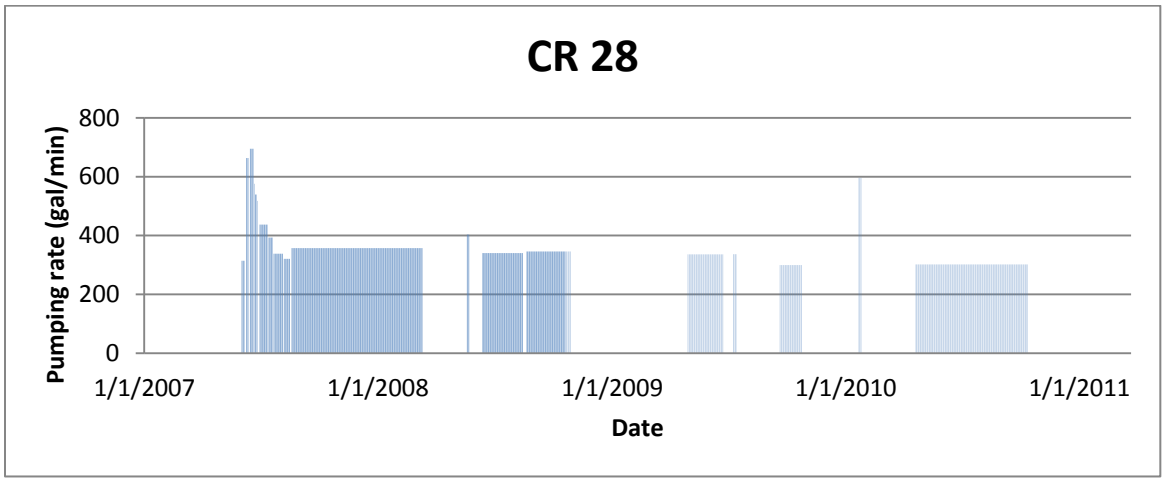
CR 28
Pumping rate (gal/min)
800
600
400
200
0
1/1/2007
1/1/2008
1/1/2009
1/1/2010
1/1/2011
Date

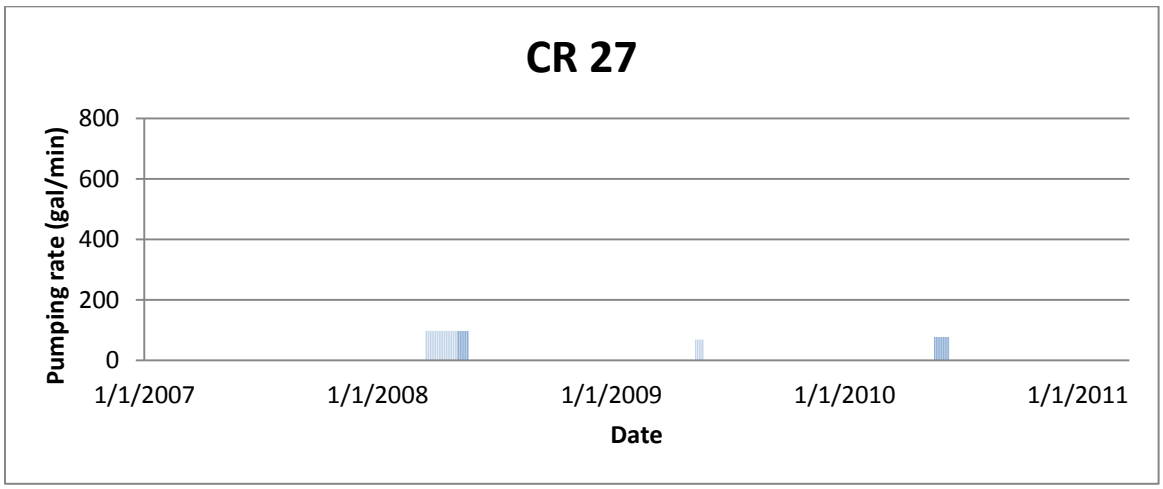
CR 27
Pumping rate (gal/min)
800
600
400
200
0
1/1/2007
1/1/2008
1/1/2009
1/1/2010
1/1/2011
Date

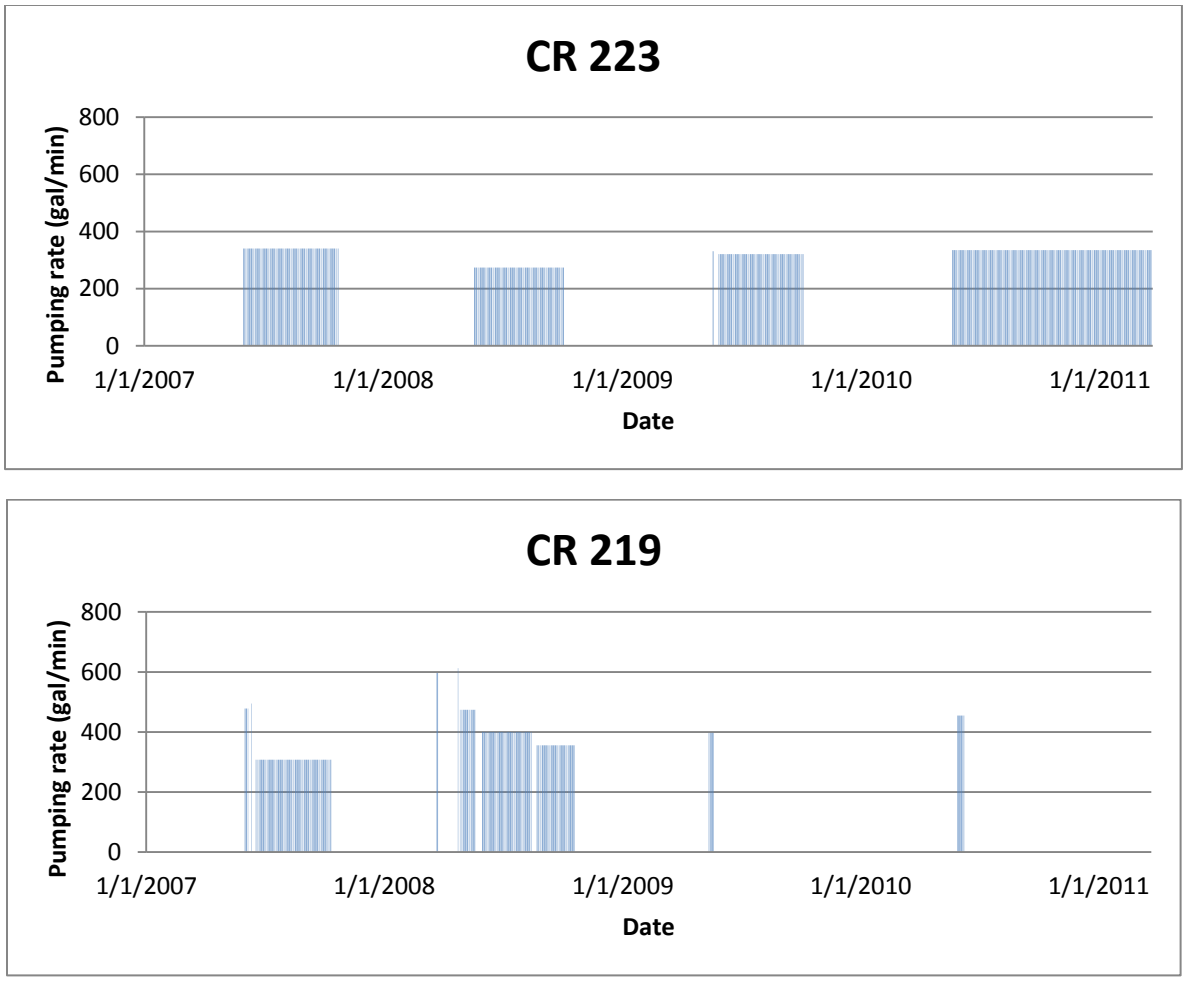

Figure 2.26: Pumping rates of eight wells at the Meadows Pumping Center, CO.

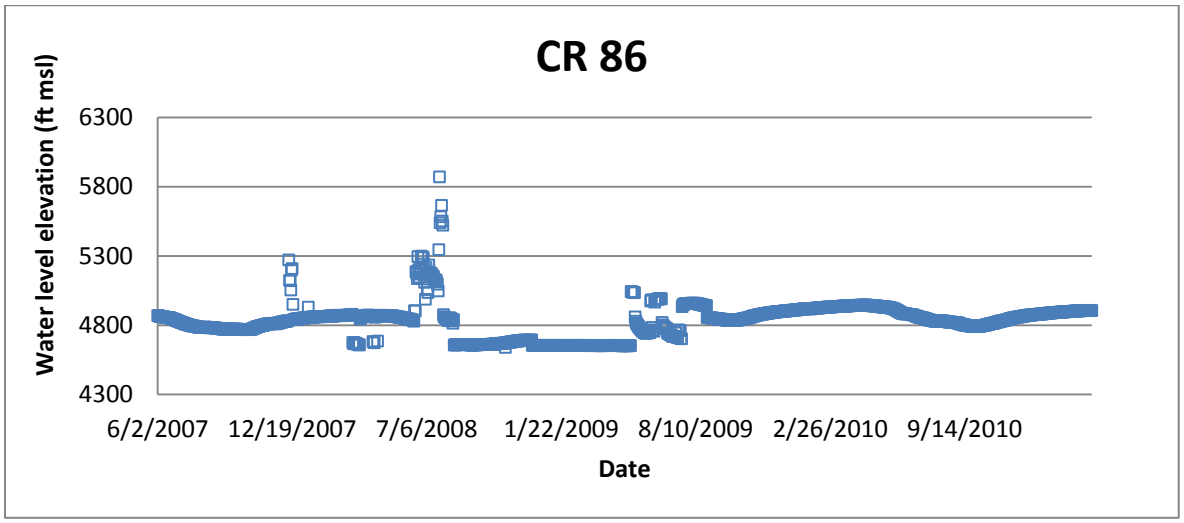

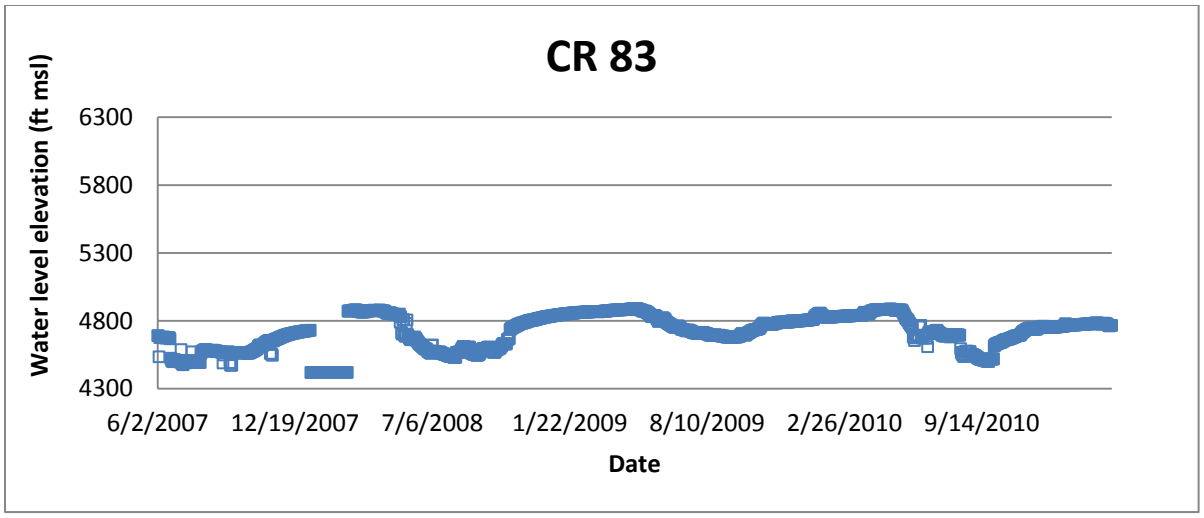
CR 83
Water level elevation (ft msl)
6300
5800
5300
4800
4300
6/2/2007
12/19/2007
7/6/2008
1/22/2009
8/10/2009
2/26/2010
9/14/2010
Date

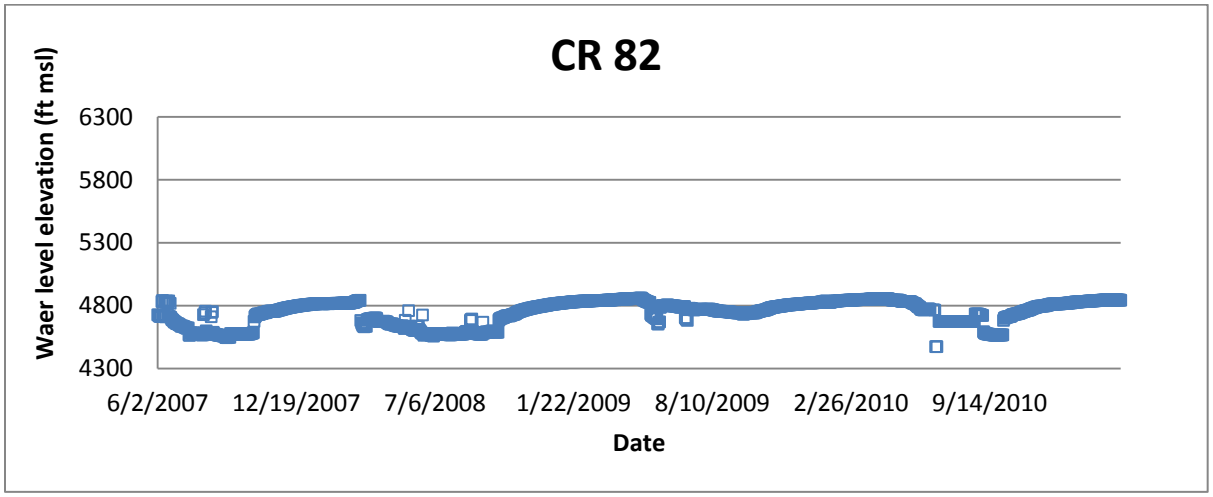
CR 82
Waer level elevation (ft msl)
6300
5800
5300
4800
4300
6/2/2007
12/19/2007
7/6/2008
1/22/2009
8/10/2009
2/26/2010
9/14/2010
Date

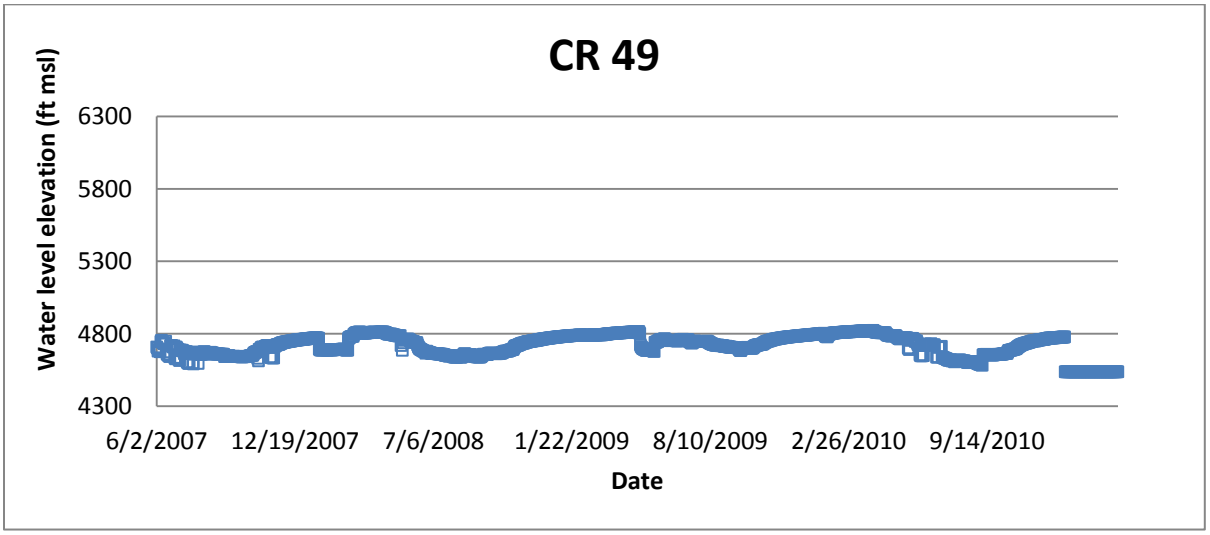
CR 49
Water level elevation (ft msl)
6300
5800
5300
4800
4300
6/2/2007
12/19/2007
7/6/2008
1/22/2009
8/10/2009
2/26/2010
9/14/2010
Date

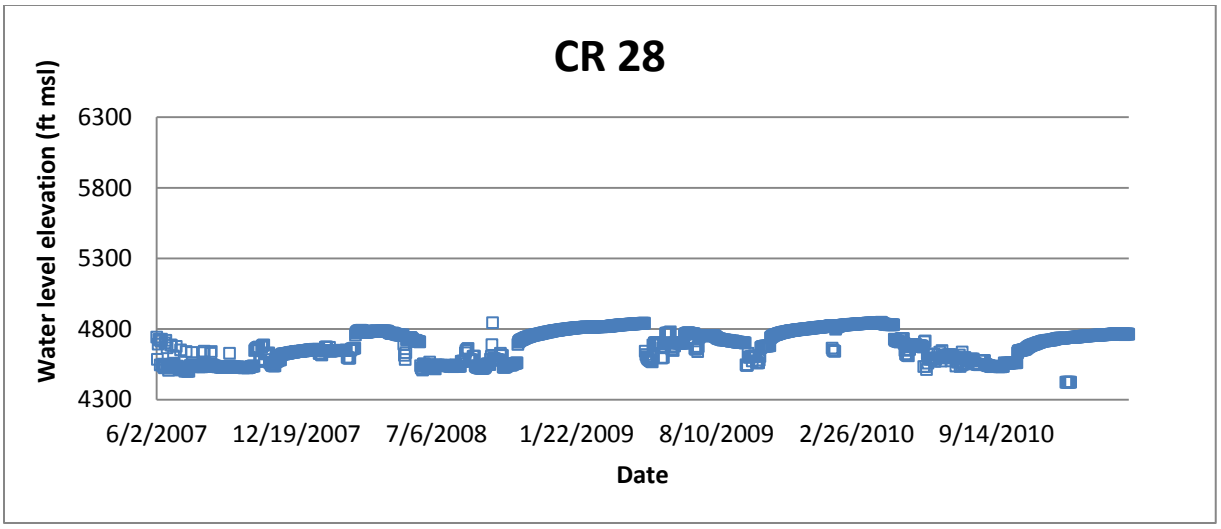
CR 28
Water level elevation (ft msl)
6300
5800
5300
4800
4300
6/2/2007
12/19/2007
7/6/2008
1/22/2009
8/10/2009
2/26/2010
9/14/2010
Date

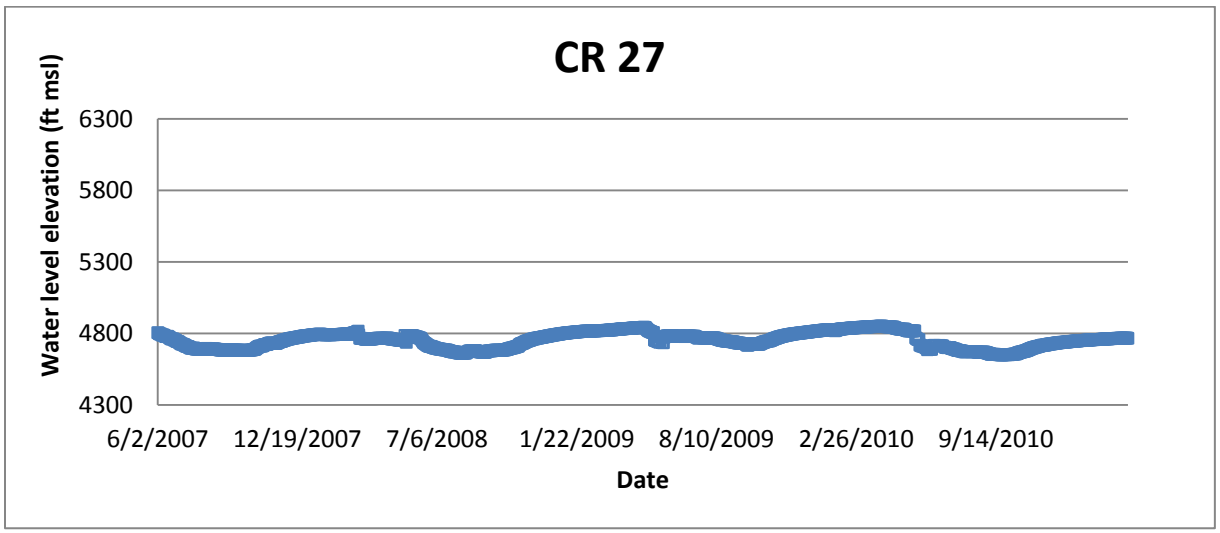
CR 27
Water level elevation (ft msl)
6300
5800
5300
4800
4300
6/2/2007
12/19/2007
7/6/2008
1/22/2009
8/10/2009
2/26/2010
9/14/2010
Date

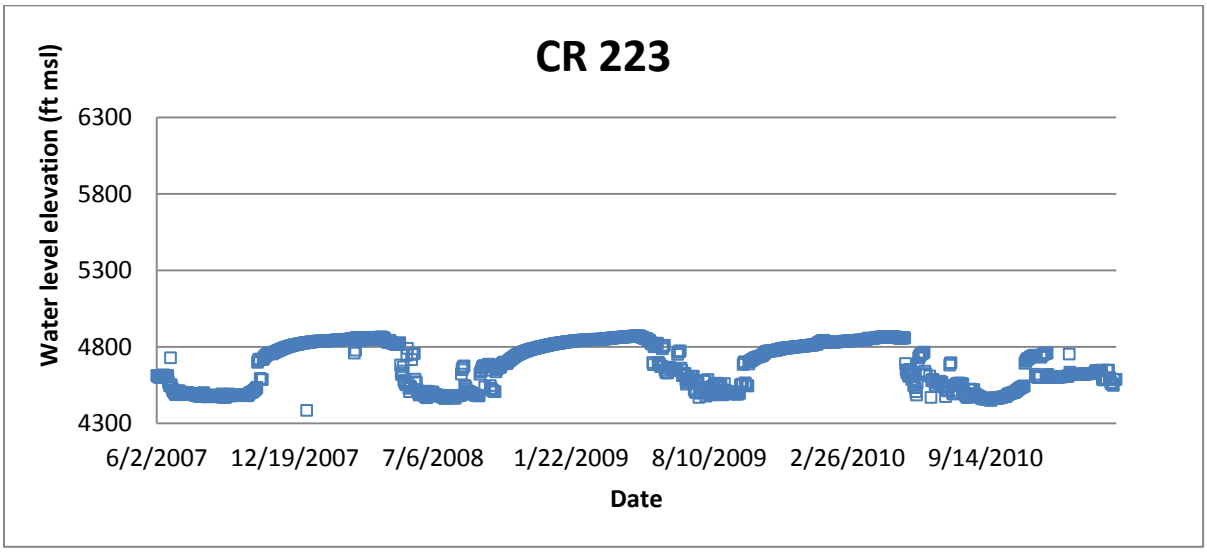
CR 223
Water level elevation (ft msl)
6300
5800
5300
4800
4300
6/2/2007
12/19/2007
7/6/2008
1/22/2009
8/10/2009
2/26/2010
9/14/2010
Date

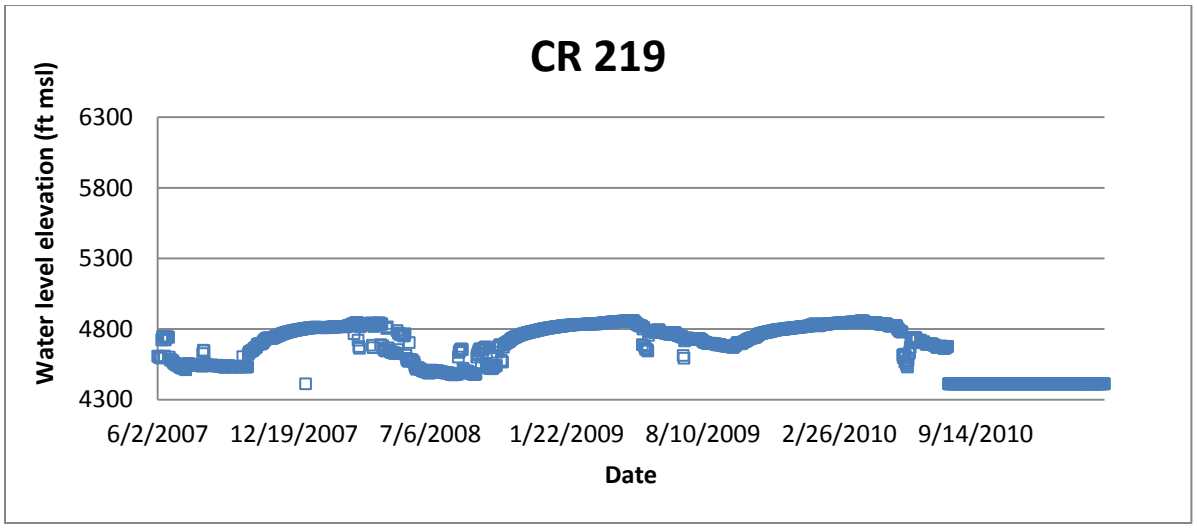

Figure 2.27: Water-level change in each well at the Meadows Pumping Center, CO.

Owing to increased demands on groundwater and increased drawdowns, technologies that use recharge options, such as aquifer storage recovery (ASR), are being used to optimize available water resources and reduce adverse effects of pumping (Lowry and Anderson, 2006). Understanding the movement of injected water can help increase the recovery efficiency, described as the percentage of water that can be recovered after injection (Lowry and Anderson, 2006).

In this study, particle tracking under dynamic pumping and injection conditions are both considered. Because there is no injection data provided, the data used for injection are assumed. Also, the injection process can be treat as the inverse process of pumping, so the injection rate in the well field is set as the negative pumping rate. Specifically, in this research, particle tracking under continuous pumping and injection conditions are studied over two periods, which are over 130 days and 6000 days, respectively. And for 130 days period, the pumping rate is 244 gal/min and injection rate is -144 gal/min. For 6000 days period, the pumping rate is 244 gal/min and injection rate is -244 gal/min. The pumping and injection rates employed in the research correspond to their periods are shown in Figure 2.28 and 2.29.

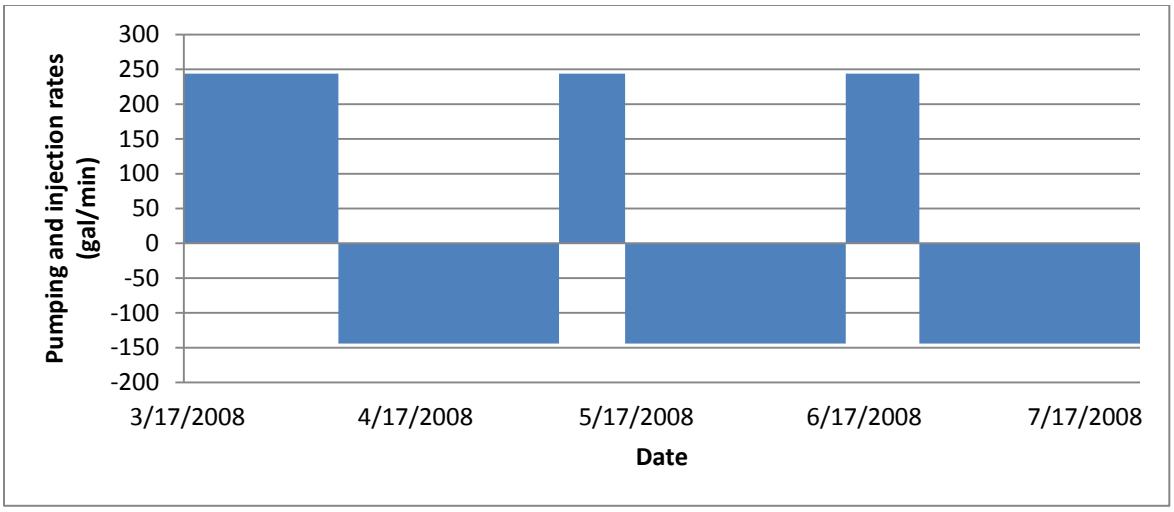

Figure 2.28: Pumping and injection rates employed for particle tracking over 130 days under continuous pumping and injection conditions at the Meadows Pumping Center, CO.

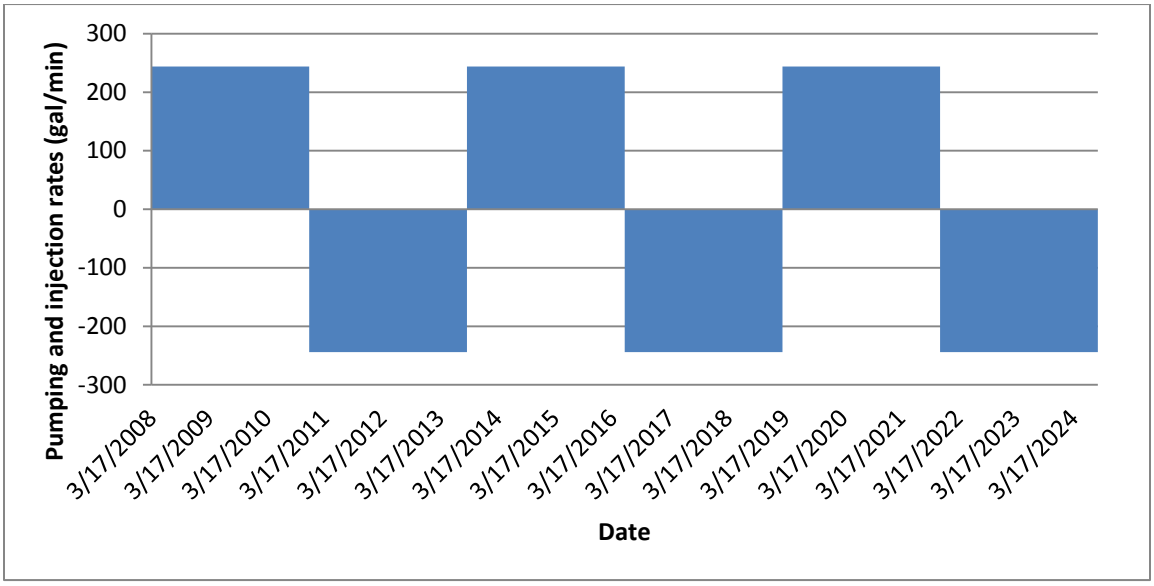

Figure 2.29: Pumping and injection rates employed for particle tracking over 6000 days under continuous pumping and injection conditions at the Meadows Pumping Center, CO.

CHAPTER 3 – METHODS

Numerical models have been widely employed to track the movement of fluid particles (e.g., Yidana, 2010; Shamsuddin et al., 2014). Unfortunately, numerical models, depending on spatial and temporal discretization, may not be able to capture dynamic aspects of groundwater flow for complex water surface with dynamic water levels. Analytical methods are useful techniques that can be applied to many ground water flow problems, including estimation of time-related capture areas of wells in hydrogeologic settings with predominantly two-dimensional flow regimes. These methods also may represent the most appropriate technology to use in the early development of a wellhead-protection strategy in complex hydrogeologic settings (Bair et al., 1991). This research provides a novel method to predict the movement of subsurface fluid particles or contaminants at field sites and in pumping well fields.

The basic idea for tracking fluid particles is: particles are placed in the system at an initial position, x_0, y_0, at an initial time, t_0. The position of the particles at any later time, t, is computed by solving the equations defined by the seepage velocity $v_x = q_x/\varphi = dx/dt$, and $v_y = q_y/\varphi = dy/dt$, where φ is the effective porosity and q_x and q_y are Darcy velocity in the *x* and *y* direction, respectively (Perini and Wilson, 1991). Two general approaches are applied in this thesis. The first approach centers on using continuous-field water-level data obtained using pressure transducer data from monitoring wells. Three or more wells are used to resolve the plane of the groundwater surface below an area of interest at a prescribed time (Figure 3.1). Gradients in the *x* and *y* directions are employed in resolving the movement of fluid particles over a defined period of time. For each time step, the plane of the potentiometric surface is resolved, and transport vectors are added to one another, head to tail.

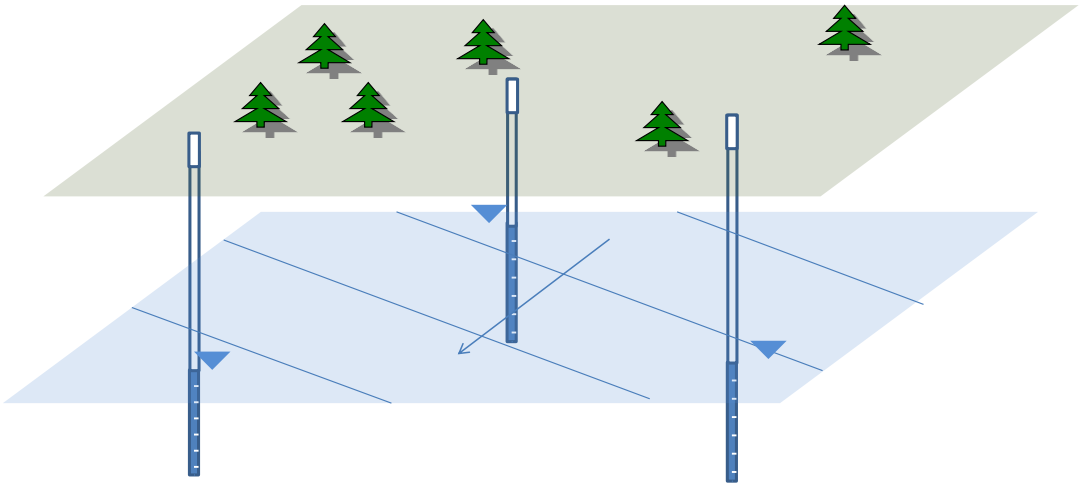

Figure 3.1: Three wells used to resolve the plane of the groundwater surface below an area of interest.

The second approach relies on a Theis superposition model for well fields developed by Davis (2013). The analytical solution is used to resolve the hydraulic gradient through a point of interest at a specified time. Figure 3.2 illustrates a potentiometric surface proven using the Theis superposition model. Potentiometric surface can be used to resolve hydraulic gradient. As with the field data approach, hydraulic gradients in the *x* and *y* directions are employed in resolving the movement of fluid particles over a defined period of time. For each time step, the hydraulic gradient at the point of interest is resolved, and transport vectors are added to one another, head to tail.

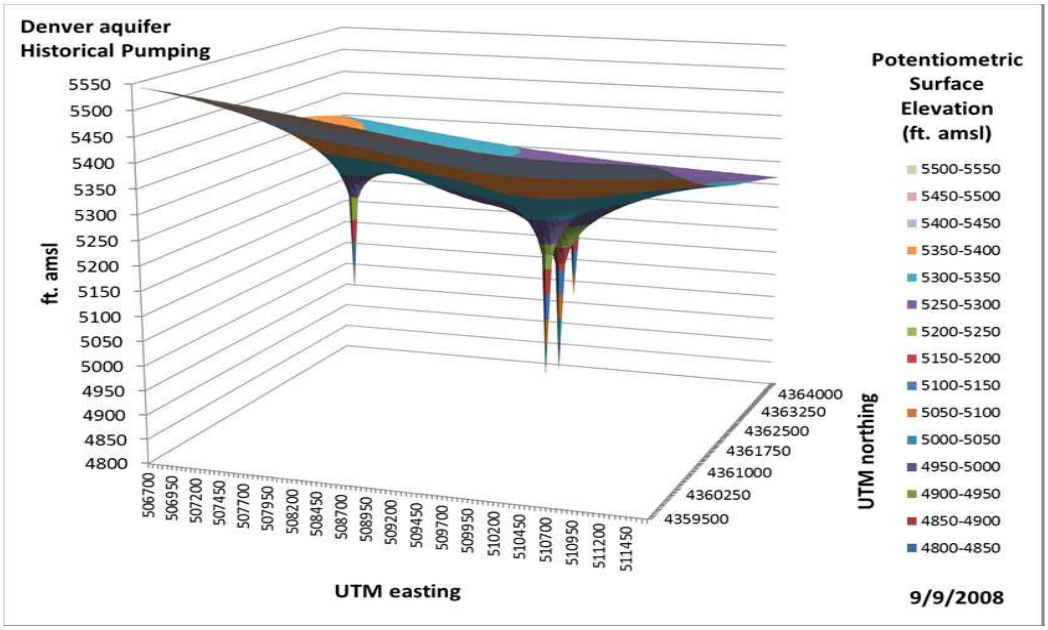

Figure 3.2: Groundwater surface at pumping conditions at a well field in the Denver aquifer (Davis, 2013).

3.1 Application of Darcy's Law

Darcy's Law is used to resolve the movement of a particle in *x*, *y*, and *z* directions. Assuming a homogeneous and anisotropic material (Domenico and Schwartz, 1997):

$$q_x = -K_{xx}\frac{\partial h}{\partial x} - K_{xy}\frac{\partial h}{\partial y} - K_{xz}\frac{\partial h}{\partial z} \tag{3.1}$$

$$q_y = -K_{yx}\frac{\partial h}{\partial x} - K_{yy}\frac{\partial h}{\partial y} - K_{yz}\frac{\partial h}{\partial z} \tag{3.2}$$

$$q_z = -K_{zx}\frac{\partial h}{\partial x} - K_{zy}\frac{\partial h}{\partial y} - K_{zz}\frac{\partial h}{\partial z} \tag{3.3}$$

where, q is the Darcy velocity [L/T], K is hydraulic conductivity[L/T], h is hydraulic head [L], *x*, *y*, and *z* are the positions [L]. In this form, there are nine components of the

hydraulic conductivity in an anisotropic material. These components can be placed in matrix form to give what is known as the "*hydraulic conductivity tensor*" (Domenico and Schwartz, 1997):

$$K = \begin{bmatrix} K_{xx} & K_{xy} & K_{xz} \\ K_{yx} & K_{yy} & K_{yz} \\ K_{zx} & K_{zy} & K_{zz} \end{bmatrix} \tag{3.4}$$

Assuming that the principal directions of anisotropy coincide with the *x*, *y*, and *z* directions of the coordinate axes, the six components K_{xy}, K_{xz}, K_{yx}, K_{yz}, K_{zx}, and K_{zy} are all equal to zero. In this case, Equation 3.4 is simplified as (Domenico and Schwartz, 1997):

$$K = \begin{bmatrix} K_{xx} & 0 & 0 \\ 0 & K_{yy} & 0 \\ 0 & 0 & K_{zz} \end{bmatrix} \tag{3.5}$$

In this research, only flow in the *x* and *y* directions is considered. Therefore, for homogeneous and anisotropic conditions in this research, Equation 3.4 is simplified to:

$$K = \begin{bmatrix} K_{xx} & 0 \\ 0 & K_{yy} \end{bmatrix} \tag{3.6}$$

3.2 Particle Tracking Under Homogeneous and Isotropic Conditions

For homogeneous and isotropic conditions, where the material properties do not differ with direction

$$K = K_{xx} = K_{yy} \tag{3.7}$$

The homogeneous and isotropic form of Darcy's law is

$$q = -K\frac{dh}{dl} \tag{3.8}$$

where, l is the position in the direction of flow [L]. The seepage velocity [L/T] is

$$v = \frac{q}{\varphi} = \frac{-K\frac{dh}{dl}}{\varphi} \tag{3.9}$$

where, φ is effective porosity [dimensionless].

This research uses field data from three or more wells at a time interval (i). A regression is performed to obtain a solution for the plane of the potentiometric surface or water table elevation (h):

$$h(x,y)_i = A_i x + B_i y + C \tag{3.10}$$

where, x and y is a position of interest, A is the gradient of head in the *x* direction [dimensionless], B is the gradient of head in the *y* direction [dimensionless], and C is a constant defined as the elevation of the water table at *(0,0)* [L], and *i* is the time interval.

The driving force for the groundwater flow is the hydraulic gradient. Given the plane of the potentiometric surface/water table elevation in this research, gradients in the *x* and *y* directions can be resolved for specified time intervals. For homogeneous and isotropic conditions, the positions of particle moving at each time step *i* are

$$x_{i=0} = x_{initial}, \text{ and } y_{i=0} = y_{initial} \tag{3.11}$$

When taking a particle forward in time:

$$x_{i+1} = x_i + \Delta x_i, \text{ and } y_{i+1} = y_i + \Delta y_i \tag{3.12}$$

where

$$\Delta x_i = v_x \Delta t_i = \frac{-KA_i}{\varphi}\Delta t_i, \text{ and } \Delta y_i = v_y \Delta t_i = \frac{-KB_i}{\varphi}\Delta t_i \tag{3.13}$$

where, Δt = time [T], v_x and v_y is the seepage velocity for the x and y directions, respectively [L/T].

Finally, the movement of a fluid particle is resolved by plotting the position of the fluid particle through time. The model is used to evaluate how particle moves: (1) in an aquifer adjacent to a large river with seasonable changes, (2) in a shallow aquiver with precipitation and evapotranspiration, and (3) near a tidal harbor under homogeneous and isotropic conditions over a specific time period. The model code at each site is presented in Appendix A, B, and C.

3.3 Particle Tracking by Continuous Water Level Data under Homogeneous and Anisotropic Conditions with Retardation

For homogeneous and anisotropic conditions, the velocity of the particle in the *x* direction, v_x is shown below:

$$v_x = \frac{-K_x A_i}{\varphi} \tag{3.14}$$

where, K_x is the hydraulic conductivity or LNAPL conductivity in the x direction [L/T]. The velocity of the particle in y direction, v_y is as below:

$$v_y = \frac{-K_y B_i}{\varphi} \tag{3.15}$$

where, K_y is the hydraulic conductivity or LNAPL conductivity in y direction [L/T].

The positions of particles moving under homogeneous and anisotropic conditions at each time step are calculated as follows,

$$x_{i=0} = x_{initial}, \text{ and } y_{i=0} = y_{initial} \tag{3.16}$$

$$x_{i+1} = x_i + \Delta x_i, \text{ and } y_{i+1} = y_i + \Delta y_i \tag{3.17}$$

where,

$$\Delta x_i = v_x \Delta t_i = \frac{-K_x A_i}{R\varphi} \Delta t_i, \text{ and } \Delta y_i = v_y \Delta t_i = \frac{-K_y B_i}{R\varphi} \Delta t_i \tag{3.18}$$

where, R is the retardation factor.

The data used in the model are described in Chapter 2. The model is used to evaluate how particle moves in three sites under homogeneous and anisotropic conditions with retardation over a specific time period. The first site is in an aquifer adjacent to a large river with seasonal changes. The second one is in a shallow aquiver with precipitation and evapotranspiration. And the third one is near a tidal harbor. The model for particle tracking for each site is shown in Appendix A, B, and C, respectively. For each site, inputs to the model are presented in Chapter 2. The model employed the following equation to calculate a retardation factor:

$$R = 1 + \frac{K_{oc} f_{oc} \rho_b}{\varphi}$$

(3.19)

where, K_{oc} is the partition coefficient [L^3/M], f_{oc} is the weight fraction of organic carbon [dimensionless], ρ_b is bulk density [M/L^3], and φ is porosity [dimensionless]. Every contaminant has a specific K_{oc}. Benzene and RDX are considered in this study as described in Chapter 2. Values of hydraulic conductivity, porosity, fraction organic carbon, and bulk density depend on the specific geological conditions at each site. Values of partition coefficient are fixed for specific contaminants. Note, because in a equivalent system, where the velocities of groundwater and contaminant are the same, there is no influence of retardation on the contaminant transport. Therefore, use of *R* values greater than 1 are only applicable to circumstances where the contaminant is advancing into media that has not been previously contacted by contaminants.

3.4 Modeling of Time for the Degradation of Contaminants

It is assumed that the degradation of a subsurface contaminant follows the pseudo first-order kinetic reaction. The following equation was employed in the model:

$$C_i = C_0 e^{-k \sum_{i=0}^{n} \Delta t_i}$$

(3.20)

where, C_i is the concentration at the time interval i [M/L^3], C_0 is the initial concentration[M/L^3], k is rate constant[T^{-1}], and Δt_i is the i^{th} time interval [T].

As described in Chapter 2, different sites have different contaminants, so the value of the rate constant depends on the specific contaminant. In this research, the requirement of minimum concentration of subsurface contaminant at each site is assumed to be 0.005 mg/L, and the kinetic reaction of the degradation of the contaminant at each site is assumed to be the first-order.

Retardation and transport are evaluated so long as $C > 0.005$ mg/L. The programming code that implements the analytical model at each site is provided in Appendix A, B, and C.

3.5 Method to Calculate Conductivity of LNAPL

There are two fluids contained in the saturated zones at Honolulu, HI, including groundwater and LNAPL. The following equations are used to resolve LNAPL conductivity.

$$K_w = \frac{kk_{rW}\rho_W g}{\mu_W} \text{ and } K_{LNAPL} = \frac{kk_{rLNAPL}\rho_{LNAPL} g}{\mu_{LNAPL}} \tag{3.21}$$

where, K_w and K_{LNAPL} are the hydraulic conductivity of groundwater and conductivity of LNAPL [L/T], k is the permeability of the porous medium [L^2]. k_{rW} and k_{rLNAPL} are the relative permeabilities to water and LNAPL [dimensionless]. k_{rW} and k_{rLNAPL} are assumed to be 1 and 0.1 in this research, respectively. ρ_W and ρ_{LNAPL} are the densities of water and LNAPL at 20℃ [M/L^3], which are 62.43 lb/ft^3 and 54.31 lb/ft^3, respectively. μ_W and μ_{LNAPL} are viscosities of water and LNAPL at 20℃ [M/L/T], which are 1.002 mPa·s, and 0.652 mPa·s, respectively, and g is the gravitational acceleration [L/T^2]. Further, by transferring the equation of K_w, permeability of the porous medium (k) can be obtained.

$$k = \frac{K_w \mu_W}{k_{rW}\rho_W g} \tag{3.22}$$

Then, put the values of permeability of the porous medium (k) to the following equation,

$$K_{LNAPL} = \frac{K_w k_{rLNAPL}\mu_W \rho_{LNAPL}}{k_{rW}\rho_W \mu_{LNAPL}} \tag{3.23}$$

the results of conductivity of LNAPL can be obtained, which is 4.39×10^{-7} ft/sec.

3.6 Particle Tracking in a Well Field Using Analytical Solution

Analytical methods are useful tools that can be applied to many groundwater flow problems, including estimation of travel time-related capture areas of wells in hydrogeologic settings with predominantly two-dimensional flow regimes (Bair et al., 1991). Davis (2013) established a Theis superposition model under the assumptions used in the development of the Theis equation. This equation can successfully predict drawdown produced by multiple wells in well fields that are cycled on and off. Dynamic water-level data are through time with time-variant flow rates obtained using the Theis superposition model. Davis (2013) provides more than three years of hourly water levels and pumping rate data from operational well fields in Castle Rock, CO. Further Davis (2013) input well locations, pumping times associated with flow rates, as well as variables including transmissivity, storativity, natural slope of the potentiometric surface, and individual well loss constants into the Theis superposition model to calculate the drawdowns for all of its operational wells for more than a three-year period. Based on the Theis superposition model (Davis, 2013), this research developed a new analytical model to track particle under dynamic pumping conditions. The code that implements the analytical model is provided in Appendix D.

Following Davis (2013), the dynamic water head values are resolved as a function of position and time using superposition of the Theis solution in time and space for multiple wells with transient pumping. Inclusive to the methods of Davis (2013) is consideration of a regionally sloping potentiometric surface. Lewis et al. (2015) presents additional developments for temporal and spatial superposition of the Theis solution for analysis of water levels in well fields. Head can be calculated by employing the static water surface elevations (Davis, 2013) minus the drawdown at any time,

$$h(x,y,t)_i = A_i x + B_i y + C - \sum_{j=1}^{n}\sum_{i=1}^{m} s(x,y,t)_{ij} \tag{3.24}$$

and

$$t = t_{initial} + i\Delta t \tag{3.25}$$

where, *n* is the total number of wells, *m* is the total number of time steps. *i* is the number of time step, and *j* is the number of well. $t_{initial}$ is the initial time when particles start to move [T]. s_{ij} is the drawdown at time step *i* in the well *j* [L].

Applying this solution to the finite difference method, the hydraulic gradient is the difference of hydraulic head at two points adjacent to each other at any time divided by the distance between these the two points (Figure 3.3). Hydraulic gradients in the *x* and *y* directions are used to drive particles based on hydraulic conductivity values. The equations are as below:

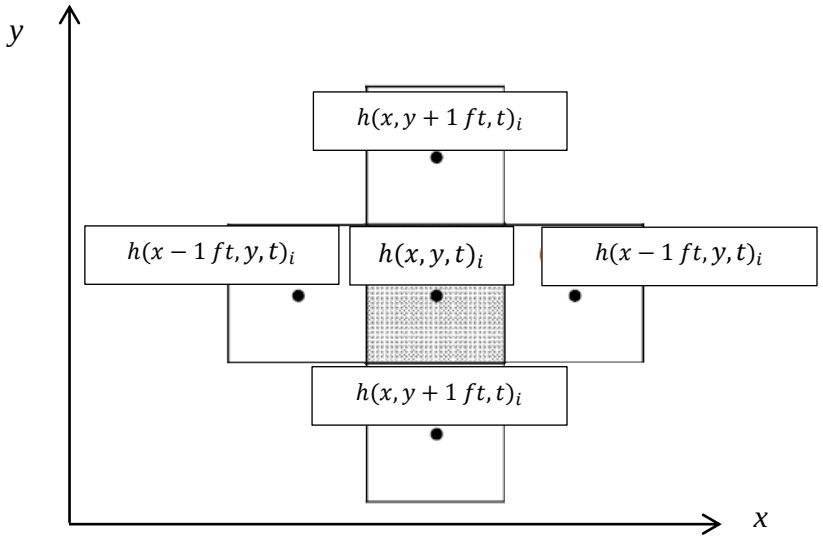

Figure 3.3: Hydraulic gradients at points adjacent to each other in *x* and *y* directions in a homogeneous, isotropic aquifer.

$$A_i = \frac{h(x - 1\ ft, y, t)_i - h(x + 1\ ft, y, t)_i}{2\ ft}$$

(3.26)

$$B_i = \frac{h(x, y - 1\ ft, t)_i - h(x, y + 1\ ft, t)_i}{2\ ft}$$

(3.27)

where, $h(x - 1\ ft, y, t)_i, h(x + 1\ ft, y, t)_i, h(x, y - 1\ ft, t)_i$, and $h(x, y + 1\ ft, t)_i$ are the two hydraulic head at two points off set by 2 ft on either side of the point of at time interval i respectively [L] (Figure 3.3).

The use of points 2 ft about the position of interest is based on a desire to accurately capture the local gradient, while not being close enough to the point of interest to introduce errors in the local gradient associated with computational accuracy of the method employed by Davis (2013) for estimating values of the well function.

According to Darcy's law and employing a succession of steady states, as with the field data approach, the initial positions of particle moving when time started are:

$$x_{i=0} = x_{initial}, \text{ and } y_{\ i=0} = y_{initial}$$

(3.28)

When taking a particle forward in time:

$$x_{i+1} = x_i + \Delta x_i, \text{ and } y_{i+1} = y_i + \Delta y_i$$

(3.29)

where

$$\Delta x_i = \frac{-T}{b\varphi} A_i \Delta t_i, \text{ and } \Delta y_i = \frac{-T}{b\varphi} B_i \Delta t_i$$

(3.30)

where, T is transmissivity [L^2/T], b is aquifer thickness [L]. The code designed to illustrate how groundwater flows under dynamic pumping conditions in a well field over a specific time period, is shown in Appendix D.

3.7 Methods to Measure Water-level and LNAPL Elevation Data

In this research, most of the data are collected from corporations, institutes and researchers. Description of how to measure water-level and LNAPL elevation data presented in the following can help better understand the way the data worked in the results.

3.7.1 Methods to Resolve Head

Head is a primary input for dynamic particle tracking. When collecting field data, as an example, level logger (Solinst®) is submerged and recorded the combination of barometric pressure and water pressure. The actual pressure of only water above the sensor of the level logger (Solinst®) is obtained by subtracting barometer pressure from the total pressure (Figure 3.4 and Solinst, 2014). Subsequently, water-level can be obtained by transferring the actual pressure as following equation shows.

$$W_{telev} = TOC - DTT_P + \frac{P_w}{\rho_w g} \tag{3.31}$$

where, *TOC* is the elevation of top of casing [L], DTT_P [L] is the depth to the pressure transducer below the *TOC*, P_w [$M/T^2/L$] is the water pressure measured by the pressure transducer, ρ_w [M/L^3] is the density of water, and g is the gravitational constants [L/T^2].

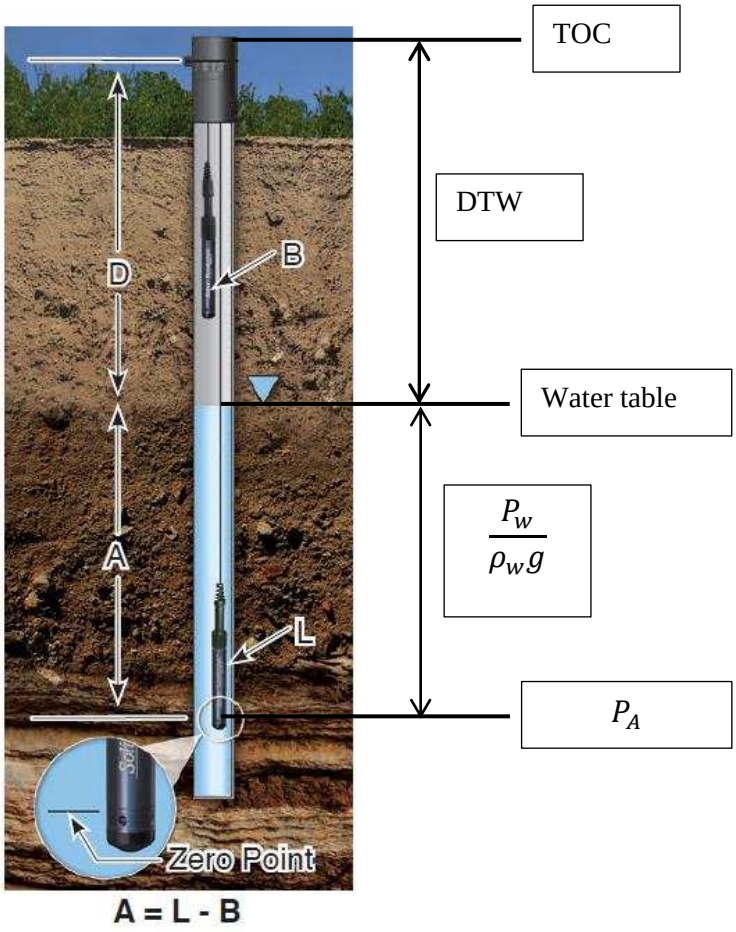

Figure 3.4: Level Logger measurement fundamentals (Solinst, 2014). (A = actual water column height, B = barometric pressure, L = level logger total pressure readings, and D = depth to water level, below reference datum)

As described in Chapter 2, water-level data are not completed for Kansas City, MO, and Pueblo, CO in this research. Furthermore, there are no injection rates for the Meadows Pumping Center, CO. The methods to treat missing data for Kansas City, MO and Pueblo, CO are skipping them. For the injection rates, it was assumed based on the pumping rates which were provided by the Meadows Pumping Center, CO.

3.7.2 Methods to Calculate Water-level and LNAPL Elevation at Honolulu, HI

The Honolulu, HI site used the Continuous Fluid Level Monitoring System (CFLMS, Environmental Data Solutions Group, LLC) to measure water level and LNAPL, shown in Figure 3.5. The method to calculate head of groundwater and LNAPL are as follows,

$$h_{water} = TOC - DTW + H_{LNAPL}\frac{\rho_{LNAPL}}{\rho_w} \tag{3.32}$$

$$h_{LNAPL} = TOC - DTO \tag{3.33}$$

where, h_{water} and h_{LNAPL} are head of groundwater and LNAPL [L], DTO is the depth to LNAPL [L], and H_{LNAPL} is the thickness of LNAPL [L].

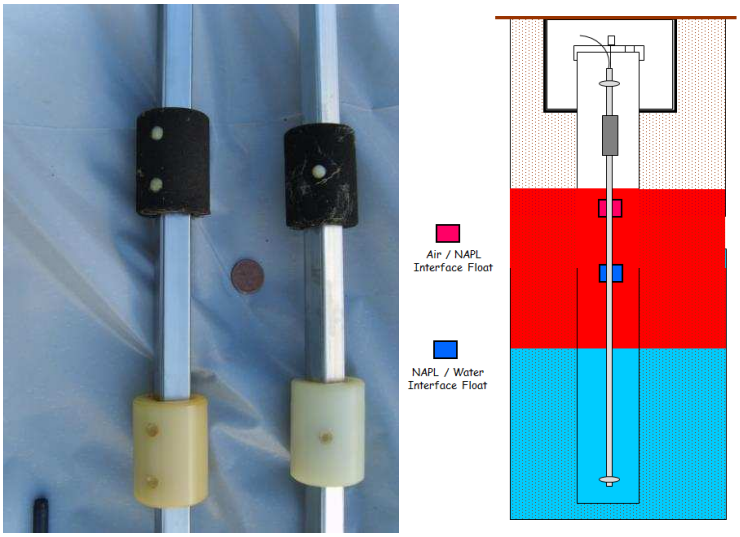

Figure 3.5: Continuous fluid level monitoring system method (CFLMS, Environmental Data Solutions Group, LLC).

CHAPTER 4 – RESULTS AND DISCUSSION

The following presents results and related discussion. First, insights from dynamic particle tracking at field sites are presented. Secondly, insights from dynamic particle tracking at a well field are advanced.

4.1 Continuous Water-Level Data from Field Sites

4.1.1 Kansas City, MO

Table 4.1 provides the quantitative results from four scenarios at the Terminal in Kansas City, MO. Particle tracking under homogeneous and isotropic conditions without reactions at the Terminal in Kansas City, Missouri from the model (see in Appendix A) is shown in Figure 4.1. Figure 4.2 adds a site map and the river hydrograph, so that the position of the particle tracking can be seen with respect to site features and periods of reversals can be correlated to river stage. Furthermore, as described in Chapter 2, because of the missing data, just three water-level peaks marked with red cycles appeared in the hydrograph instead of six peaks. High river stages occur in the middle of 2011 to 2012, 2014 to 2015, and 2015 to 2016 made water-level risen to peaks of Missouri River at Kansas City, MO, so that caused the flow direction of groundwater changed, which are correspond to the three flow direction reversals in the path line as shown in Figure 4.1 and 4.2.

Table 4.1 The distance particle moved in each scenario at Kansas City, MO

Anisotropy	Direction	Retardation	Degradation	Δx (Particle moves in the *x* direction) (ft)	Δy (Particle moves in the *y* direction) (ft)	Total distance (ft)
No	Forward	No	No	1285.14	502.07	1379.73
No	Backward	No	No	1285.14	502.07	1379.73
Yes	Forward	Yes	No	186.25	36.38	189.77
Yes	Forward	Yes	Yes	186.02	36.38	189.54

Because hydraulic gradient is the driving force for groundwater flow, groundwater flow in each direction should be same with the hydraulic gradient direction shown in Figure 2.5. However, as shown in Figure 4.1, groundwater flow at this site is mainly in one direction, from northwest to southeast. Groundwater does not flow as the same change in each direction of hydraulic gradients in this area. The proper explanation for this phenomenon is that the hydraulic gradients with greater magnitude are mainly in the northwest to southeast direction, and hydraulic gradients with small magnitudes are varied in other directions (Figure 2.5). Moreover, time interval for each groundwater flow driven by each hydraulic gradient is the same, according to the Darcy's equation, hydraulic gradient in the direction with small magnitude cannot drive particles flow long enough to make particles flow away from the main direction-northwest to southeast, the direction which is driven by hydraulic gradient with greater magnitude.

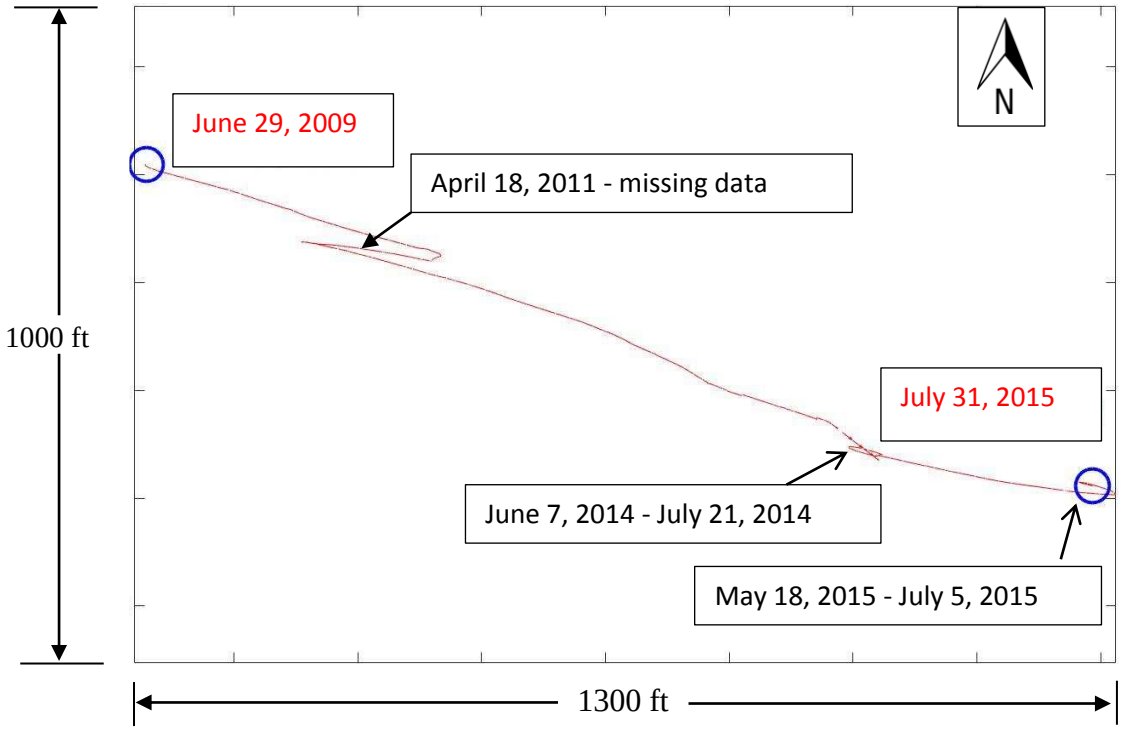

Figure 4.1: Particle tracking under homogeneous and isotropic conditions without reactions at Kansas City, MO.

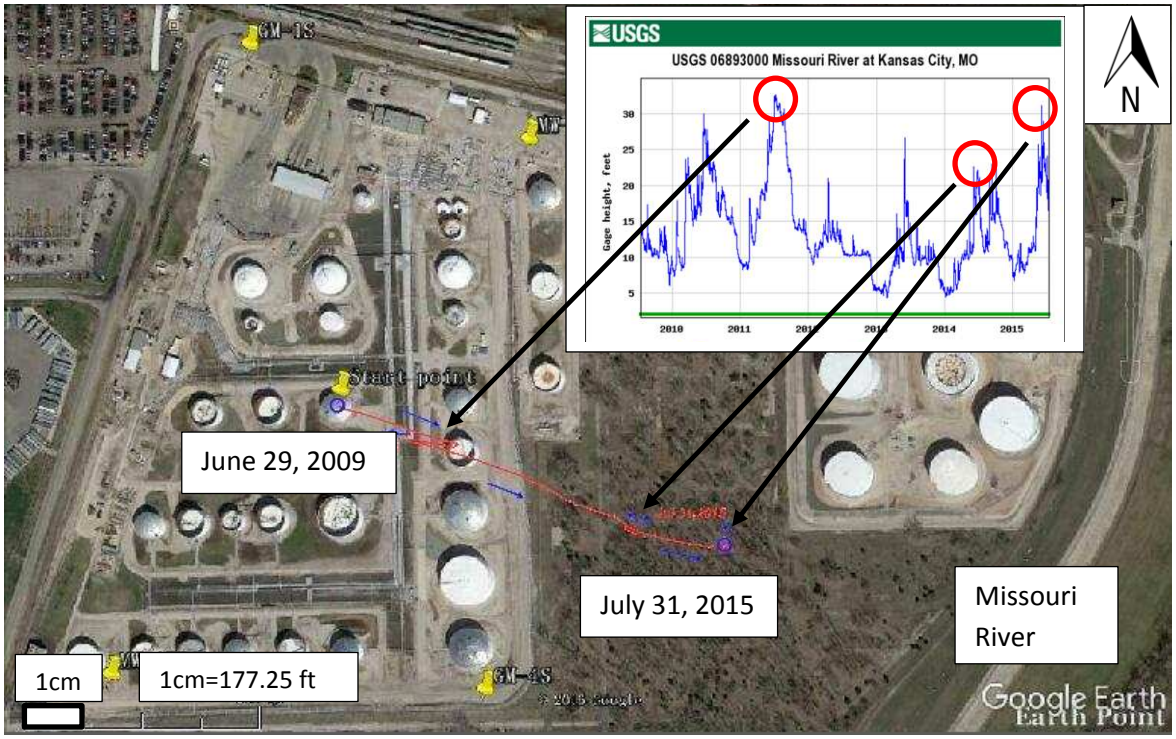

Figure 4.2: Particle tracking on the site map under homogeneous and isotropic conditions without reactions at Kansas City, MO.

Figure 4.3 shows the backward tracking from June 29, 2009 to July 31, 2015 under homogeneous and isotropic conditions without reactions at Kansas City, MO. Under homogeneous and isotropic conditions, for backward tracking, particle flow direction in every part of the aquifer should be the same with each time step of forward tracking. Therefore, the pattern of particle flow path line for backward tracking is the same with the path line for forward tracking. And by using backward tracking, the source of particle can be traced out.

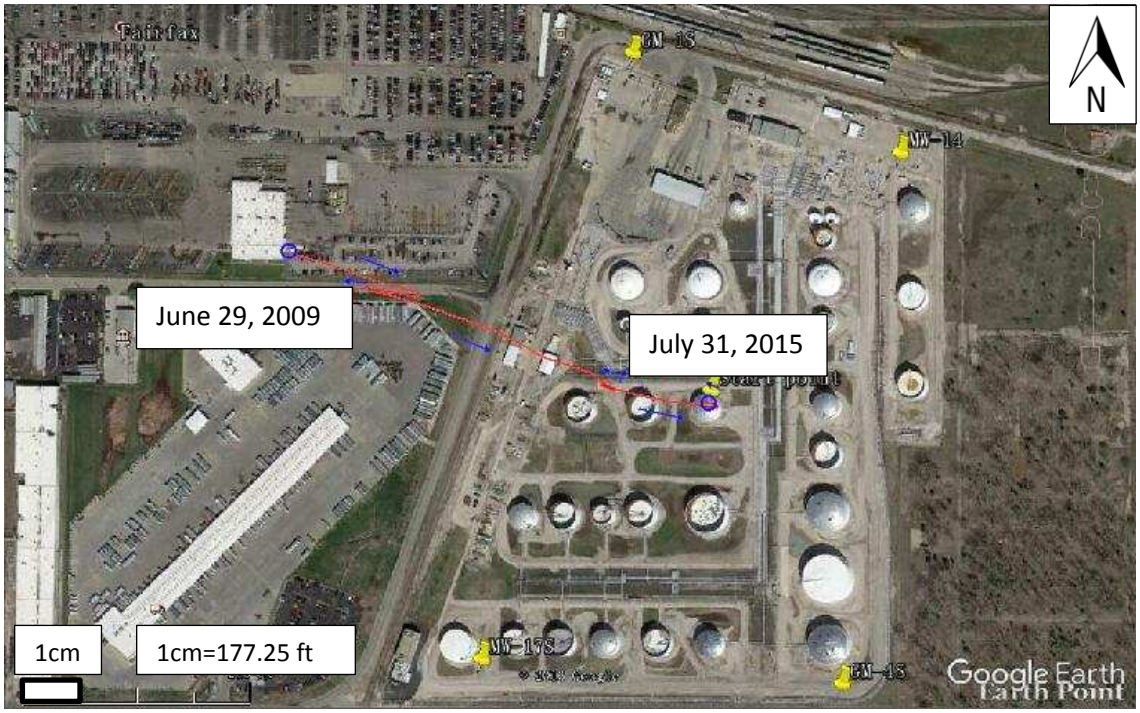

Figure 4.3: Particle tracking on the site map to trace out the source of particles under homogeneous and isotropic conditions without reactions at Kansas City, MO.

Subsurface conditions in the real world are notably more complex. There is no aquifer comprised of only one geologic material so that the permeability in a given direction is the same from point to point (Schwartz and Zhang, 2002). Subsurfaces are not homogeneous, but heterogeneous, composed of layered geological units with variable hydraulic conductivities. Moreover, the sorption of dissolved compounds to aquifer materials 1) reduces the rate at which a contaminant moves on in an aquifer, 2) increases the pumping required to flush compounds out of an aquifer relative to non-sorbing compounds, and 3) can affect transformation rate (Pankow and Cherry, 1996). For more precise predictions to capture analytical processes, consideration is given to homogeneous, anisotropic conditions with retardation factor without reactions. Time period for this condition was also from June 29, 2009 to July 31, 2015.

The result of particle tracking under homogeneous and anisotropic conditions with retardation and without reactions at the Terminal in Kansas City, Missouri from the model (see

in Appendix A) is shown in Figure 4.4. In Figure 4.4, particle flow direction was almost the same as with it under homogeneous and isotropic conditions without reactions. However, due to absorption, particles under homogeneous and anisotropic conditions with retardation and without reactions moved less than under homogeneous and isotropic conditions without reactions (see in Table 4.1). Moreover, because the hydraulic conductivity in the *x* direction is greater than in the *y* direction, the direction of the flow path line was more toward to the *x* direction than under homogeneous and isotropic conditions without reactions.

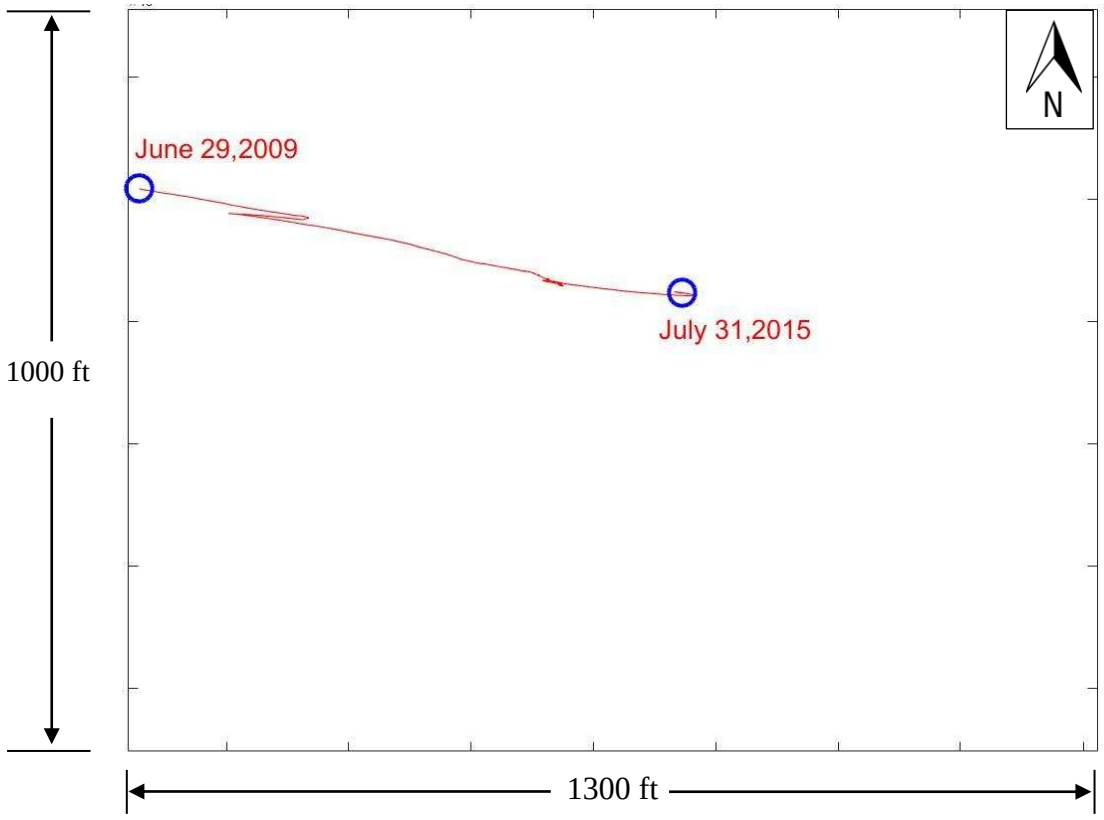

Figure 4.4: Particle tracking under homogeneous and anisotropic conditions with retardation and without reactions at Kansas City, MO.

Degradation of organic contaminants in groundwater can occur naturally, supported by available electron donors, electron acceptors and nutrients, or through human intervention using enhanced or engineered bioremediation technologies (Scow and Hicks, 2005). The model of

kinetic reaction of benzene and the minimum concentration of benzene of local groundwater quality standard are described in Chapter 3. Assuming the initial benzene concentration in the subsurface of this area is 1 mg/L, based on the rate constant of the first order kinetic reaction of benzene (see in Chapter 2) and the code (see in Appendix A), the flow-path line of benzene within the limited concentration in the subsurface under homogeneous and anisotropic conditions with retardation in this area is shown in Figure 4.5. Due to natural attenuation in the subsurface, the concentration of benzene is degraded from 1 mg/L on June 29, 2009 to 0.005 mg/L on May 12, 2015. The path line is a little shorter than the scenario without natural attenuation (Table 4.1 and Figure 4.4).

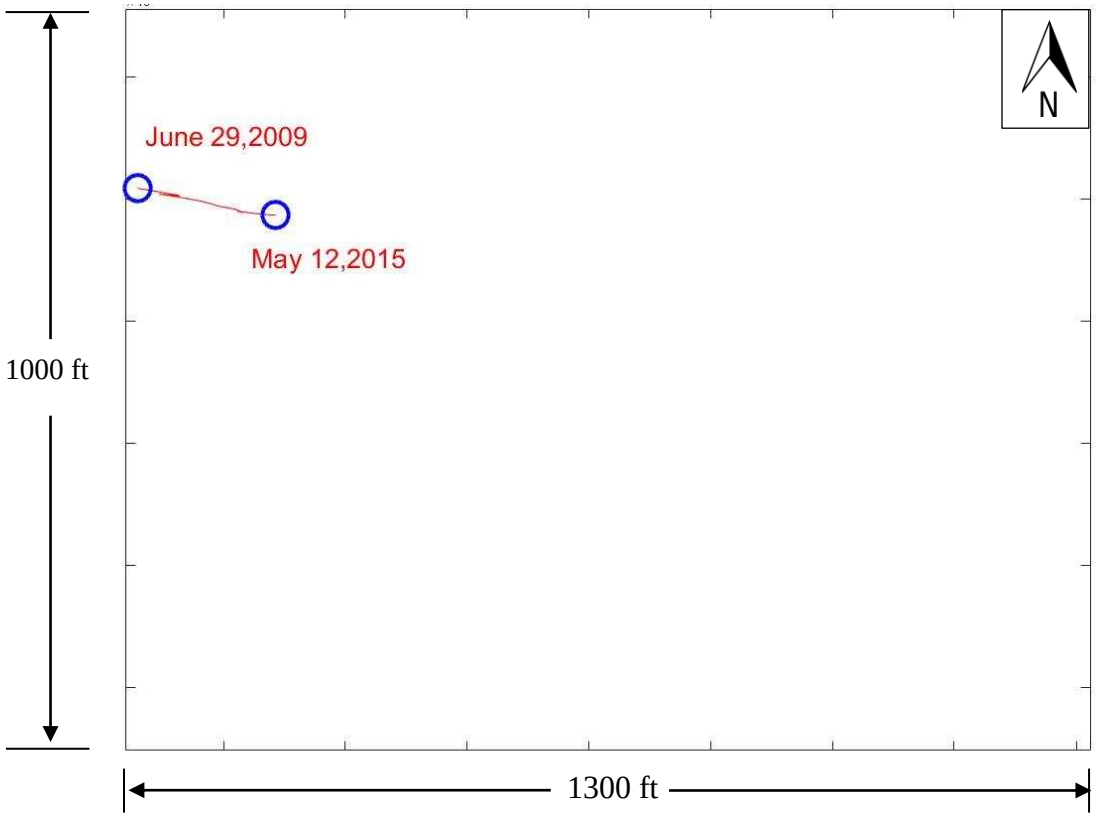

Figure 4.5: Particle tracking under homogeneous and anisotropic conditions with retardation and the first-order degradation at Kansas City, MO.

4.1.2 Particle Tracking at Pueblo Chemical Depot (PCD), CO

Table 4.2 provides the quantitative results from four scenarios at the PCD, CO introduced in the following. In this section, methods for tracking particle at field sites are applied to a site located at Pueblo Chemical Depot, CO. The result of particle tracking under homogeneous and isotropic conditions without reactions at PCD, Colorado from the model (see in Appendix B) is shown in Figure 4.6. As described in Chapter 2, precipitation and transpiration of the vegetations contribute to the water-level changes in this area. From the end of the spring to the summer, transpiration contributes to the water-surface-elevation decline so that the groundwater flow directions are reversed shown in Figure 4.6. From the beginning of fall to the summer, precipitation forces the water surface elevation to rise. This period is much longer so the main groundwater flow is from the northeast to the south west (Figure 4.6). Therefore, although the direction of groundwater flow is mainly from northeast to southwest from March 1, 2006 to September 16, 2008, there are three particle flow changes during this period. Figure 4.7 adds a site map and the hydrograph of the aquifer, so that the position of the particle tracking can be seen with respect to site features and periods of reversals can be correlated to water-level.

Table 4.2 The distance particle moved in each scenario at PCD, CO

Anisotropy	Direction	Retardation	Degradation	Δx (Particle moves in the x direction) (ft)	Δy (Particle moves in the y direction) (ft)	Total distance (ft)
No	Forward	No	No	58.70	83.45	102.03
No	Backward	No	No	58.70	83.45	102.03
Yes	Forward	Yes	No	32.06	22.79	39.33
Yes	Forward	Yes	Yes	9.65	5.79	11.25

As shown in Figure 4.6, groundwater flow at this site is also mainly in one direction, from northeast to southwest. Groundwater also does not flow as the same change in each direction of hydraulic gradients in this area (Figure 2.9). It is because hydraulic gradients with greater magnitude are mainly in the northeast to southwest direction, and hydraulic gradients

vary in other directions they have small magnitudes (Figure 2.9). Moreover, time interval for each groundwater flow driven by each hydraulic gradient is the same, according to the Darcy's equation, hydraulic gradient in the direction with small magnitude cannot drive particles flow long enough to make particles flow away from the main direction-northeast to southwest, the direction which is driven by hydraulic gradient with greater magnitude.

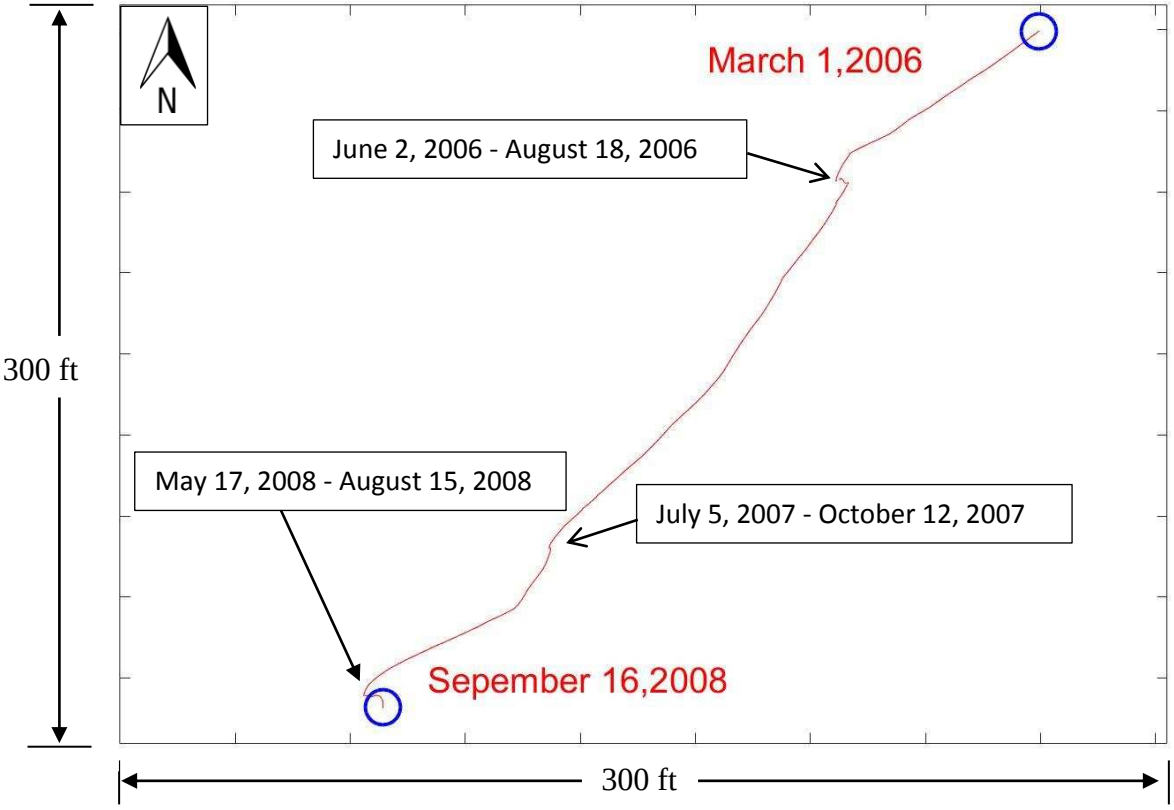

Figure 4.6: Particle tracking under homogeneous and isotropic conditions without reactions at PCD in Pueblo, CO.

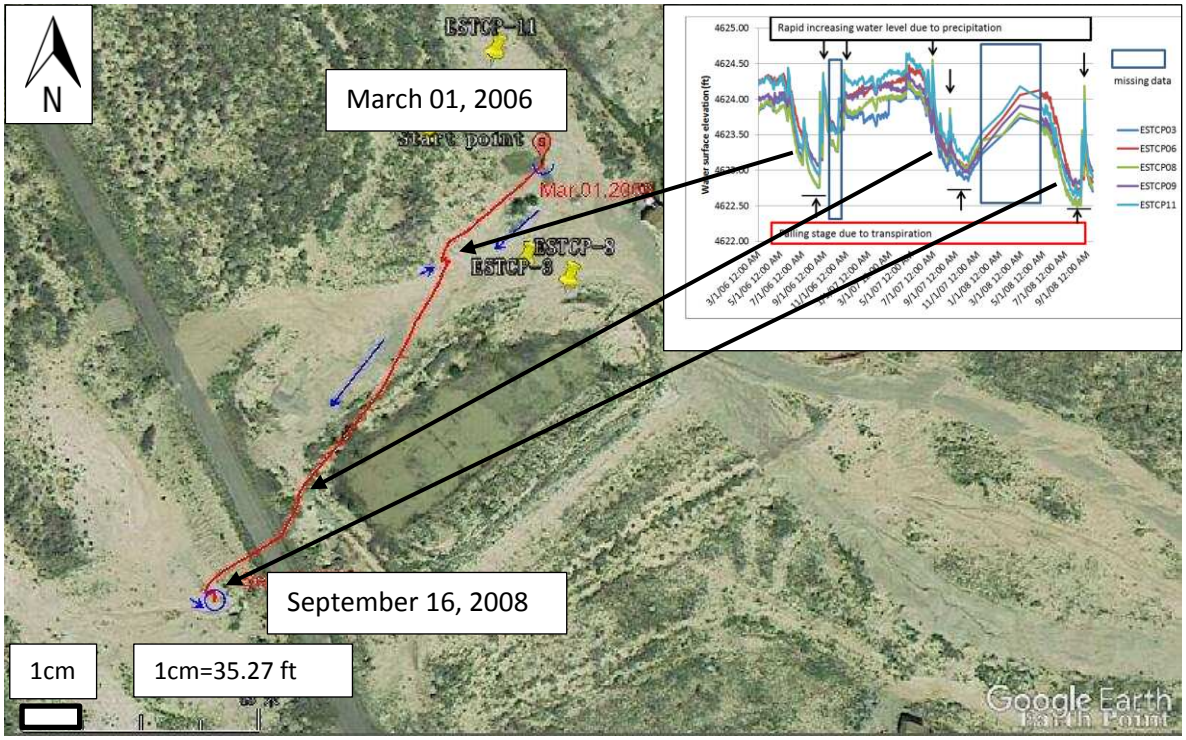

Figure 4.7: Particle tracking on the site map under homogeneous and isotropic conditions without reactions at PCD, CO.

Figure 4.8 shows the backward tracking from March 1, 2006 to September 16, 2008 under homogeneous and isotropic conditions without reactions at PCD, CO. Under homogeneous and isotropic conditions without reactions, for backward tracking, particle-flow direction in every part of the aquifer at PCD, CO should be the same with each time step of forward tracking. Therefore, the pattern of particle flow path line for backward tracking is the same with the path line for forward tracking. And by using backward tracking, the source of particle can also be traced out at PCD, CO.

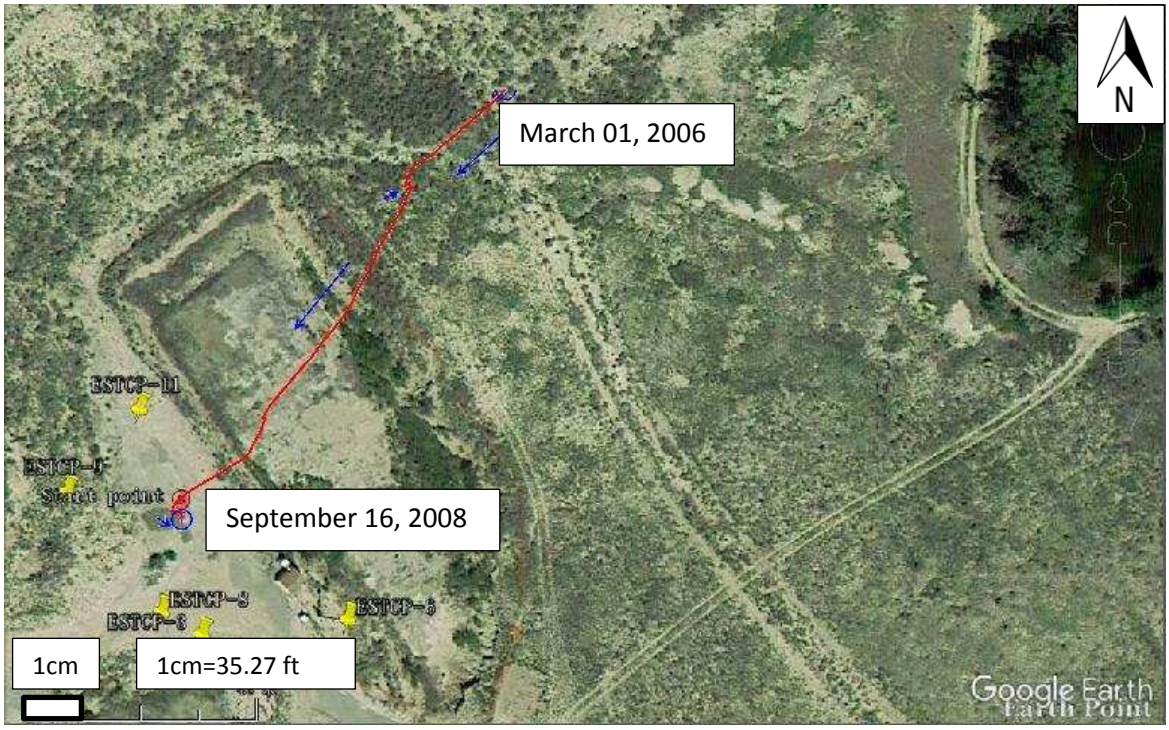

Figure 4.8: Particle tracking on the site map to trace out the source of particles under homogeneous and isotropic conditions without reactions at PCD, CO.

Particle tracking under homogeneous and anisotropic conditions with retardation and without reactions at PCD, CO from the model (see in Appendix B) is shown in Figure 4.9.The period was also from March 1, 2006 to September 16, 2008. In Figure 4.9, similar to the conditions at Kansas City, MO, due to absorption, particles under the homogeneous and anisotropic conditions with retardation and without reactions moved less than under homogeneous and isotropic conditions without reactions (see in Table 4.2).

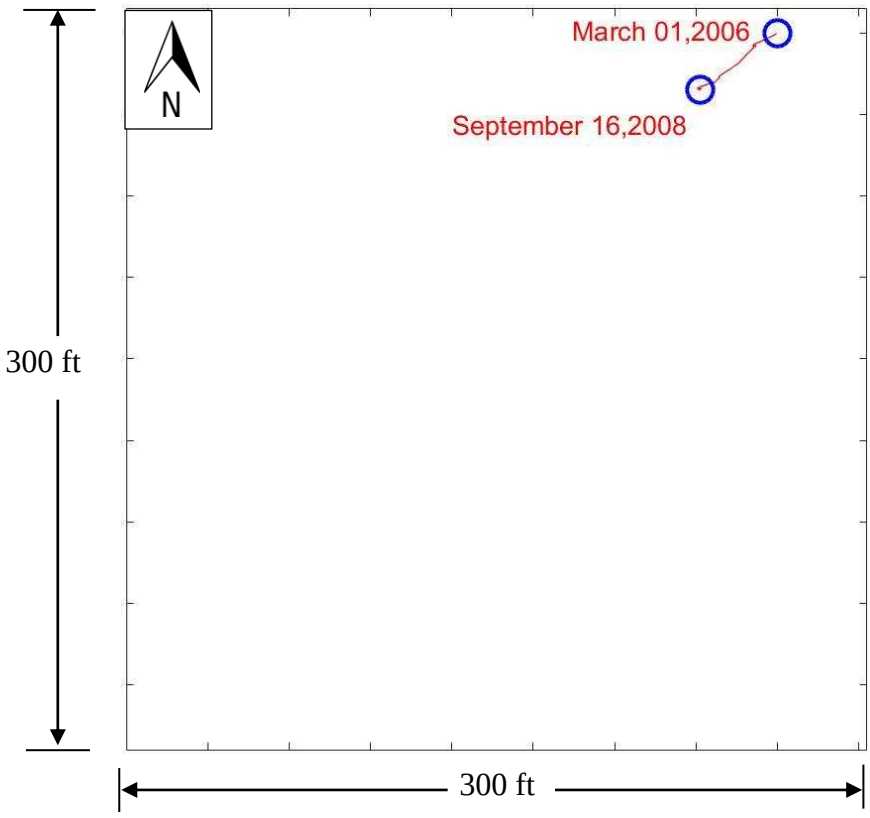

Figure 4.9: Particle tracking under homogeneous and anisotropic conditions with retardation and without reactions at PCD, CO.

At this field site, the model of kinetic reaction of RDX and the minimum concentration of RDX of local groundwater quality standard are described in Chapter 3. Further, assuming the initial RDX concentration in the subsurface of this area is 1000 mg/L, basing the rate constant of the first-order kinetic reaction of RDX (see in Chapter 2) and the code (see in Appendix B), the flow path line of RDX within the limited concentration in the subsurface in this area is shown in Figure 4.10. Due to natural attenuation in the subsurface, the concentration of RDX is degraded from 1000 mg/L on March 1, 2006 to 0.005 mg/L on October 25, 2006. The path line is shorter than the scenario without natural attenuation (Table 4.2 and Figure 4.9).

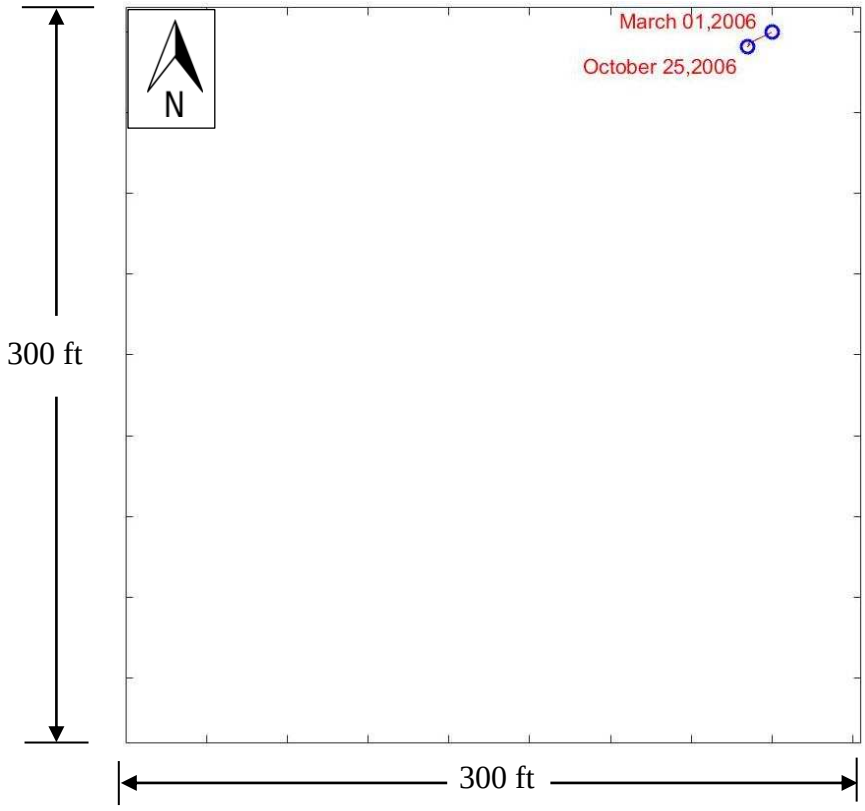

Figure 4.10: Particle tracking under homogeneous and anisotropic conditions with retardation and the first-order degradation at PCD, CO.

4.1.3 Particle Tracking at Honolulu, HI

Groundwater in coastal areas is commonly governed by tidal fluctuations (Tang and Jiao, 2001). For many environmental and engineering problems, understanding the response of groundwater to tidal fluctuation of coastal water is important (Pontin, 1986). In coastal aquifers, the groundwater level (hydraulic head or water table) fluctuates with time in response to the water level fluctuations of the tidal water body (ocean or river) (Li and Jiao, 2002).

The gradients of groundwater and LNAPL for a 39-day period are shown in Figure 4.11. This time period includes 78 high and low tides. The tides are influenced by moon (Figure 2.12). The gradients of two fluids do not exactly follow the changing of tides over this period. For groundwater, the pattern of hydraulic gradients in the *x* direction is similar to the tides (Figure

4.11 (a)). In the *y* direction, the amplitude of the changes in hydraulic gradients are diminished through time (Figure 4.11 (b)). Similarly, for LNAPL, the amplitude of the changes in the gradients in the *y* direction diminishes through time (Figure 4.11 (d)).

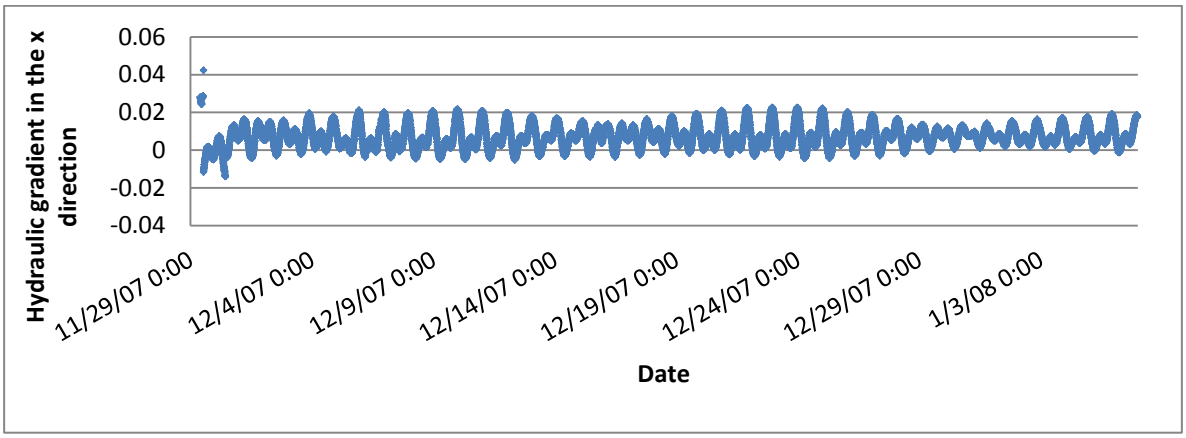

(a)

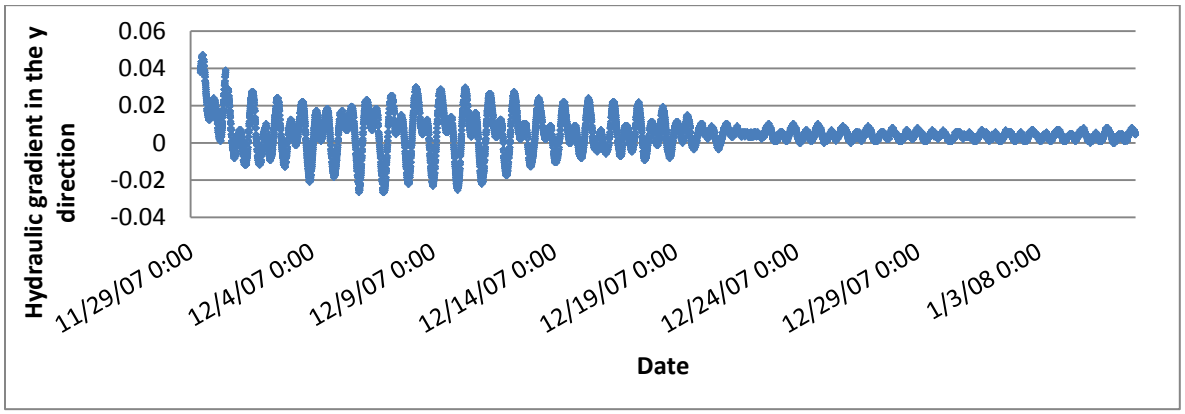

(b)

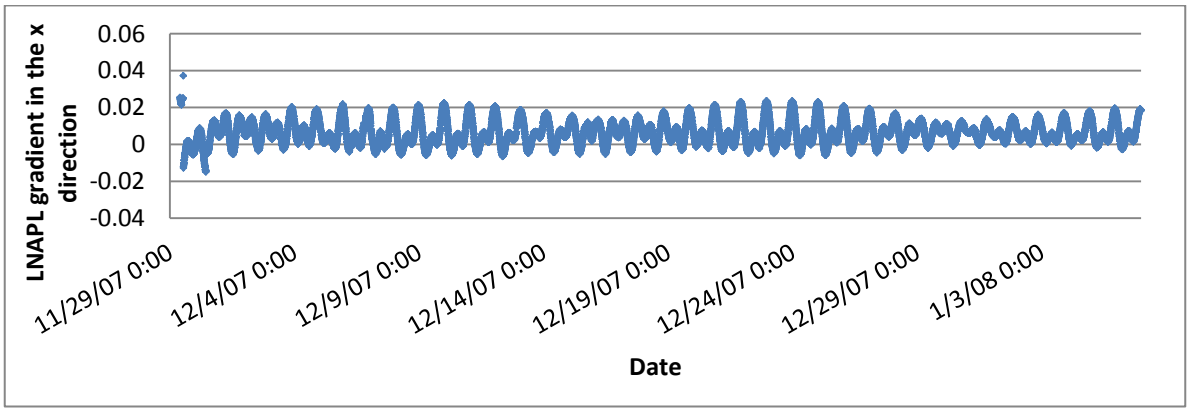

(c)

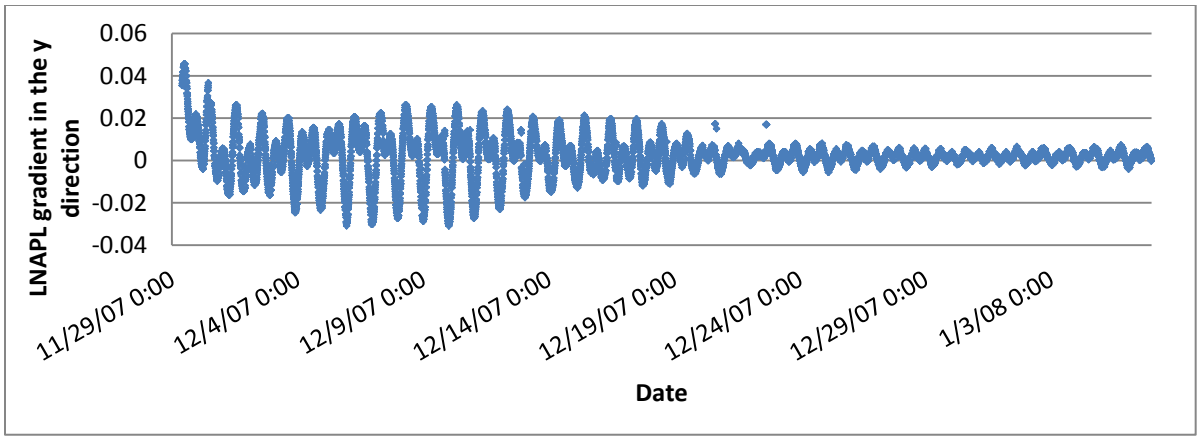

(d)

Figure 4.11: Gradients of groundwater and LNAPL through time. (a) hydraulic gradient of groundwater in the *x* direction; (b) hydraulic gradient of groundwater in the *y* direction; (c) gradient of LNAPL in the *x* direction; (d) gradient of LNAPL in the *y* direction.

Table 4.3 provides the quantitative results for particle tracking in groundwater and LNAPL from four scenarios at the harbor site in Honolulu, HI introduced in the following. Figure 4.12 and 4.13 present the particle tracking for groundwater and LNAPL over a 39-day period. The code is shown in Appendix C. The amplitude of variation in the direction of groundwater and LNAPL flow reduced over time. Given the close proximity of the study area to the harbor, tides are the primary factor governing driving gradients. However, because the gradients of groundwater and LNAPL both diminished over this period (Figure 4.11), another explanation for the diminishing fluctuations of groundwater and LNAPL flow maybe due to increased recharge during the later portion of the study period.

Hydraulic gradients of groundwater and gradients of LNAPL varied at every direction in the half part of rose charts (Figure 2.23). However, groundwater and LNAPL flow mainly in the northeast to southwest direction, and the fluctuations in the main flow path lines are in the northwest to southeast direction, these are two main flow directions shown in Figure 4.12 and 4.13. Groundwater and LNAPL do not flow as the same change in each direction of hydraulic

gradients and LNAPL gradients in this area. It is because hydraulic gradients and LNAPL gradients with big magnitude are mainly in the northeast to southwest direction and northwest to southeast direction, and the magnitudes of hydraulic gradients and LNAPL gradients in the northeast to southwest direction are bigger than the hydraulic gradients and LNAPL gradients in the northwest to southeast direction. Further, hydraulic gradients and LNAPL gradients varied in other directions all have small magnitudes (Figure 2.23). Moreover, time interval for each groundwater flow driven by each hydraulic gradient is the same, according to Darcy's equation, hydraulic gradient and LNAPL gradient in the direction with small magnitude cannot drive particles flow long enough to drive groundwater and LNAPL flow away from the main direction.

Table 4.3 The distance particle moved in each scenario at Honolulu, HI

Groundwater						
Anisotropy	Direction	Retardation	Degradation	Δx (Particle moves in the x direction) (ft)	Δy (Particle moves in the y direction) (ft)	Total distance (ft)
No	Forward	No	No	0.312	0.22	0.38
Yes	Forward	Yes	No	0.045	0.016	0.048
Yes	Forward	Yes	Yes	0.015	0.0074	0.005
LNAPL						
No	Forward	No	No	0.037	0.014	0.04
Yes	Forward	Yes	No	0.0042	0.0037	0.0056

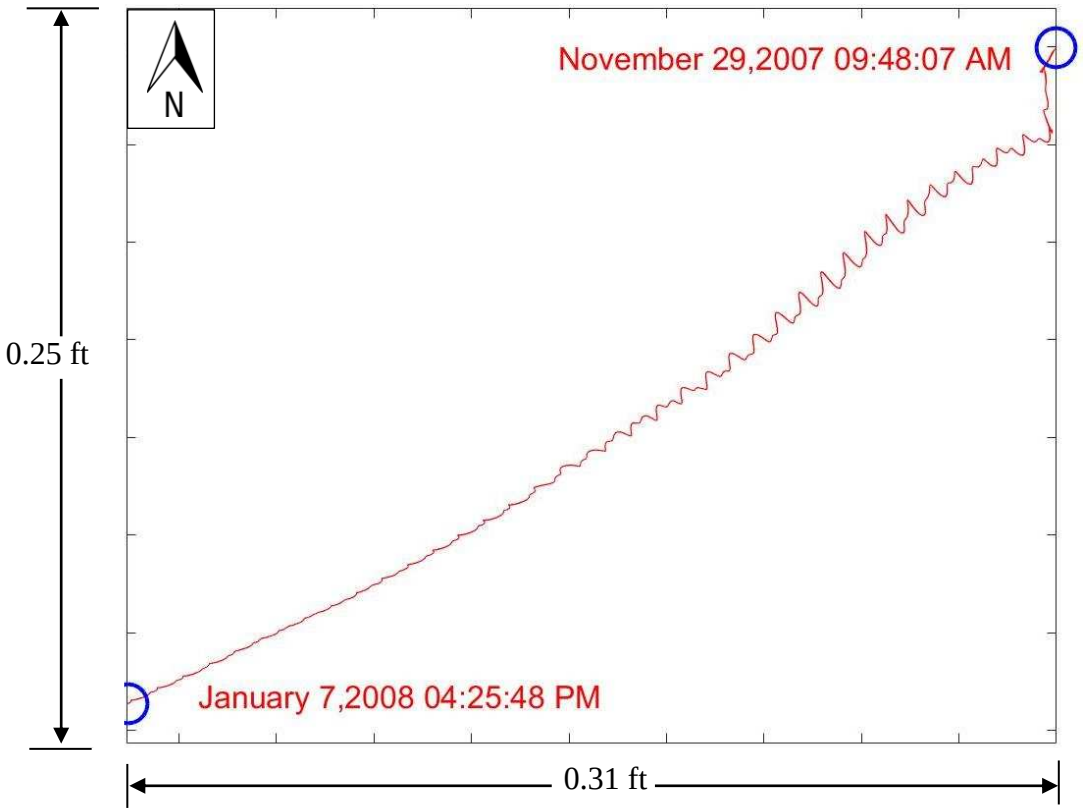

Figure 4.12: Groundwater flow path line under homogeneous and isotropic conditions without reactions at Honolulu, HI.

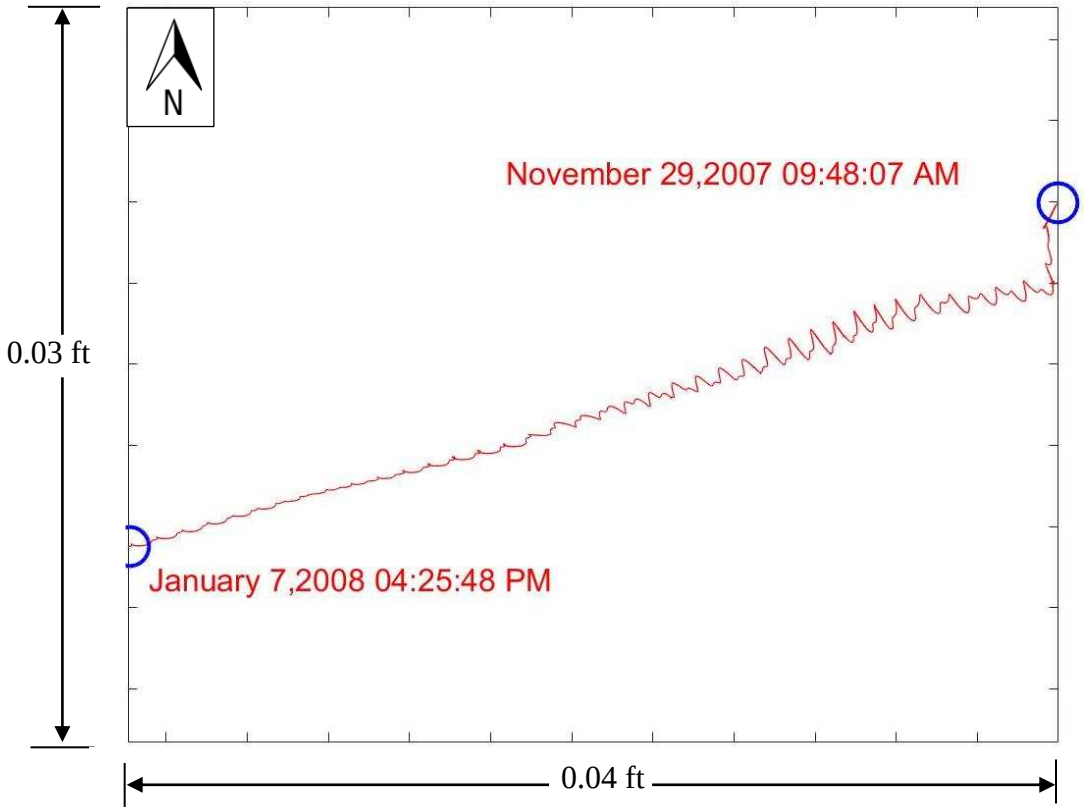

Figure 4.13: LNAPL flow path line under homogeneous and isotropic conditions without reactions at Honolulu, HI.

Under homogeneous and isotropic conditions without reactions, compared to the groundwater flow, LNAPL flow is much smaller. The reason for the smaller movement of LNAPL flow is due to the smaller relative permeability and other factors for LNAPL, the details are described in Chapter 3. Other factors except the smaller relative conductivity of LNAPL contributing to the small magnitude of the measures LNAPL fluxes could be head gradients in LNAPL that are smaller than head gradients in groundwater and natural losses of LNAPL through dissolution, evaporation, and degradation (Mahler et al., 2011).

The flow directions of groundwater and LNAPL under homogeneous and anisotropic conditions with retardation and without reactions are shown in Figure 4.14 and 4.15. The code is

shown in Appendix C. They have different flow paths and directions compared to the scenario under homogeneous and isotropic conditions without reactions.

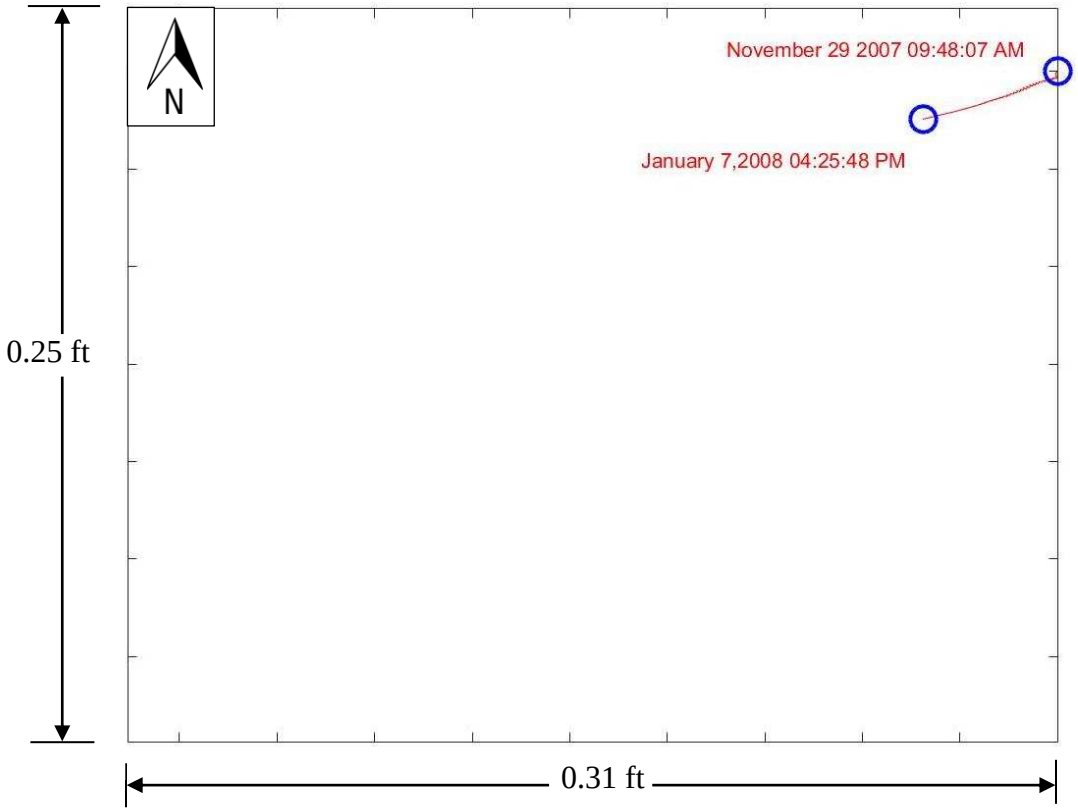

Figure 4.14: Particle-flow path line in groundwater under homogeneous and anisotropic conditions with retardation and without reactions at Honolulu, HI.

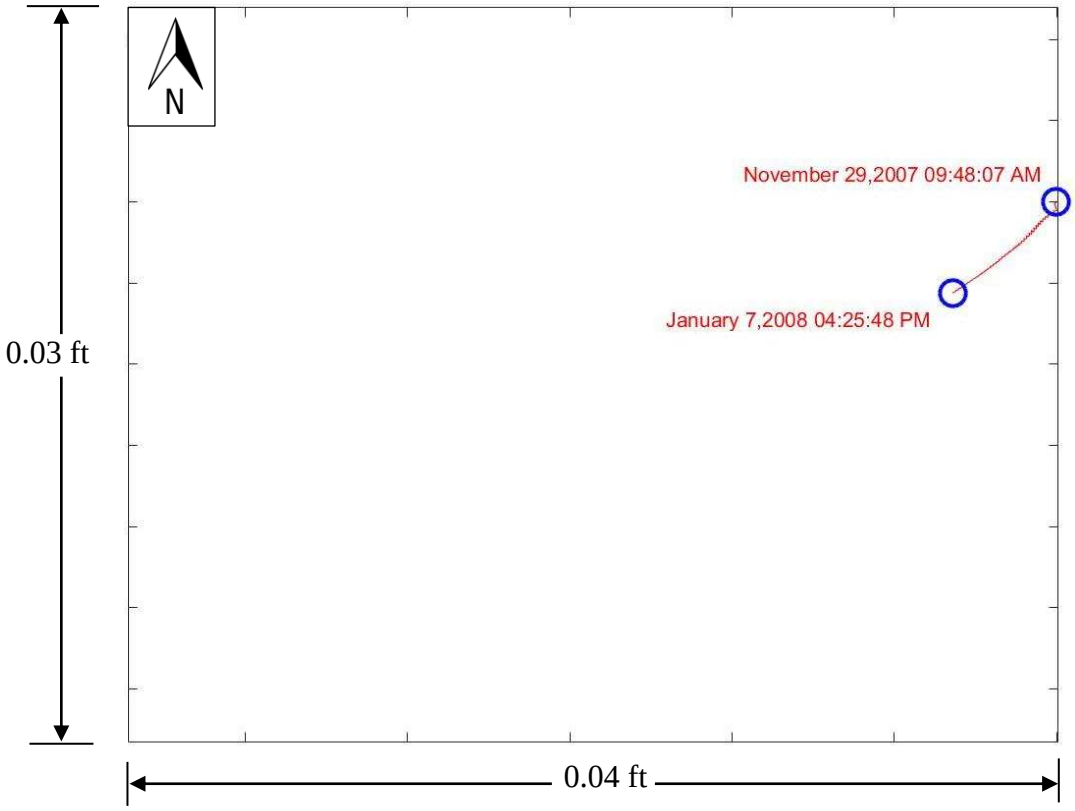

Figure 4.15: Particle-flow path line of LNAPL under homogeneous and anisotropic conditions with retardation and without reactions at Honolulu, HI.

The model of kinetic reaction of benzene and the minimum concentration of benzene of local groundwater quality standard are described in Chapter 3. Further, assume the initial benzene concentration in the subsurface at this site is 1000 mg/L. Figure 4.16 shows the flow path line of benzene within the limited concentration in the subsurface in this area. The code is shown in Appendix C. Due to natural attenuation in subsurface, the concentration of benzene is degraded from 1000 mg/L on November 29, 2007 to 0.005 mg/L on December 13, 2007. And distance of benzene moved in this area is shown in Table 4.3.

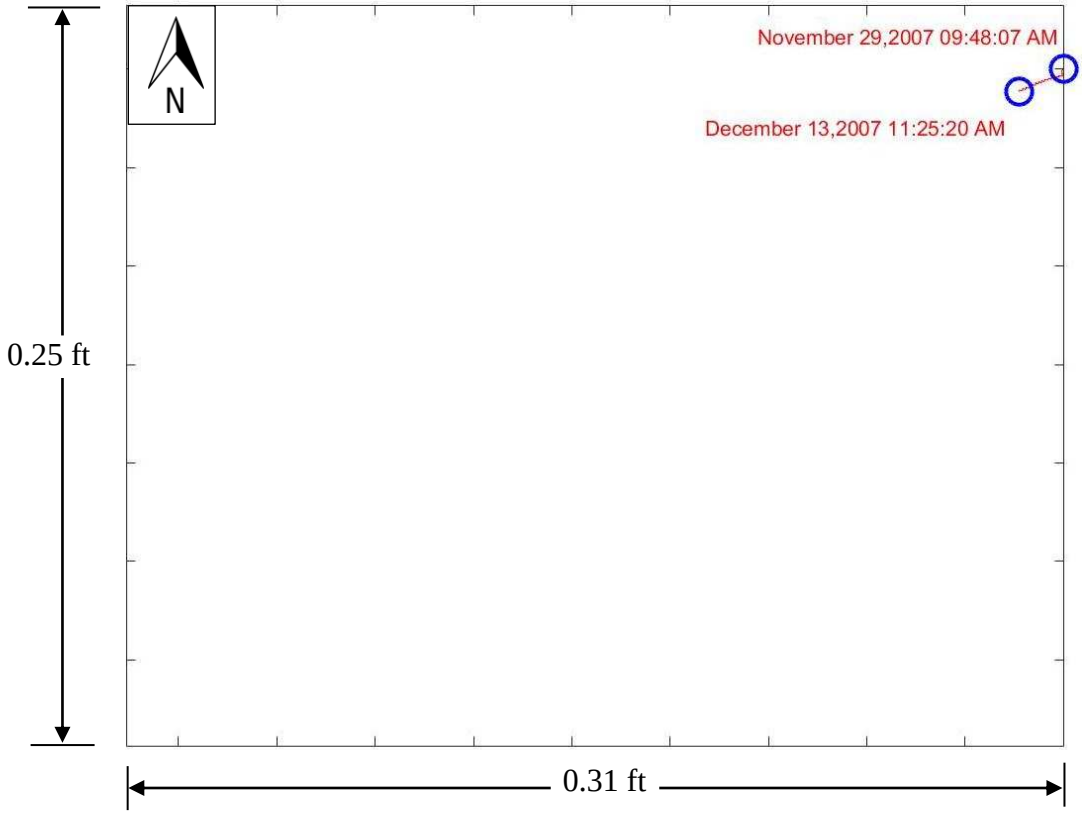

Figure 4.16: Particle tracking under homogeneous and anisotropic conditions with retardation and the first-order degradation at Honolulu, HI.

4.2 Analytical Modeling of Particle Tracking For Dynamic Pumping Conditions

4.2.1 Particle Tracking Results from Production and Injection Wells

The analytical solution used in this research is designed to obtain the time-dependent capture zone by placing particles around pumping wells in it, moving the particles backward from wells into pumping field for injection conditions, and moving the particles forward from the pumping field into wells for pumping conditions, and then connecting the particle positions at any given time with line segments. This solution captures the movement of subsurface fluid particles in pumping fields with dynamic water levels. Movement of particles is evaluated by 1) backward tracking of particles from the pumping field into the production wells, 2) forward

tracking of particles from the injection wells into the pumping field, and 3) continuous pumping and injection conditions.

For pumping conditions, particle tracking were studied by backward methods. Initially, particles were tracked by starting with eight particles around one well, moving the particles from the field to the well in time, and connecting the particle positions with line segments over 21 days. For injection conditions, particle tracking were studied by forward methods, where particles were tracked from the well to the field in time. Figures 4.17 and 4.18 show the flow paths of particles under pumping and injection conditions, respectively. The code is presented in Appendix D. As Figures 4.17 and 4.18 shown, if we know the current particle position, we can use particle tracking to determine where the particles were and even a few days prior under pumping and injection conditions.

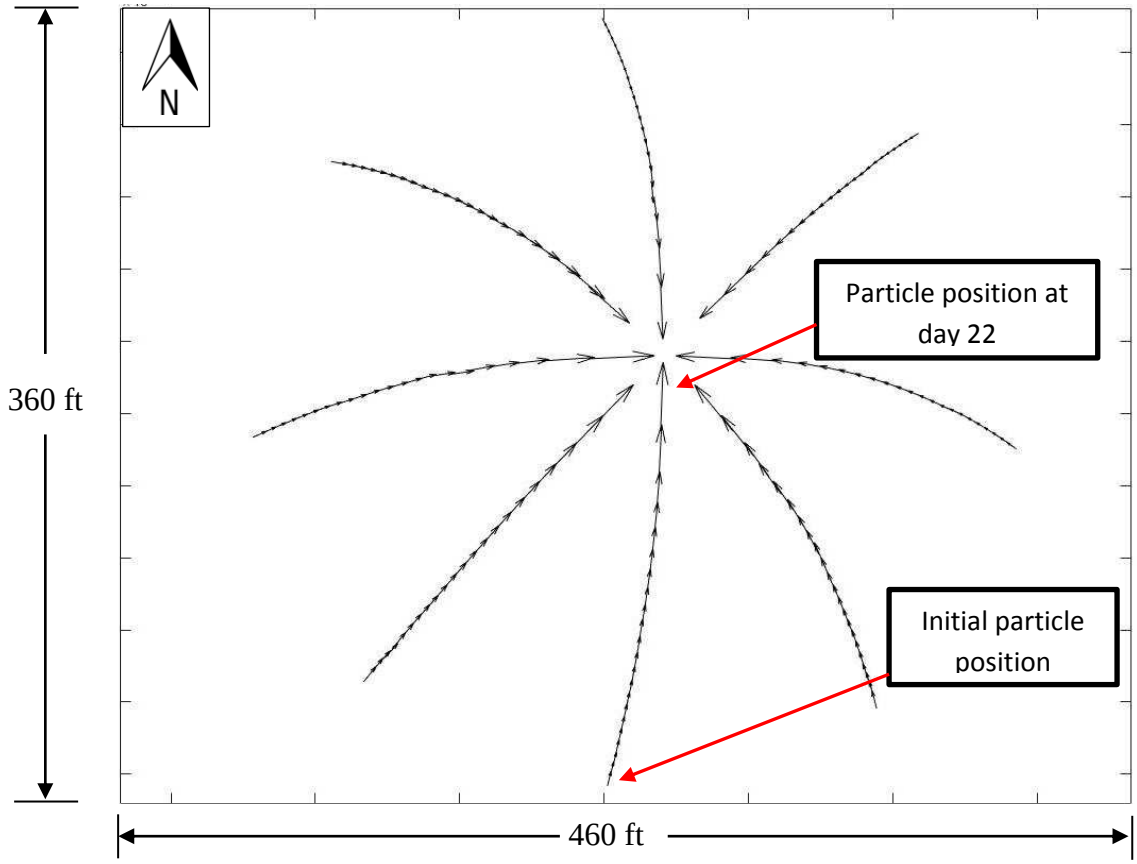

Figure 4.17: Movement of particles around one representative of eight wells for 22 days under pumping conditions at the Meadows Pumping Center, CO.

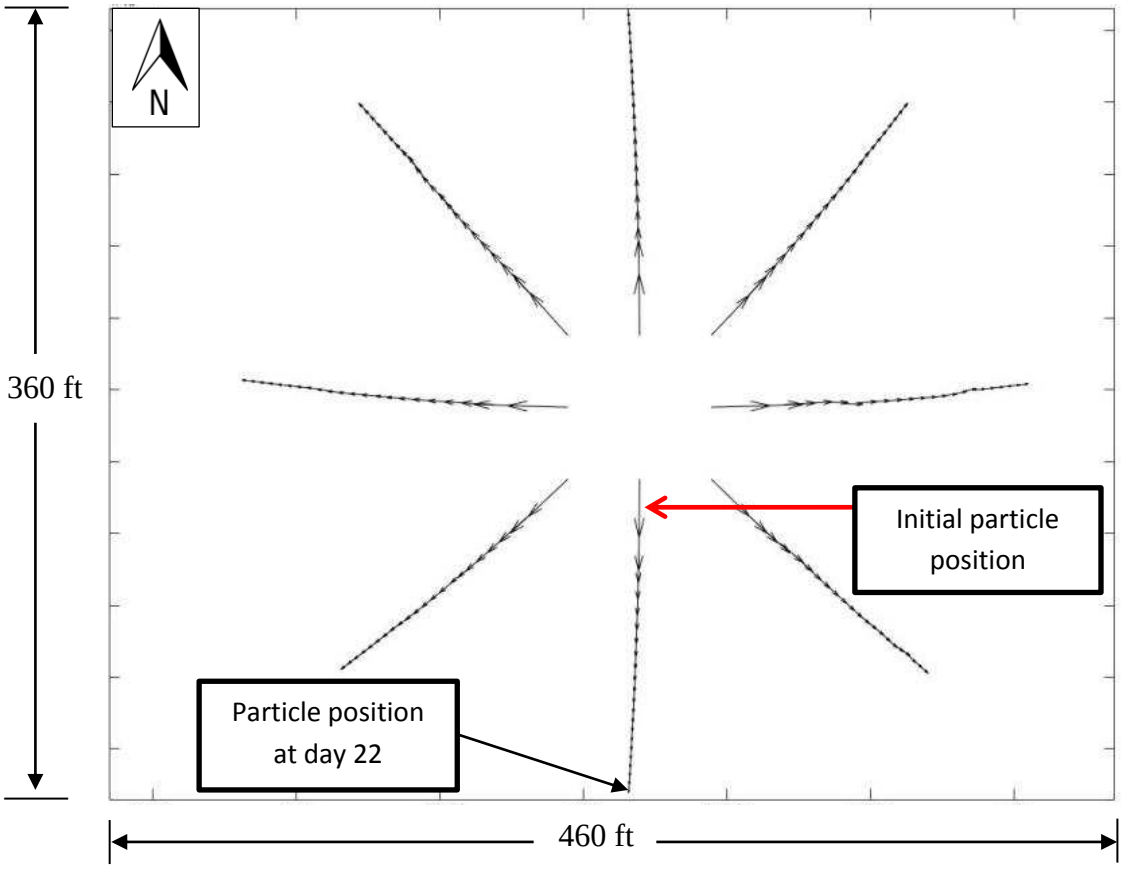

Figure 4.18: Movement of particles around one representative of eight wells for 22 days under injection conditions at the Meadows Pumping Center, CO.

When pumping stops, well and aquifer water levels rise toward their pre-pumping levels (Sterrett, 2007). Because pumps were on and off continuously, uninterrupted drawdowns and recoveries happened successively. Figure 4.19 shows how particles move under continuous pumping and injection conditions in a well over time. Pumping stress is shown in Chapter 2 of this Thesis. The code is shown in Appendix D. In Figure 4.19, water was initially pumped from a well for 21 days (0-1 shown in the Figure), and then the water injected into the well for 30 days (1-2 shown in the Figure), and the pumping and injection processes were continued for a total of 130 days. The movement of water under each pumping and injection process is shown in Figure 4.20. The red circle represents the water position under each pumping and injection process. When the pumps are on and off, the groundwater levels fall and rise continuously. The injection

process drives rising water levels. Accordingly, particles flow toward the well when the pump is on and flow away from the well when the water is injected. The injection curve nearly is an inverted image of the drawdown curve. The resulting inverted paths occurred not so symmetric is because the well in Figure 4.19 is in a well field that influenced by seven other wells although they are far away from each other; drawdown in this well is accordingly influenced by other drawdowns during the pumping. Pumping in the adjacent wells was introduced in the Methods section of this Thesis.

In the first pumping process (Figure 4.20 (a)), water moved 112.89 ft from the aquifer to the well in the first 21 days. In the first injection process (Figure 4.20 (b)), water moved 62.93 ft from the well back to the aquifer over the following 30 days. Likewise, for process (c), water moved 37.47 ft from the aquifer to the well again; and water moved 41.93 ft from the well to the aquifer in process (d); for process (e), water moved 30.22 ft from the aquifer to the well and it moved 25.62 ft from the well into the aquifer in process (f). Red circles in Figure 4.20 show that for a single well, water positions under each pumping and injection process do not flow far away from the well, indicating that the pumping and injection process will not make water flow far away from the well for a short period.

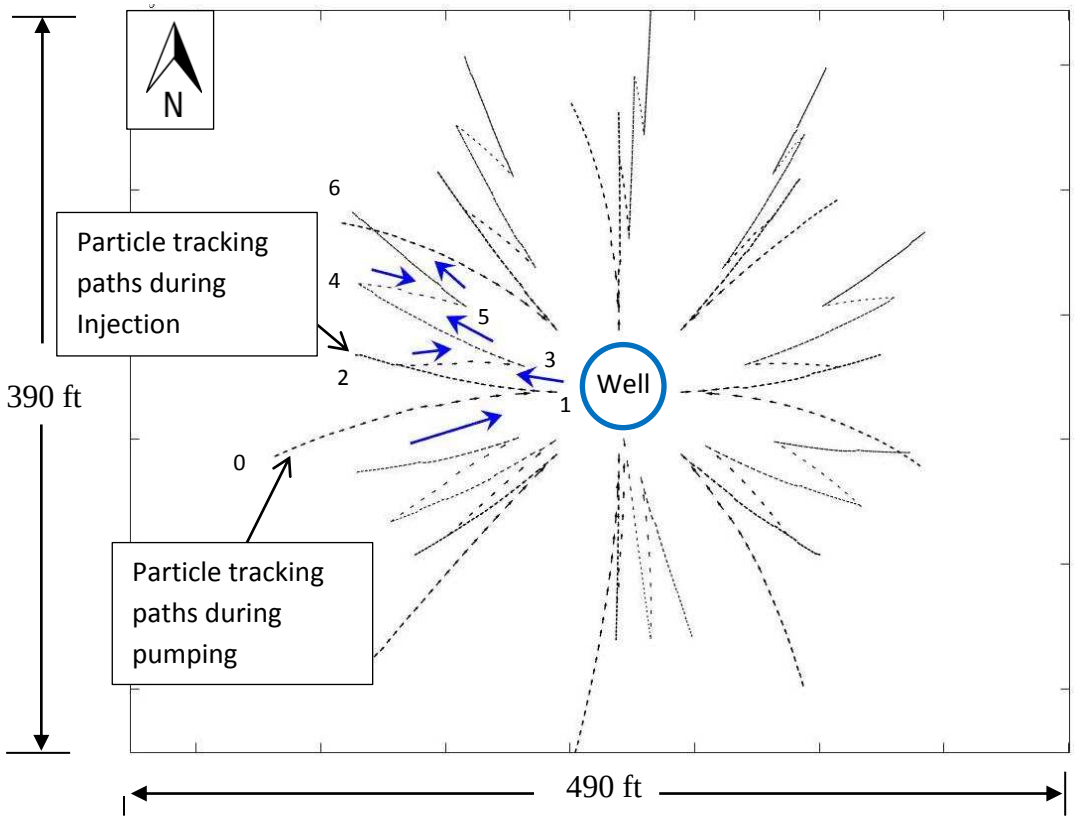

Figure 4.19: Movement of particles around one representative of eight wells for 130 days under continuous pumping and injection conditions at the Meadows Pumping Center, CO.

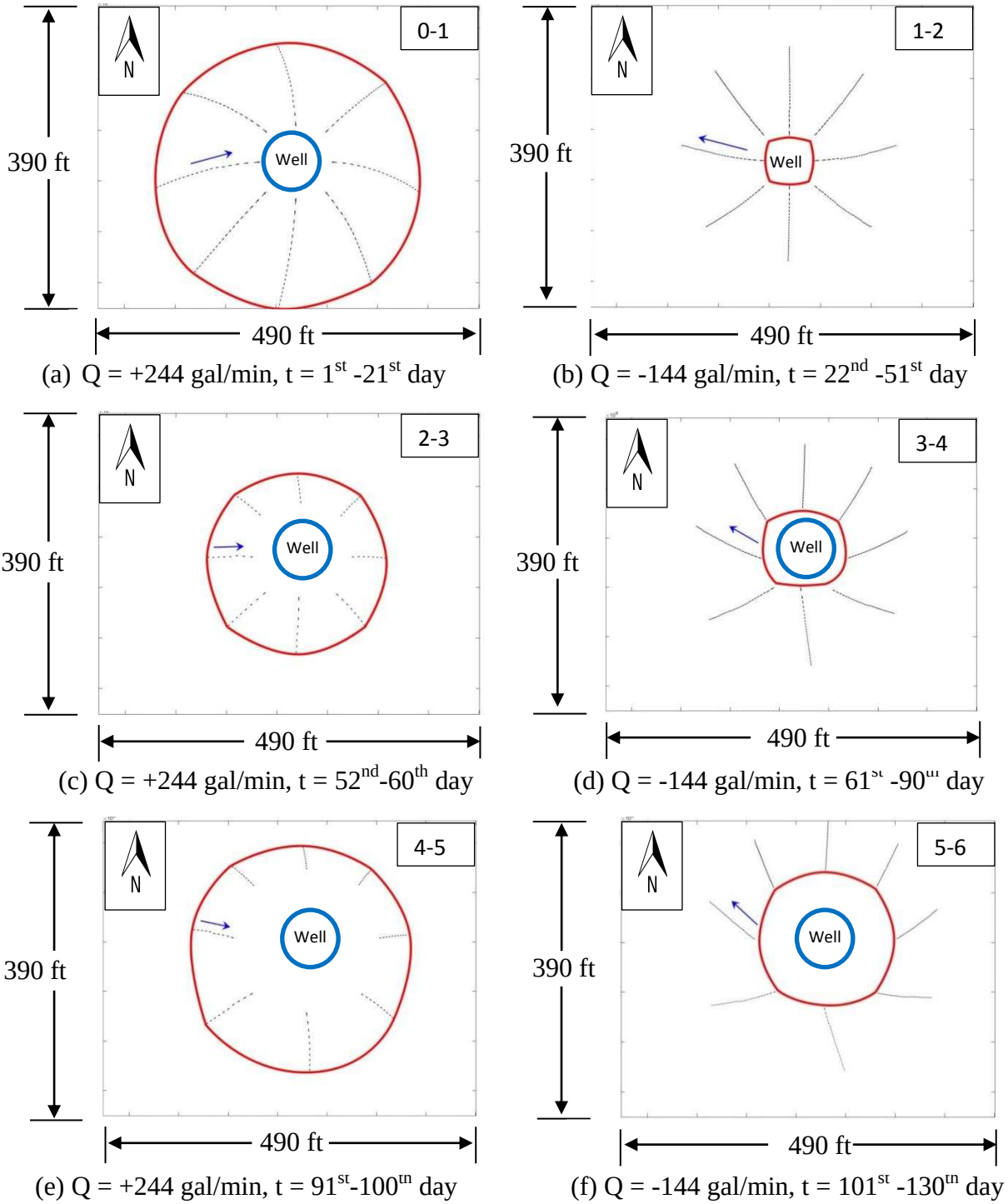

(a) Q = +244 gal/min, t = 1st -21st day

(b) Q = -144 gal/min, t = 22nd -51st day

(c) Q = +244 gal/min, t = 52nd-60th day

(d) Q = -144 gal/min, t = 61st -90th day

(e) Q = +244 gal/min, t = 91st-100th day

(f) Q = -144 gal/min, t = 101st -130th day

Figure 4.20: Water circles around a well for 130 days under each pumping and injection conditions at the Meadows Pumping Center, CO.

Particle tracking under continuous pumping and injection conditions was also studied for a longer period of time, in order to see if the similar results can be obtained. Figure 4.21 shows water moved for 6000 days under continuous pumping and injection conditions. Also, uninterrupted drawdowns and recoveries occurred successively because of continuous pumping and injection. Pumping stress is shown in Chapter 2 of this Thesis. The movement of water under each pumping and injection process is shown in Figure 4.22. The red circle represents as the water position under each pumping and injection process.

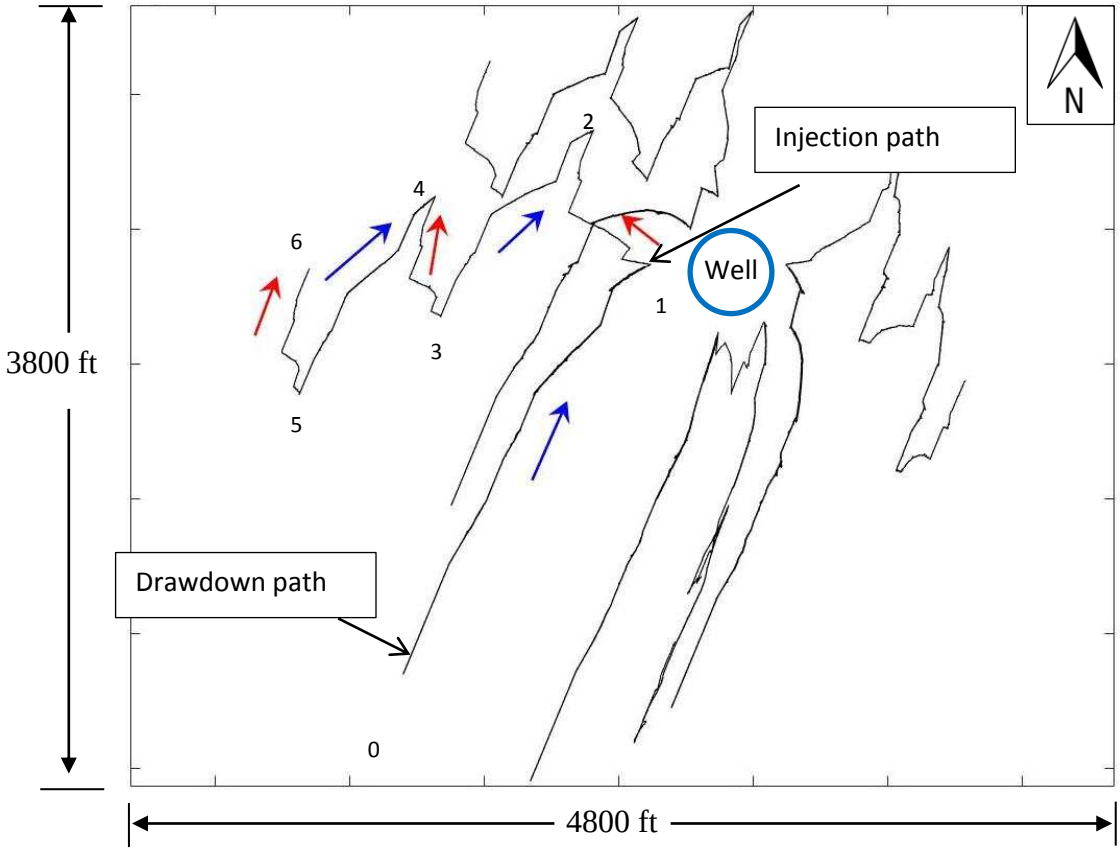

Figure 4.21: Movement of particles around one representative of eight wells for 6000 days under continuous pumping and injection conditions at the Meadows Pumping Center, CO.

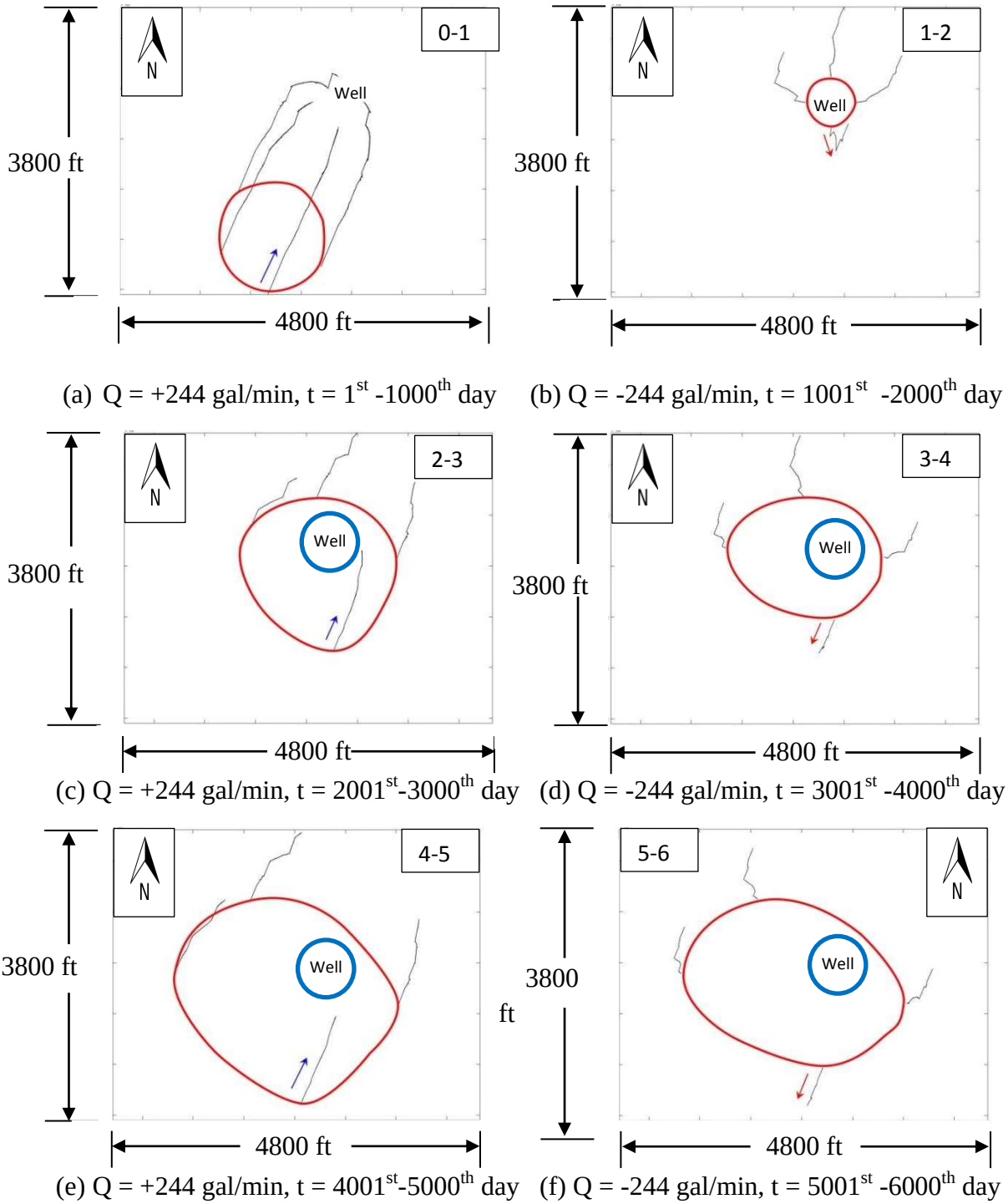

(a) Q = +244 gal/min, t = 1st -1000th day (b) Q = -244 gal/min, t = 1001st -2000th day

(c) Q = +244 gal/min, t = 2001st-3000th day (d) Q = -244 gal/min, t = 3001st -4000th day

(e) Q = +244 gal/min, t = 4001st-5000th day (f) Q = -244 gal/min, t = 5001st -6000th day

Figure 4.22: Water circles around a well for 6000 days under each pumping and injection conditions at the Meadows Pumping Center, CO.

For a longer period of time, 6000 days in this case, for a single well, water also did not flow far away from the well under continuous pumping and injection. For the first 1000 days (Figure 4.22(a)), water moved 861.12 ft from the aquifer to the well during the pumping. In the process (b), water was injected into the aquifer and moved 183.1 ft back to the aquifer from the well. In the following processes (c) and (d), water moved 513.81 ft from the aquifer to the well and 176.41 ft from the well back to the aquifer, respectively. Finally, water again moved 659.45 ft from the aquifer to the well and 180.84 ft from the well back to the aquifer.

CHAPTER 5 – CONCLUSIONS

5.1 Overview

Groundwater at industrial sites and well fields has potential to become contaminated by organic or inorganic compounds from releases. Three field sites with pressure transducers data and a well field are studied in this Thesis. The objective of this research is to explore a novel method to predict the movement of subsurface contaminants and groundwater by tracking particles, relying on dynamic water-level data from pressure transducers or analytical solutions. The positive results generated from this research are simple methods for predicting the movement of subsurface contaminants given dynamic water levels at sites.

5.1.1 Methods

Numerical models are often employed to help people solve particle tracking problems. However, there are limitations to use numerical models. The biggest problem is that numerical models track particle in an element with a uniform head through time steps. For selected problems, temporal and spatial discretization may be insufficient to accurately track particles. For particle tracking at field sites without pumping conditions, this research employed dynamic water-level data in three or more wells to solve particle tracking. Specifically, to determine the particle flow path lines at three field sites, this research first employs three or more wells to measure water levels at each time step. Secondly, these water-level data from wells were used to determine the plain of the water table at each time step. Thirdly, using the slope of the water table and Darcy's equation, particle position at each time step and flow path line at field sites are obtained. The particle flow path lines at three sites are dependent on temporally varying recharge and discharge conditions at each site. Not only for the three field sites described in this Thesis,

but if 1) hydrogeological conditions can be known, 2) establishing three or more wells in a field site, and 3) collecting water-level data from each well at each time step, contaminants flow in the saturated zone at other sites can be obtained.

For the field site with dynamic pumping conditions, numerical models are limited in tracking particle close to wells under dynamic conditions. This research employed a Theis superposition model (Davis, 2013) and analytical solutions to solve particle tracking under dynamic pumping conditions with great space and time. The Theis superposition model (Davis, 2013) provides exact solutions for gradients about pumping wells under dynamic pumping conditions. Based on the Theis superposition model (Davis, 2013) and analytical solutions, flow path lines of fluid particles under dynamic pumping and injection conditions at well fields can be obtained.

5.1.2 Influence of Recharge and Discharge Factors to Groundwater Flow

The three field sites studied in this research all have recharge and discharge factors in the local area, which contribute the changes of the groundwater level. Correspondingly the changes of groundwater level make the directions of groundwater flow changed at these sites. For particle tracking at the field site in Kansas City, MO, Missouri River flows pass the field site of interest. Water-level in the Missouri River mainly declines in the summer, and rises up after the summer. The decline of water-level in the Missouri River in the summer makes the water-level in the aquifer declined. Accordingly, this change of water-level at the field of interest has direction of hydraulic gradient changed from one direction to the inversed direction. Similarly, the rise of water-level in the Missouri River after the summer makes the water-level in the aquifer rise. Also this change of water-level makes the direction of hydraulic gradient shifted. So based on the data provided in this Thesis, there are three main changes of water-level at the field site in Kansas

City, MO, which causes three reversals directions occurred in the particle flow path line at Kansas City, MO.

For particle tracking at PCD, CO, compared to the field site in Kansas City, MO, there is no river flows pass this area. The main factors that make the water-level changed at this site are seasonal precipitation and transpiration. Transpiration mainly occur from the beginning of the summer to the early fall. And groundwater level mainly declines in this period. After the early fall, transpiration decreased and precipitation makes the groundwater level risen up and gradually stable till the next summer. Similar to the field site at Kansas City, MO, the rise and decline of water-level can change the hydraulic gradient, so that change the direction of groundwater flow in this area. Also, the periods of three reversals directions occurred in the particle flow path line at PCD, CO just corresponds to the periods when precipitation and transpiration make the water-level rise and declined.

For particle tracking at Honolulu, HI, the field site of interest is adjacent to the harbor. The groundwater level at this site is influenced by the tides. However, in the period of interest in this research, hydraulic gradients and LNAPL gradients in the *y* direction do not exactly follow the changing of tides. For groundwater and LNAPL, the amplitudes of the changes in hydraulic gradients are diminished through time in the *y* direction. Also, the amplitude of variation in the direction of groundwater and LNAPL flow reduced over time. Because the period of interest for this site is 39 days, which is a short period, probably the increased recharge during the later portion of the study period caused the diminishing fluctuations of groundwater and LNAPL flow.

Therefore, the changes of water-level in the recharge and discharge source and precipitation and transpiration at the field site can give people some clues to direction of groundwater or contaminant flow. Especially, the big changes of water-level in the recharge and

discharge and seasonal changes of precipitation and transpiration will make main direction of groundwater or contaminant changed.

5.1.3 Key Results

For particle tracking at the field site in Kansas City, MO, the direction of hydraulic gradient varies through almost 360° with temporally changing gradient. Interestingly, despite these variations, particle tracking shows a clear trend of flow to east-southeast with brief period of flow reversals.

For particle tracking at PCD, CO, hydraulic gradients are also varied almost at every direction with temporally changing gradients. During brief periods, the groundwater flow direction shifts to the northwest. But groundwater flow at this site is mainly in one direction, from northeast to southwest.

For particle tracking at the field site in Honolulu, HI, hydraulic gradients and gradients of LNAPL varied with different magnitudes in almost every direction in the southwest part of rose charts on a daily basis. The main directions of hydraulic gradient and LNAPL gradient are concentrated in the northwest to southeast and southwest. And the magnitude of hydraulic gradient and LNAPL gradient in the northwest to southeast direction is smaller to the magnitude of hydraulic gradient and LNAPL gradient in the northeast to southwest direction. However, groundwater and LNAPL flow mainly in the northeast to southwest direction, and the fluctuations in the main flow path lines are in the northwest to southeast direction.

Based on the results, groundwater and LNAPL flow mainly follows the direction of hydraulic gradients and LNAPL gradients with big magnitudes. The proper explanation for this phenomena is that because the time interval for each groundwater flow driven by each hydraulic gradient is the same, according to the Darcy’s equation, the gradient with small magnitude

cannot drive particles flow long enough to make particles flow away from the main direction, which is driven by hydraulic gradient and LNAPL gradient with big magnitude. So in a groundwater or contaminant flow process over a time period, hydraulic gradient with small magnitude and short time period cannot change main direction of groundwater or contaminant flow.

5.1.4 Influence of Dynamic Pumping Conditions to Groundwater Flow

Under dynamic pumping conditions, the results of this research provide a relatively uniform capture zones. Also, the results of this research show that although groundwater may flow away from the well to the well field during the pumping process and flow toward to the well from the well field during the injection process, position of the groundwater may change following each process but does not flow far away from the well. Accordingly, groundwater positions can be evaluated based on the research for dynamic pumping. At the same time, particle tracking under dynamic pumping conditions can simply help people evaluate particle movement about well used to both store and recovery water.

5.2 Other Potential Applications and Future Research

This research gives us a simple method, based on simple assumptions, to track contaminants and groundwater in the saturated zones. There are some future works that may help make the methods and results of particle tracking more realistic and wonderful. Firstly, to make particle tracking results more efficiently, water level data should be acquired via wireless connections for real-time monitoring.

Secondly, in this research, geological conditions were assumed to be 1) homogeneous, and isotropic 2) homogeneous, and anisotropic. Also, consideration is given to reactions including sorption and degradation. Furthermore, the particles and groundwater flow direction

were assumed to be two-dimensional. And the geologic parameters were hypothesized simply based on the geological information of these field sites. To obtain more precise and real results of the movements of contaminants and groundwater in subsurface, more exact and complex geologic and biogeochemical conditions and assumptions need to be considered both in the saturated and unsaturated zones: (1) heterogeneous and anisotropic conditions, (2) varying geologic parameters in varying regions, (3) flow directions of contaminants and groundwater in *x*, *y*, and *z* axes, (4) varying retardation factors across the whole geologic setting, (5) different areas having specific contaminants corresponding to different kinetic reactions, (6) diffusion, dispersion, sorption, and desorption considerations for the influence of flow and degradation of contaminants, (7) not only the chemical impact but physical influence, such as temperature, on the flow and transport and, (8) local microbial influence on the transport of contaminants, 9) different redox zone. Therefore, if more comprehensive and exact factors can be obtained and considered in the model, more sound results can be generated.

Thirdly, if establish a laboratory study of particle movement using the same geological conditions as this research, it would verify the results of the model and confine users to apply it. Additionally, in this research, the water level data, parameters, and coordinates are input to the model manually before the model can be operated. This process is time-consuming. So computational methods should be compiled into a user friendly software package would greatly increase the efficiency of the modeling processes. And appropriate time and space discretization should be resolved in the computational methods.

REFERENCES

Bair, E. S., A. E. Springer, and G. S. Roadcap. 1991. Delineation of traveltime-related capture areas od wells using analytical flow models and particle-tracking analysis. *Ground Water* 29, no.3: 387-397.

Cunningham, W. L., R. A. Sheets, and C. W. Schalk. 1994. Evaluation of ground-water flow by particle tracking, Wright-Patterson Air Force Base. U.S. Geologocal Survey Water-Resources Investigation Report 94-4243.

Davis, J. A. 2013. Coupled analytical modeling of water level dynamics and energy use for operational well fields in the Denver basin aquifers. Masters thesis, Colorado State University, Fort Collins, Colorado.

Domenico, P. A., and F. W. Schwartz. 1997. Physical and chemical hydrogeology. John Wiley & Sons, Inc.

Frind, E.O., J.W. Molson, and D.L. Rudolph. 2006. Well vulnerability: A quantitative approach for source water protection. *Ground Water* 44, no.5: 732-742.

Jackson, C.R. 2002. Steady-state particle tracking in the object-oriented regional groundwater model ZOOMQ3D. *British Geological Survey*: 9.

Lewis, R. A., M.J. Ronayne, and T.C. Sale. 2015. Estimating aquifer properties using derivative analysis of water level time series from active well fields. *Groundwater* 54, no.3: 414-424.

Li, H. L. and J. J. Jiao. 2002. Analytical solutions of tidal groundwater flow in coastal two-aquifer system. *Advances in Water Resources* 25, no.4: 417-426.

Lowry, C. S., and M. P. Anderson. 2006. An assessment of aquifer storage recovery using ground water flow models. *Ground Water* 44, no.5: 661-667.

Lu, N. 1994. A semianalytical method of path line computation for transient finite-difference groundwater flow models. *Water Resources Research* 30, no.8: 2449-2459.

Mahler, N., T. Sale, T. Smith, and M. Lyverse. 2011. Use of single-welltracer dilution tests to evaluate LNAPL flux at seven field sites. *Ground Water* 50, no.6: 851-860.

Maskey,S., A. Jonoski, and D. P. Solomatine. 2002. Groundwater remediation strategy using global optimization algorithms. *Journal of water resources planning and management* 128, no.6: 431-440.

Moutsopoulos, K. N., A. Gemitzi, and V. A. Tsihrintzis. 2008. Delineation of groundwater protection zones by the backward particle tracking method: theoretical background and GIS-based stochastic analysis. *Environmental Geology* 54, no.5:1081-1090.

Murdoch, L. Charles and Hensley, L. David. 1994. Physical properties of Hawaiian golf course sands. *Hort Technology* 4, no.2: 150-153.

Pankow, J. F. and J. A. Cherry. 1996. Dense Chlorinated Solvent and Other DNAPLs in Groundwater: History, Behavior, and Remediation. Waterloo Press.

Pollock, D.W. 1988. Semianalytical computation of path lines for finite-difference models. *Ground Water* 26, no.6: 743-750.

Pontin, J.M.A. 1986. Prediction of groundwater Pressures and uplift below excavations in tidal limits. *Geological Society, London, Engineering Geology Special Publication* 3: 333-366.

Rifai, S. Hanadi, and Newell, J. Charles. 1998. Estimating first-order decay rates for BTEX using data from 115 sites. Proceedings of the petroleum hydrocarbons and organic chemicals in ground water: prevention, detection and remediation conference: 31-4.

Robinson, B. A., Z. V. Dash, and G. Srinivasam. 2010. A particle tracking transport method for the simulation of resident and flux-averaged concentration of solute plumes in groundwater models. *Computational Geosciences* 14, no.4: 779-792.

Robson, S. G. and E. R. Banta. 1995. Ground Water Atlas of the United States, "Arizona, Colorado, New Mexico, Utah, HA730=C". Available on World Wide Web, URL: USGS HA730-C: http://pubs.usgs.gov/ha/ha730/ch_c/C-text6.html Retrieved 4/16/2013.

Sale, T., A. Eldiery, and A. Baily. 2009. Compilation and preliminary analysis of hydrogeologic data from the Denver basin aquifers in the vicinity of Castle Rock, Colorado.

Sale, T., M. Olson, D. Gilbert, and M. Petersen. 2010. Field demonstration/validation of electrolytic barriers for energetic compounds at Pueblo Chemical Depot. *ESTCP Project ER-0519*.

Schafer-Perini, A. L., and J. L. Wilson. 1991. Efficient and accurate front tracking for two-dimensional groundwater flow models. *Water Resources Research* 27, no.7: 1471-1485.

Schwartz, F. W., and H. Zhang. 2002. Fundamentals of Groundwater Water. John Wiley & Sons, Inc.

Scow, K. M., and K. A. Hicks. 2005. Natural attenuation and enhanced bioremediation of organic contaminants in groundwater. *Current Opinion in Biotechnology* 16, no.3: 246-253.

Shamsuddin, M. K., N. S. Suratman, M. P. Zakaria, A. Z. Aris, and W. N. A. Sulaiman. 2014. Particle tracking analysis of river-aquifer interaction via bank infiltration techniques, *Environmental Earth Sciences* 72, no.8: 3129-3142.

Solinst. 2014. Levelogger Model 3001 User guide.

Sterrett, R. J. 2007. Groundwater and wells. Johnson screens.

Tang, Z. H., and J. J. Jiao. 2001. A two-dimensional analytical solution for groundwater flow in a leaky confined aquifer system near open tidal water. *Hydrological Processes* 15: 573-585.

TRC. 2012. LNAPL distribution and recoverability assessment.

U.S. Department of Health and Human Services, 1995. *Toxicological profile for RDX*.

USGS. 2005. Fate and transport of petroleum hydrocarbons in soil and ground water at Big Fork National River and Recreation Area, Tennessee and Kentucky, 2002-2003.

Yidana, S. M. 2011. Groundwater flow modeling and particle tracking for chemical transport in the southern Voltaian aquifers. *Environmental Earth Sciences* 63, no.4: 709-721.

APPENDIX A – MODELING CODE FOR PARTICLE TRACKING AT KANSAS CITY, MO

This appendix contains programming code used for the particle tracking modeling and first-order kinetic reaction modeling at Kansas City, MO using PTC Mathcad 15® Engineering Software.

Particle tracking under homogeneous and isotropic conditions without reactions at Kansas City, MO.

$$
\begin{aligned}
XX := \;& X_{old} \leftarrow X_{initial} \\
& Y_{old} \leftarrow Y_{initial} \\
& \text{for } j \in 1..N_{data} \\
& \quad zz \leftarrow \begin{pmatrix} z_{1,j} \\ z_{2,j} \\ z_{3,j} \\ z_{4,j} \end{pmatrix} \\
& \quad R \leftarrow \text{regress}(M_{xy}, zz, 1) \\
& \quad Slope_x \leftarrow R_4 \\
& \quad Slope_y \leftarrow R_5 \\
& \quad ZZ_{j,1} \leftarrow Slope_x \\
& \quad ZZ_{j,2} \leftarrow Slope_y \\
& \quad ZZ_{j,3} \leftarrow \left| \sqrt{Slope_x^{\,2} + Slope_y^{\,2}} \right| \\
& \quad ZZ_{j,4} \leftarrow \text{atan}\left(\frac{-Slope_y}{-Slope_x} \right) \text{ if } Slope_x \le 0 \wedge Slope_y \le 0 \\
& \quad ZZ_{j,4} \leftarrow \text{atan}\left(\frac{Slope_x}{-Slope_y} \right) + \frac{\pi}{2} \text{ if } Slope_x > 0 \wedge Slope_y \le 0 \\
& \quad ZZ_{j,4} \leftarrow \text{atan}\left(\frac{Slope_y}{Slope_x} \right) + \pi \text{ if } Slope_x \ge 0 \wedge Slope_y \ge 0 \\
& \quad ZZ_{j,4} \leftarrow \text{atan}\left(\frac{-Slope_x}{Slope_y} \right) + \frac{3 \cdot \pi}{2} \text{ if } Slope_x \le 0 \wedge Slope_y \ge 0 \\
& \quad ZZ_{j,5} \leftarrow X_{old} - \frac{ZZ_{j,1} \cdot 0.0033 \cdot 86400}{0.25} \\
& \quad ZZ_{j,6} \leftarrow Y_{old} - \frac{ZZ_{j,2}\, 0.0033}{0.25} \cdot 86400 \\
& \quad X_{old} \leftarrow ZZ_{j,5} \\
& \quad Y_{old} \leftarrow ZZ_{j,6} \\
& ZZ
\end{aligned}
$$

Particle tracking under homogeneous and anisotropic conditions with retardation factor and without reactions at Kansas City, MO.

$$
\begin{aligned}
XX :=\ & X_{old} \leftarrow X_{initial} \\
& Y_{old} \leftarrow Y_{initial} \\
& \text{for } j \in 1..N_{data} \\
& \quad zz \leftarrow \begin{pmatrix} z_{1,j} \\ z_{2,j} \\ z_{3,j} \\ z_{4,j} \end{pmatrix} \\
& \quad R \leftarrow \text{regress}(M_{xy}, zz, 1) \\
& \quad Slope_x \leftarrow R_4 \\
& \quad Slope_y \leftarrow R_5 \\
& \quad ZZ_{j,1} \leftarrow Slope_x \\
& \quad ZZ_{j,2} \leftarrow Slope_y \\
& \quad ZZ_{j,3} \leftarrow \left| \sqrt{Slope_x^{\,2} + Slope_y^{\,2}} \right| \\
& \quad ZZ_{j,4} \leftarrow \text{atan}\left(\frac{-Slope_y}{-Slope_x}\right) \text{ if } Slope_x \le 0 \wedge Slope_y \le 0 \\
& \quad ZZ_{j,4} \leftarrow \text{atan}\left(\frac{Slope_x}{-Slope_y}\right) + \frac{\pi}{2} \text{ if } Slope_x > 0 \wedge Slope_y \le 0 \\
& \quad ZZ_{j,4} \leftarrow \text{atan}\left(\frac{Slope_y}{Slope_x}\right) + \pi \text{ if } Slope_x \ge 0 \wedge Slope_y \ge 0 \\
& \quad ZZ_{j,4} \leftarrow \text{atan}\left(\frac{-Slope_x}{Slope_y}\right) + \frac{3\cdot\pi}{2} \text{ if } Slope_x \le 0 \wedge Slope_y \ge 0 \\
& \quad K_{ioc} \leftarrow 59.\frac{mL}{gm} \\
& \quad f_{oc} \leftarrow 0.01 \\
& \quad K_{id} \leftarrow f_{oc} \cdot K_{ioc} \\
& \quad R \leftarrow 1 + \frac{K_{id} \cdot \rho_b}{\phi} \\
& \quad ZZ_{j,5} \leftarrow X_{old} - \frac{ZZ_{j,1} \cdot 0.0033 \cdot 86400}{0.25 \cdot R} \\
& \quad ZZ_{j,6} \leftarrow Y_{old} - \frac{ZZ_{j,2}^{\,0.00164}}{0.25 \cdot R} \cdot 86400 \\
& \quad X_{old} \leftarrow ZZ_{j,5} \\
& \quad Y_{old} \leftarrow ZZ_{j,6} \\
& ZZ
\end{aligned}
$$

First-Order Kinetic Reactions at Kansas City, MO.

$n := 1552$ $\Delta t := 1day$

$$M := \left| \begin{array}{l} C_0 \leftarrow 1 \frac{mg}{L} \\ k \leftarrow 0.0036 \frac{1}{day} \\ \text{for } i \in 1,2..n \\ \quad \left| \begin{array}{l} C_i \leftarrow C_0 \cdot e^{-k \cdot \Delta t \cdot i} \\ \text{break if } C_i < 0.005 \frac{mg}{L} \end{array} \right. \\ C \end{array} \right.$$

APPENDIX B – MODELING CODE FOR PARTICLE TRACKING AT PCD, CO

This appendix contains programming code used for the particle tracking modeling and first-order kinetic reaction modeling at PCD, CO using PTC Mathcad 15® Engineering Software.

Particle tracking under homogeneous and isotropic conditions without reactions at PCD, CO.

$$
\begin{aligned}
XX :- \;& X_{old} \leftarrow X_{initial} \\
& Y_{old} \leftarrow Y_{initial} \\
& \text{for } j \in 1..N_{data} \\
& \quad zz \leftarrow \begin{bmatrix} (zT)_{1,j} \\ (zT)_{2,j} \\ (zT)_{3,j} \\ (zT)_{4,j} \\ (zT)_{5,j} \end{bmatrix} \\
& \quad R \leftarrow regress(M_{xy}, zz, 1) \\
& \quad Slope_x \leftarrow R_4 \\
& \quad Slope_y \leftarrow R_5 \\
& \quad ZZ_{j,1} \leftarrow Slope_x \\
& \quad ZZ_{j,2} \leftarrow Slope_y \\
& \quad ZZ_{j,3} \leftarrow \left| \sqrt{Slope_x^{\,2} + Slope_y^{\,2}} \right| \\
& \quad ZZ_{j,4} \leftarrow atan\left(\frac{-Slope_y}{-Slope_x}\right) \text{ if } Slope_x \le 0 \wedge Slope_y \le 0 \\
& \quad ZZ_{j,4} \leftarrow atan\left(\frac{Slope_x}{-Slope_y}\right) + \frac{\pi}{2} \text{ if } Slope_x > 0 \wedge Slope_y \le 0 \\
& \quad ZZ_{j,4} \leftarrow atan\left(\frac{Slope_y}{Slope_x}\right) + \pi \text{ if } Slope_x \ge 0 \wedge Slope_y \ge 0 \\
& \quad ZZ_{j,4} \leftarrow atan\left(\frac{-Slope_x}{Slope_y}\right) + \frac{3 \cdot \pi}{2} \text{ if } Slope_x \le 0 \wedge Slope_y \ge 0 \\
& \quad ZZ_{j,5} \leftarrow X_{old} - \frac{ZZ_{j,1} \cdot 0.00033 \cdot 86400}{0.25} \\
& \quad ZZ_{j,6} \leftarrow Y_{old} - \frac{ZZ_{j,2} \cdot 0.00033}{0.25} \cdot 86400 \\
& \quad X_{old} \leftarrow ZZ_{j,5} \\
& \quad Y_{old} \leftarrow ZZ_{j,6} \\
& ZZ
\end{aligned}
$$

Particle tracking under homogeneous and anisotropic conditions with retardation factor and without reactions at PCD, CO.

$$
\begin{aligned}
XX := \;& X_{old} \leftarrow X_{initial} \\
& Y_{old} \leftarrow Y_{initial} \\
& \text{for } j \in 1..N_{data} \\
& \quad zz \leftarrow \begin{bmatrix} (zT)_{1,j} \\ (zT)_{2,j} \\ (zT)_{3,j} \\ (zT)_{4,j} \\ (zT)_{5,j} \end{bmatrix} \\
& \quad R \leftarrow \text{regress}(M_{xy}, zz, 1) \\
& \quad Slope_x \leftarrow R_4 \\
& \quad Slope_y \leftarrow R_5 \\
& \quad ZZ_{j,1} \leftarrow Slope_x \\
& \quad ZZ_{j,2} \leftarrow Slope_y \\
& \quad ZZ_{j,3} \leftarrow \left| \sqrt{Slope_x^{\,2} + Slope_y^{\,2}} \right| \\
& \quad ZZ_{j,4} \leftarrow \text{atan}\left(\frac{-Slope_y}{-Slope_x}\right) \text{ if } Slope_x \le 0 \wedge Slope_y \le 0 \\
& \quad ZZ_{j,4} \leftarrow \text{atan}\left(\frac{Slope_x}{-Slope_y}\right) + \frac{\pi}{2} \text{ if } Slope_x > 0 \wedge Slope_y \le 0 \\
& \quad ZZ_{j,4} \leftarrow \text{atan}\left(\frac{Slope_y}{Slope_x}\right) + \pi \text{ if } Slope_x \ge 0 \wedge Slope_y \ge 0 \\
& \quad ZZ_{j,4} \leftarrow \text{atan}\left(\frac{-Slope_x}{Slope_y}\right) + \frac{3 \cdot \pi}{2} \text{ if } Slope_x \le 0 \wedge Slope_y \ge 0 \\
& \quad K_{ioc} \leftarrow 63 \cdot \frac{mL}{gm} \\
& \quad f_{oc} \leftarrow 0.01 \\
& \quad K_{id} \leftarrow f_{oc} \cdot K_{ioc} \\
& \quad R \leftarrow 1 + \frac{K_{id} \cdot \rho_b}{\phi} \\
& \quad ZZ_{j,5} \leftarrow X_{old} - \frac{ZZ_{j,1} \cdot 0.00033 \cdot 86400}{0.25 \cdot R} \\
& \quad ZZ_{j,6} \leftarrow Y_{old} - \frac{ZZ_{j,2}^{\,0.000164}}{0.25 \cdot R} \cdot 86400 \\
& \quad X_{old} \leftarrow ZZ_{j,5} \\
& \quad Y_{old} \leftarrow ZZ_{j,6} \\
& ZZ
\end{aligned}
$$

First-Order Kinetic Reactions at Pueblo Chemical Depot (PCD), CO.

$n := 723 \qquad \Delta t := 1day$

$$M := \left| \begin{array}{l} C_0 \leftarrow 1000 \dfrac{mg}{L} \\ k \leftarrow 0.063 \dfrac{1}{day} \\ \text{for } i \in 1,2..n \\ \quad \left| \begin{array}{l} C_i \leftarrow C_0 \cdot e^{-k \cdot \Delta t \cdot i} \\ \text{break if } C_i < 0.005 \dfrac{mg}{L} \end{array} \right. \\ C \end{array} \right.$$

APPENDIX C – MODELING CODE FOR PARTICLE TRACKING AT HONOLULU, HI

This appendix contains programming code used for the particle tracking modeling and first-order kinetic reaction modeling at Honolulu, HI using PTC Mathcad 15® Engineering Software.

Particle tracking for groundwater under homogeneous and isotropic conditions without reactions at Honolulu, HI.

$$
\begin{aligned}
XX := \;& X_{old} \leftarrow X_{initial} \\
& Y_{old} \leftarrow Y_{initial} \\
& \text{for } j \in 1..N_{data} \\
& \quad zz \leftarrow \begin{bmatrix} (z^T)_{1,j} \\ (z^T)_{2,j} \\ (z^T)_{3,j} \end{bmatrix} \\
& \quad R \leftarrow \text{regress}(M_{xy}, zz, 1) \\
& \quad Slope_x \leftarrow R_4 \\
& \quad Slope_y \leftarrow R_5 \\
& \quad ZZ_{j,1} \leftarrow Slope_x \\
& \quad ZZ_{j,2} \leftarrow Slope_y \\
& \quad ZZ_{j,3} \leftarrow \left| \sqrt{Slope_x^{\,2} + Slope_y^{\,2}} \right| \\
& \quad ZZ_{j,4} \leftarrow \text{atan}\left(\frac{-Slope_y}{-Slope_x}\right) \text{ if } Slope_x \le 0 \wedge Slope_y \le 0 \\
& \quad ZZ_{j,4} \leftarrow \text{atan}\left(\frac{Slope_x}{-Slope_y}\right) + \frac{\pi}{2} \text{ if } Slope_x > 0 \wedge Slope_y \le 0 \\
& \quad ZZ_{j,4} \leftarrow \text{atan}\left(\frac{Slope_y}{Slope_x}\right) + \pi \text{ if } Slope_x \ge 0 \wedge Slope_y \ge 0 \\
& \quad ZZ_{j,4} \leftarrow \text{atan}\left(\frac{-Slope_x}{Slope_y}\right) + \frac{3\cdot\pi}{2} \text{ if } Slope_x \le 0 \wedge Slope_y \ge 0 \\
& \quad ZZ_{j,5} \leftarrow X_{old} - \frac{ZZ_{j,1}\cdot 3.28\cdot 10^{-6}\cdot 360}{0.25} \\
& \quad ZZ_{j,6} \leftarrow Y_{old} - \frac{ZZ_{j,2}\left(3.28\cdot 10^{-6}\right)}{0.25}\cdot 360 \\
& \quad X_{old} \leftarrow ZZ_{j,5} \\
& \quad Y_{old} \leftarrow ZZ_{j,6} \\
& ZZ
\end{aligned}
$$

Particle tracking for groundwater under homogeneous and anisotropic conditions with retardation factor and without reactions at Honolulu, HI.

$$
\begin{aligned}
XX := \;& X_{old} \leftarrow X_{initial} \\
& Y_{old} \leftarrow Y_{initial} \\
& \text{for } j \in 1..N_{data} \\
& \quad zz \leftarrow \begin{bmatrix} (zT)_{1,j} \\ (zT)_{2,j} \\ (zT)_{3,j} \end{bmatrix} \\
& \quad R \leftarrow \text{regress}(M_{xy}, zz, 1) \\
& \quad Slope_x \leftarrow R_4 \\
& \quad Slope_y \leftarrow R_5 \\
& \quad ZZ_{j,1} \leftarrow Slope_x \\
& \quad ZZ_{j,2} \leftarrow Slope_y \\
& \quad ZZ_{j,3} \leftarrow \left| \sqrt{Slope_x^{\,2} + Slope_y^{\,2}} \right| \\
& \quad ZZ_{j,4} \leftarrow \text{atan}\left(\frac{-Slope_y}{-Slope_x}\right) \text{ if } Slope_x \le 0 \wedge Slope_y \le 0 \\
& \quad ZZ_{j,4} \leftarrow \text{atan}\left(\frac{Slope_x}{-Slope_y}\right) + \frac{\pi}{2} \text{ if } Slope_x > 0 \wedge Slope_y \le 0 \\
& \quad ZZ_{j,4} \leftarrow \text{atan}\left(\frac{Slope_y}{Slope_x}\right) + \pi \text{ if } Slope_x \ge 0 \wedge Slope_y \ge 0 \\
& \quad ZZ_{j,4} \leftarrow \text{atan}\left(\frac{-Slope_x}{Slope_y}\right) + \frac{3 \cdot \pi}{2} \text{ if } Slope_x \le 0 \wedge Slope_y \ge 0 \\
& \quad K_{ioc} \leftarrow 59 \cdot \frac{mL}{gm} \\
& \quad f_{oc} \leftarrow 0.01 \\
& \quad K_{id} \leftarrow f_{oc} \cdot K_{ioc} \\
& \quad R \leftarrow 1 + \frac{K_{id} \cdot \rho_b}{\phi} \\
& \quad ZZ_{j,5} \leftarrow X_{old} - \frac{ZZ_{j,1} \cdot 3.28 \cdot 10^{-6} \cdot 360}{0.25 \cdot R} \\
& \quad ZZ_{j,6} \leftarrow Y_{old} - \frac{ZZ_{j,2}\, 1.64 \cdot 10^{-6}}{0.25 \cdot R} \cdot 360 \\
& \quad X_{old} \leftarrow ZZ_{j,5} \\
& \quad Y_{old} \leftarrow ZZ_{j,6} \\
& ZZ
\end{aligned}
$$

Particle tracking for LNAPL under homogeneous and isotropic conditions without reactions at Honolulu, HI.

$$
\begin{aligned}
XX := \;& X_{old} \leftarrow X_{initial} \\
& Y_{old} \leftarrow Y_{initial} \\
& \text{for } j \in 1..N_{data} \\
& \quad zz \leftarrow \begin{bmatrix} (z^T)_{1,j} \\ (z^T)_{2,j} \\ (z^T)_{3,j} \end{bmatrix} \\
& \quad R \leftarrow \text{regress}(M_{xy}, zz, 1) \\
& \quad Slope_x \leftarrow R_4 \\
& \quad Slope_y \leftarrow R_5 \\
& \quad ZZ_{j,1} \leftarrow Slope_x \\
& \quad ZZ_{j,2} \leftarrow Slope_y \\
& \quad ZZ_{j,3} \leftarrow \left| \sqrt{Slope_x^{\,2} + Slope_y^{\,2}} \right| \\
& \quad ZZ_{j,4} \leftarrow \text{atan}\left(\frac{-Slope_y}{-Slope_x}\right) \text{ if } Slope_x \le 0 \wedge Slope_y \le 0 \\
& \quad ZZ_{j,4} \leftarrow \text{atan}\left(\frac{Slope_x}{-Slope_y}\right) + \frac{\pi}{2} \text{ if } Slope_x > 0 \wedge Slope_y \le 0 \\
& \quad ZZ_{j,4} \leftarrow \text{atan}\left(\frac{Slope_y}{Slope_x}\right) + \pi \text{ if } Slope_x \ge 0 \wedge Slope_y \ge 0 \\
& \quad ZZ_{j,4} \leftarrow \text{atan}\left(\frac{-Slope_x}{Slope_y}\right) + \frac{3\cdot\pi}{2} \text{ if } Slope_x \le 0 \wedge Slope_y \ge 0 \\
& \quad ZZ_{j,5} \leftarrow X_{old} - \frac{ZZ_{j,1}\cdot\left(4.39\cdot10^{-7}\right)\cdot360}{0.25} \\
& \quad ZZ_{j,6} \leftarrow Y_{old} - \frac{ZZ_{j,2}\left(4.39\cdot10^{-7}\right)}{0.25}\cdot360 \\
& \quad X_{old} \leftarrow ZZ_{j,5} \\
& \quad Y_{old} \leftarrow ZZ_{j,6} \\
& ZZ
\end{aligned}
$$

Particle tracking for LNAPL under homogeneous and anisotropic conditions with retardation factor and without reactions at Honolulu, HI.

$$
\begin{aligned}
XX :- \;& X_{old} \leftarrow X_{initial} \\
& Y_{old} \leftarrow Y_{initial} \\
& \text{for } j \in 1..N_{data} \\
& \quad zz \leftarrow \begin{bmatrix} (zT)_{1,j} \\ (zT)_{2,j} \\ (zT)_{3,j} \end{bmatrix} \\
& \quad R \leftarrow \text{regress}(M_{xy}, zz, 1) \\
& \quad Slope_x \leftarrow R_4 \\
& \quad Slope_y \leftarrow R_5 \\
& \quad ZZ_{j,1} \leftarrow Slope_x \\
& \quad ZZ_{j,2} \leftarrow Slope_y \\
& \quad ZZ_{j,3} \leftarrow \left| \sqrt{Slope_x^{\,2} + Slope_y^{\,2}} \right| \\
& \quad ZZ_{j,4} \leftarrow \text{atan}\left(\frac{-Slope_y}{-Slope_x}\right) \text{ if } Slope_x \le 0 \wedge Slope_y \le 0 \\
& \quad ZZ_{j,4} \leftarrow \text{atan}\left(\frac{Slope_x}{-Slope_y}\right) + \frac{\pi}{2} \text{ if } Slope_x > 0 \wedge Slope_y \le 0 \\
& \quad ZZ_{j,4} \leftarrow \text{atan}\left(\frac{Slope_y}{Slope_x}\right) + \pi \text{ if } Slope_x \ge 0 \wedge Slope_y \ge 0 \\
& \quad ZZ_{j,4} \leftarrow \text{atan}\left(\frac{-Slope_x}{Slope_y}\right) + \frac{3\cdot\pi}{2} \text{ if } Slope_x \le 0 \wedge Slope_y \ge 0 \\
& \quad K_{ioc} \leftarrow 59\cdot\frac{mL}{gm} \\
& \quad f_{oc} \leftarrow 0.01 \\
& \quad K_{id} \leftarrow f_{oc}\cdot K_{ioc} \\
& \quad R \leftarrow 1 + \frac{K_{id}\cdot\rho_b}{\phi} \\
& \quad ZZ_{j,5} \leftarrow X_{old} - \frac{ZZ_{j,1}\cdot 4.39\cdot 10^{-7}\cdot 360}{0.25R} \\
& \quad ZZ_{j,6} \leftarrow Y_{old} - \frac{ZZ_{j,2}\left(2.19\cdot 10^{-7}\cdot 360\right)}{0.25R} \\
& \quad X_{old} \leftarrow ZZ_{j,5} \\
& \quad Y_{old} \leftarrow ZZ_{j,6} \\
& ZZ
\end{aligned}
$$

First-Order Kinetic Reactions at Honolulu, HI.

$n := 9400$ $\Delta t := 1day$

$$M := \left| \begin{array}{l} C_0 \leftarrow 1000 \dfrac{mg}{L} \\ k \leftarrow 0.0036 \dfrac{1}{day} \\ \text{for } i \in 1,2..n \\ \quad \left| \begin{array}{l} C_i \leftarrow C_0 \cdot e^{-k \cdot \Delta t \cdot i} \\ \text{break if } C_i < 0.005 \dfrac{mg}{L} \end{array} \right. \\ C \end{array} \right.$$

APPENDIX D – MODELING CODE FOR PARTICLE TRACKING UNDER DYNAMIC PUMPING CONDITIONS

This appendix contains programming code used for water-level modeling, generations of potentiometric surfaces, a Theis superposition model, and analytical solutions for modeling particle tracking under dynamic pumping conditions. Program codes of water-level modeling, generations of potentiometric surfaces, and a Theis superposition model were developed by T. Sale at Colorado State University using PTC Mathcad 15® Engineering Software.

Well Function

Subroutine for obtaining W(u) as a function of u

$$W(u) := \begin{cases} X \leftarrow \int_u^{\infty} \frac{e^{-x}}{x}\,dx & \text{if } u > 0.01 \\ X \leftarrow -0.5772 - \ln(u) & \text{otherwise} \\ X \end{cases}$$

Theis Equation

$$s = \frac{Q}{4\pi \cdot T} W\left(\frac{r^2 S}{4 \cdot T \cdot t}\right)$$

Drawdown Calculation

$$DD(x, y, N_{wells}, t) := \begin{cases} s \leftarrow 0 \cdot ft \\ \text{for } j \in 1 .. N_{wells} \\ \quad \text{for } i \in 1 .. N_{steps} \\ \quad\quad \text{if } t > W_{Time_{i,j}} \\ \quad\quad\quad s \leftarrow s + \frac{W_{Q_{i,j}}}{4 \cdot \pi \cdot T} \cdot W\left[\frac{\left[\sqrt{(x - X_j)^2 + (y - Y_j + 0.5 \cdot ft)^2}\right]^2 \cdot S}{4 \cdot T \cdot (t - W_{Time_{i,j}})}\right] & \text{if } t \le W_{Time_{i+1,j}} \\ \quad\quad\quad s \leftarrow s + \frac{W_{Q_{i,j}}}{4 \cdot \pi \cdot T} \cdot \left[W\left[\frac{\left[\sqrt{(x - X_j)^2 + (y - Y_j + 0.5 \cdot ft)^2}\right]^2 \cdot S}{4 \cdot T \cdot (t - W_{Time_{i,j}})}\right] - W\left[\frac{\left[\sqrt{(x - X_j)^2 + (y - Y_j + 0.5 \cdot ft)^2}\right]^2 \cdot S}{4 \cdot T \cdot (t - W_{Time_{i+1,j}})}\right]\right] & \text{otherwise} \\ s \end{cases}$$

Water surface about dynamically opearted pumping wells in a well fields

$$WaterSurface(N_{wells}, x, y, t) := A \cdot x + B \cdot y + Ref - DD(x, y, N_{wells}, t)$$

For 130 days, particle tracking in 1st to 21st day (process 1 described in Chapter 4) during the pumping period under homogeneous and isotropic conditions without reactions at the Meadows Pumping Center, CO.

$$\begin{aligned}
&\textbf{Positions} := \textbf{for}\ \ i \in 0..7 \\
&\quad XXX_{1,2\cdot i+1} \leftarrow x_{i+1} \\
&\quad XXX_{1,2\cdot i+2} \leftarrow y_{i+1} \\
&\quad t \leftarrow t_{initial} \\
&\quad \textbf{for}\ \ k \in 1..21 \\
&\qquad WSminusx_{i+1} \leftarrow WaterSurface\left(N_{wells}, XXX_{k,2\cdot i+1} - 1ft, XXX_{k,2\cdot i+2}, t\right) \\
&\qquad WSplusx_{i+1} \leftarrow WaterSurface\left(N_{wells}, XXX_{k,2\cdot i+1} + 1ft, XXX_{k,2\cdot i+2}, t\right) \\
&\qquad WSminusy_{i+1} \leftarrow WaterSurface\left(N_{wells}, XXX_{k,2\cdot i+1}, XXX_{k,2\cdot i+2} - 1ft, t\right) \\
&\qquad WSplusy_{i+1} \leftarrow WaterSurface\left(N_{wells}, XXX_{k,2\cdot i+1}, XXX_{k,2\cdot i+2} + 1ft, t\right) \\
&\qquad Gradx_{i+1} \leftarrow \frac{WSminusx_{i+1} - WSplusx_{i+1}}{2ft} \\
&\qquad Grady_{i+1} \leftarrow \frac{WSminusy_{i+1} - WSplusy_{i+1}}{2ft} \\
&\qquad \Delta x_{i+1} \leftarrow \frac{T}{32.81ft \cdot n_e} \cdot Gradx_{i+1} \cdot \Delta t \\
&\qquad \Delta y_{i+1} \leftarrow \frac{T}{32.81ft \cdot n_e} \cdot Grady_{i+1} \cdot \Delta t \\
&\qquad XXX_{k+1,2\cdot i+1} \leftarrow XXX_{k,2\cdot i+1} - \Delta x_{i+1} \\
&\qquad XXX_{k+1,2\cdot i+2} \leftarrow XXX_{k,2\cdot i+2} - \Delta y_{i+1} \\
&\qquad t \leftarrow t_{initial} + k \cdot \Delta t \\
&\quad XXX
\end{aligned}$$

For 130 days, particle tracking in 22nd to 51st day (process 2 described in Chapter 4) during the injection period under homogeneous and isotropic conditions without reactions at the Meadows Pumping Center, CO.

$$
\begin{aligned}
&\textbf{Positions} := \textbf{for}\ \ i \in 0..7 \\
&\quad XXX_{1,2\cdot i+1} \leftarrow x_{i+1} \\
&\quad XXX_{1,2\cdot i+2} \leftarrow y_{i+1} \\
&\quad t \leftarrow t_{initial} \\
&\quad \textbf{for}\ \ k \in 1..30 \\
&\qquad WSminusx_{i+1} \leftarrow WaterSurface\left(N_{wells}, XXX_{k,2\cdot i+1} - 1m, XXX_{k,2\cdot i+2}, t\right) \\
&\qquad WSplusx_{i+1} \leftarrow WaterSurface\left(N_{wells}, XXX_{k,2\cdot i+1} + 1m, XXX_{k,2\cdot i+2}, t\right) \\
&\qquad WSminusy_{i+1} \leftarrow WaterSurface\left(N_{wells}, XXX_{k,2\cdot i+1}, XXX_{k,2\cdot i+2} - 1m, t\right) \\
&\qquad WSplusy_{i+1} \leftarrow WaterSurface\left(N_{wells}, XXX_{k,2\cdot i+1}, XXX_{k,2\cdot i+2} + 1m, t\right) \\
&\qquad Gradx_{i+1} \leftarrow \frac{WSminusx_{i+1} - WSplusx_{i+1}}{2ft} \\
&\qquad Grady_{i+1} \leftarrow \frac{WSminusy_{i+1} - WSplusy_{i+1}}{2ft} \\
&\qquad \Delta x_{i+1} \leftarrow \frac{T}{32.81ft \cdot \varphi} \cdot Gradx_{i+1} \cdot \Delta t \\
&\qquad \Delta y_{i+1} \leftarrow \frac{T}{32.81ft \cdot \varphi} \cdot Grady_{i+1} \cdot \Delta t \\
&\qquad XXX_{k+1,2\cdot i+1} \leftarrow XXX_{k,2\cdot i+1} + \Delta x_{i+1} \\
&\qquad XXX_{k+1,2\cdot i+2} \leftarrow XXX_{k,2\cdot i+2} + \Delta y_{i+1} \\
&\qquad t \leftarrow t_{initial} + k \cdot \Delta t \\
&\quad XXX
\end{aligned}
$$

For 130 days, particle tracking in 52nd to 60th day (process 3 described in Chapter 4) during the pumping period under homogeneous and isotropic conditions without reactions at the Meadows Pumping Center, CO.

$$\begin{aligned}
&\textbf{Positions} := \textbf{for}\ \ i \in 0..7 \\
&\quad XXX_{1,2\cdot i+1} \leftarrow x_{i+1} \\
&\quad XXX_{1,2\cdot i+2} \leftarrow y_{i+1} \\
&\quad t \leftarrow t_{initial} \\
&\quad \textbf{for}\ \ k \in 1..9 \\
&\qquad WSminusx_{i+1} \leftarrow WaterSurface\left(N_{wells}, XXX_{k,2\cdot i+1} - 1m, XXX_{k,2\cdot i+2}, t\right) \\
&\qquad WSplusx_{i+1} \leftarrow WaterSurface\left(N_{wells}, XXX_{k,2\cdot i+1} + 1m, XXX_{k,2\cdot i+2}, t\right) \\
&\qquad WSminusy_{i+1} \leftarrow WaterSurface\left(N_{wells}, XXX_{k,2\cdot i+1}, XXX_{k,2\cdot i+2} - 1m, t\right) \\
&\qquad WSplusy_{i+1} \leftarrow WaterSurface\left(N_{wells}, XXX_{k,2\cdot i+1}, XXX_{k,2\cdot i+2} + 1m, t\right) \\
&\qquad Gradx_{i+1} \leftarrow \frac{WSminusx_{i+1} - WSplusx_{i+1}}{2ft} \\
&\qquad Grady_{i+1} \leftarrow \frac{WSminusy_{i+1} - WSplusy_{i+1}}{2ft} \\
&\qquad \Delta x_{i+1} \leftarrow \frac{-T}{32.81ft \cdot \varphi} \cdot Gradx_{i+1} \cdot \Delta t \\
&\qquad \Delta y_{i+1} \leftarrow \frac{-T}{32.81ft \cdot \varphi} \cdot Grady_{i+1} \cdot \Delta t \\
&\qquad XXX_{k+1,2\cdot i+1} \leftarrow XXX_{k,2\cdot i+1} - \Delta x_{i+1} \\
&\qquad XXX_{k+1,2\cdot i+2} \leftarrow XXX_{k,2\cdot i+2} - \Delta y_{i+1} \\
&\qquad t \leftarrow t_{initial} + k \cdot \Delta t \\
&\quad XXX
\end{aligned}$$

For 130 days, particle tracking in 61st to 90th day (process 4 described in Chapter 4) during the injection period under homogeneous and isotropic conditions without reactions at the Meadows Pumping Center, CO.

$$\begin{aligned}
&\textbf{Positions} := \textbf{for}\ \ i \in 0..7 \\
&\quad XXX_{1,2\cdot i+1} \leftarrow x_{i+1} \\
&\quad XXX_{1,2\cdot i+2} \leftarrow y_{i+1} \\
&\quad t \leftarrow t_{initial} \\
&\quad \textbf{for}\ \ k \in 1..30 \\
&\qquad WSminusx_{i+1} \leftarrow WaterSurface\left(N_{wells}, XXX_{k,2\cdot i+1} - 1m, XXX_{k,2\cdot i+2}, t\right) \\
&\qquad WSplusx_{i+1} \leftarrow WaterSurface\left(N_{wells}, XXX_{k,2\cdot i+1} + 1m, XXX_{k,2\cdot i+2}, t\right) \\
&\qquad WSminusy_{i+1} \leftarrow WaterSurface\left(N_{wells}, XXX_{k,2\cdot i+1}, XXX_{k,2\cdot i+2} - 1m, t\right) \\
&\qquad WSplusy_{i+1} \leftarrow WaterSurface\left(N_{wells}, XXX_{k,2\cdot i+1}, XXX_{k,2\cdot i+2} + 1m, t\right) \\
&\qquad Gradx_{i+1} \leftarrow \frac{WSminusx_{i+1} - WSplusx_{i+1}}{2ft} \\
&\qquad Grady_{i+1} \leftarrow \frac{WSminusy_{i+1} - WSplusy_{i+1}}{2ft} \\
&\qquad \Delta x_{i+1} \leftarrow \frac{T}{32.81ft \cdot \varphi} \cdot Gradx_{i+1} \cdot \Delta t \\
&\qquad \Delta y_{i+1} \leftarrow \frac{T}{32.81ft \cdot \varphi} \cdot Grady_{i+1} \cdot \Delta t \\
&\qquad XXX_{k+1,2\cdot i+1} \leftarrow XXX_{k,2\cdot i+1} + \Delta x_{i+1} \\
&\qquad XXX_{k+1,2\cdot i+2} \leftarrow XXX_{k,2\cdot i+2} + \Delta y_{i+1} \\
&\qquad t \leftarrow t_{initial} + k \cdot \Delta t \\
&\quad XXX
\end{aligned}$$

For 130 days, particle tracking in 91st to 100th day (process 5 described in Chapter 4) during the pumping period under homogeneous and isotropic conditions without reactions at the Meadows Pumping Center, CO.

$$
\begin{aligned}
&\textbf{Positions} := \textbf{for}\ \ i \in 0..7 \\
&\quad XXX_{1,2\cdot i+1} \leftarrow x_{i+1} \\
&\quad XXX_{1,2\cdot i+2} \leftarrow y_{i+1} \\
&\quad t \leftarrow t_{initial} \\
&\quad \textbf{for}\ \ k \in 1..10 \\
&\qquad WSminusx_{i+1} \leftarrow WaterSurface\left(N_{wells}, XXX_{k,2\cdot i+1} - 1m, XXX_{k,2\cdot i+2}, t\right) \\
&\qquad WSplusx_{i+1} \leftarrow WaterSurface\left(N_{wells}, XXX_{k,2\cdot i+1} + 1m, XXX_{k,2\cdot i+2}, t\right) \\
&\qquad WSminusy_{i+1} \leftarrow WaterSurface\left(N_{wells}, XXX_{k,2\cdot i+1}, XXX_{k,2\cdot i+2} - 1m, t\right) \\
&\qquad WSplusy_{i+1} \leftarrow WaterSurface\left(N_{wells}, XXX_{k,2\cdot i+1}, XXX_{k,2\cdot i+2} + 1m, t\right) \\
&\qquad Gradx_{i+1} \leftarrow \frac{WSminusx_{i+1} - WSplusx_{i+1}}{2ft} \\
&\qquad Grady_{i+1} \leftarrow \frac{WSminusy_{i+1} - WSplusy_{i+1}}{2ft} \\
&\qquad \Delta x_{i+1} \leftarrow \frac{-T}{32.81ft \cdot \varphi} \cdot Gradx_{i+1} \cdot \Delta t \\
&\qquad \Delta y_{i+1} \leftarrow \frac{-T}{32.81ft \cdot \varphi} \cdot Grady_{i+1} \cdot \Delta t \\
&\qquad XXX_{k+1,2\cdot i+1} \leftarrow XXX_{k,2\cdot i+1} - \Delta x_{i+1} \\
&\qquad XXX_{k+1,2\cdot i+2} \leftarrow XXX_{k,2\cdot i+2} - \Delta y_{i+1} \\
&\qquad t \leftarrow t_{initial} + k \cdot \Delta t \\
&\quad XXX
\end{aligned}
$$

For 130 days, particle tracking in 101st to 130th day (process 6 described in Chapter 4) during the injection period under homogeneous and isotropic conditions without reactions at the Meadows Pumping Center, CO.

$$\text{Positions} := \text{for } i \in 0..7$$

$$XXX_{1,2\cdot i+1} \leftarrow x_{i+1}$$

$$XXX_{1,2\cdot i+2} \leftarrow y_{i+1}$$

$$t \leftarrow t_{initial}$$

$$\text{for } k \in 1..30$$

$$WSminusx_{i+1} \leftarrow WaterSurface\left(N_{wells}, XXX_{k,2\cdot i+1} - 1m, XXX_{k,2\cdot i+2}, t\right)$$

$$WSplusx_{i+1} \leftarrow WaterSurface\left(N_{wells}, XXX_{k,2\cdot i+1} + 1m, XXX_{k,2\cdot i+2}, t\right)$$

$$WSminusy_{i+1} \leftarrow WaterSurface\left(N_{wells}, XXX_{k,2\cdot i+1}, XXX_{k,2\cdot i+2} - 1m, t\right)$$

$$WSplusy_{i+1} \leftarrow WaterSurface\left(N_{wells}, XXX_{k,2\cdot i+1}, XXX_{k,2\cdot i+2} + 1m, t\right)$$

$$Gradx_{i+1} \leftarrow \frac{WSminusx_{i+1} - WSplusx_{i+1}}{2ft}$$

$$Grady_{i+1} \leftarrow \frac{WSminusy_{i+1} - WSplusy_{i+1}}{2ft}$$

$$\Delta x_{i+1} \leftarrow \frac{T}{32.81ft \cdot \varphi} \cdot Gradx_{i+1} \cdot \Delta t$$

$$\Delta y_{i+1} \leftarrow \frac{T}{32.81ft \cdot \varphi} \cdot Grady_{i+1} \cdot \Delta t$$

$$XXX_{k+1,2\cdot i+1} \leftarrow XXX_{k,2\cdot i+1} + \Delta x_{i+1}$$

$$XXX_{k+1,2\cdot i+2} \leftarrow XXX_{k,2\cdot i+2} + \Delta y_{i+1}$$

$$t \leftarrow t_{initial} + k \cdot \Delta t$$

$$XXX$$

For 6000 days, particle tracking in 1st to 1000th day (process 1 described in Chapter 4) during the injection period under homogeneous and isotropic conditions without reactions at the Meadows Pumping Center, CO.

$$\begin{aligned}
&\textbf{Positions} := \textbf{for}\ \ i \in 0..3 \\
&\quad XXX_{1,2\cdot i+1} \leftarrow x_{i+1} \\
&\quad XXX_{1,2\cdot i+2} \leftarrow y_{i+1} \\
&\quad t \leftarrow t_{initial} \\
&\quad \textbf{for}\ \ k \in 1..1000 \\
&\qquad WSminusx_{i+1} \leftarrow WaterSurface\left(N_{wells}, XXX_{k,2\cdot i+1} - 1m, XXX_{k,2\cdot i+2}, t\right) \\
&\qquad WSplusx_{i+1} \leftarrow WaterSurface\left(N_{wells}, XXX_{k,2\cdot i+1} + 1m, XXX_{k,2\cdot i+2}, t\right) \\
&\qquad WSminusy_{i+1} \leftarrow WaterSurface\left(N_{wells}, XXX_{k,2\cdot i+1}, XXX_{k,2\cdot i+2} - 1m, t\right) \\
&\qquad WSplusy_{i+1} \leftarrow WaterSurface\left(N_{wells}, XXX_{k,2\cdot i+1}, XXX_{k,2\cdot i+2} + 1m, t\right) \\
&\qquad Gradx_{i+1} \leftarrow \frac{WSminusx_{i+1} - WSplusx_{i+1}}{2ft} \\
&\qquad Grady_{i+1} \leftarrow \frac{WSminusy_{i+1} - WSplusy_{i+1}}{2ft} \\
&\qquad \Delta x_{i+1} \leftarrow \frac{T}{32.81ft \cdot \varphi} \cdot Gradx_{i+1} \cdot \Delta t \\
&\qquad \Delta y_{i+1} \leftarrow \frac{T}{32.81ft \cdot \varphi} \cdot Grady_{i+1} \cdot \Delta t \\
&\qquad XXX_{k+1,2\cdot i+1} \leftarrow XXX_{k,2\cdot i+1} - \Delta x_{i+1} \\
&\qquad XXX_{k+1,2\cdot i+2} \leftarrow XXX_{k,2\cdot i+2} - \Delta y_{i+1} \\
&\qquad t \leftarrow t_{initial} + k \cdot \Delta t \\
&\quad XXX
\end{aligned}$$

For 6000 days, particle tracking in 1001st to 2000th day (process 2 described in Chapter 4) during the injection period under homogeneous and isotropic conditions without reactions at the Meadows Pumping Center, CO.

$$
\begin{aligned}
&\textbf{Positions} := \textbf{for}\ \ i \in 0..3 \\
&\quad XXX_{1,2\cdot i+1} \leftarrow x_{i+1} \\
&\quad XXX_{1,2\cdot i+2} \leftarrow y_{i+1} \\
&\quad t \leftarrow t_{initial} \\
&\quad \textbf{for}\ \ k \in 1..1000 \\
&\qquad WSminusx_{i+1} \leftarrow WaterSurface\left(N_{wells}, XXX_{k,2\cdot i+1} - 1m, XXX_{k,2\cdot i+2}, t\right) \\
&\qquad WSplusx_{i+1} \leftarrow WaterSurface\left(N_{wells}, XXX_{k,2\cdot i+1} + 1m, XXX_{k,2\cdot i+2}, t\right) \\
&\qquad WSminusy_{i+1} \leftarrow WaterSurface\left(N_{wells}, XXX_{k,2\cdot i+1}, XXX_{k,2\cdot i+2} - 1m, t\right) \\
&\qquad WSplusy_{i+1} \leftarrow WaterSurface\left(N_{wells}, XXX_{k,2\cdot i+1}, XXX_{k,2\cdot i+2} + 1m, t\right) \\
&\qquad Gradx_{i+1} \leftarrow \frac{WSminusx_{i+1} - WSplusx_{i+1}}{2ft} \\
&\qquad Grady_{i+1} \leftarrow \frac{WSminusy_{i+1} - WSplusy_{i+1}}{2ft} \\
&\qquad \Delta x_{i+1} \leftarrow \frac{T}{32.81ft \cdot \varphi} \cdot Gradx_{i+1} \cdot \Delta t \\
&\qquad \Delta y_{i+1} \leftarrow \frac{T}{32.81ft \cdot \varphi} \cdot Grady_{i+1} \cdot \Delta t \\
&\qquad XXX_{k+1,2\cdot i+1} \leftarrow XXX_{k,2\cdot i+1} + \Delta x_{i+1} \\
&\qquad XXX_{k+1,2\cdot i+2} \leftarrow XXX_{k,2\cdot i+2} + \Delta y_{i+1} \\
&\qquad t \leftarrow t_{initial} + k \cdot \Delta t \\
&\quad XXX
\end{aligned}
$$

For 6000 days, particle tracking in 2001st to 3000th day (process 3 described in Chapter 4) during the pumping period under homogeneous and isotropic conditions without reactions at the Meadows Pumping Center, CO.

$$\begin{aligned}
&\textbf{Positions} := \textbf{for}\ \ i \in 0..3 \\
&\quad XXX_{1,2\cdot i+1} \leftarrow x_{i+1} \\
&\quad XXX_{1,2\cdot i+2} \leftarrow y_{i+1} \\
&\quad t \leftarrow t_{initial} \\
&\quad \textbf{for}\ \ k \in 1..1000 \\
&\qquad WSminusx_{i+1} \leftarrow WaterSurface\left(N_{wells}, XXX_{k,2\cdot i+1} - 1m, XXX_{k,2\cdot i+2}, t\right) \\
&\qquad WSplusx_{i+1} \leftarrow WaterSurface\left(N_{wells}, XXX_{k,2\cdot i+1} + 1m, XXX_{k,2\cdot i+2}, t\right) \\
&\qquad WSminusy_{i+1} \leftarrow WaterSurface\left(N_{wells}, XXX_{k,2\cdot i+1}, XXX_{k,2\cdot i+2} - 1m, t\right) \\
&\qquad WSplusy_{i+1} \leftarrow WaterSurface\left(N_{wells}, XXX_{k,2\cdot i+1}, XXX_{k,2\cdot i+2} + 1m, t\right) \\
&\qquad Gradx_{i+1} \leftarrow \frac{WSminusx_{i+1} - WSplusx_{i+1}}{2ft} \\
&\qquad Grady_{i+1} \leftarrow \frac{WSminusy_{i+1} - WSplusy_{i+1}}{2ft} \\
&\qquad \Delta x_{i+1} \leftarrow \frac{T}{32.81ft \cdot \varphi} \cdot Gradx_{i+1} \cdot \Delta t \\
&\qquad \Delta y_{i+1} \leftarrow \frac{T}{32.81ft \cdot \varphi} \cdot Grady_{i+1} \cdot \Delta t \\
&\qquad XXX_{k+1,2\cdot i+1} \leftarrow XXX_{k,2\cdot i+1} - \Delta x_{i+1} \\
&\qquad XXX_{k+1,2\cdot i+2} \leftarrow XXX_{k,2\cdot i+2} - \Delta y_{i+1} \\
&\qquad t \leftarrow t_{initial} + k \cdot \Delta t \\
&\quad XXX
\end{aligned}$$

For 6000 days, particle tracking in 3001st to 4000th day (process 4 described in Chapter 4) during the injection period under homogeneous and isotropic conditions without reactions at the Meadows Pumping Center, CO.

$$
\begin{aligned}
&\textbf{Positions} := \textbf{for}\ \ i \in 0..3 \\
&\quad XXX_{1,2\cdot i+1} \leftarrow x_{i+1} \\
&\quad XXX_{1,2\cdot i+2} \leftarrow y_{i+1} \\
&\quad t \leftarrow t_{initial} \\
&\quad \textbf{for}\ \ k \in 1..1000 \\
&\qquad WSminusx_{i+1} \leftarrow WaterSurface\left(N_{wells}, XXX_{k,2\cdot i+1} - 1m, XXX_{k,2\cdot i+2}, t\right) \\
&\qquad WSplusx_{i+1} \leftarrow WaterSurface\left(N_{wells}, XXX_{k,2\cdot i+1} + 1m, XXX_{k,2\cdot i+2}, t\right) \\
&\qquad WSminusy_{i+1} \leftarrow WaterSurface\left(N_{wells}, XXX_{k,2\cdot i+1}, XXX_{k,2\cdot i+2} - 1m, t\right) \\
&\qquad WSplusy_{i+1} \leftarrow WaterSurface\left(N_{wells}, XXX_{k,2\cdot i+1}, XXX_{k,2\cdot i+2} + 1m, t\right) \\
&\qquad Gradx_{i+1} \leftarrow \frac{WSminusx_{i+1} - WSplusx_{i+1}}{2ft} \\
&\qquad Grady_{i+1} \leftarrow \frac{WSminusy_{i+1} - WSplusy_{i+1}}{2ft} \\
&\qquad \Delta x_{i+1} \leftarrow \frac{T}{32.81ft \cdot \varphi} \cdot Gradx_{i+1} \cdot \Delta t \\
&\qquad \Delta y_{i+1} \leftarrow \frac{T}{32.81ft \cdot \varphi} \cdot Grady_{i+1} \cdot \Delta t \\
&\qquad XXX_{k+1,2\cdot i+1} \leftarrow XXX_{k,2\cdot i+1} + \Delta x_{i+1} \\
&\qquad XXX_{k+1,2\cdot i+2} \leftarrow XXX_{k,2\cdot i+2} + \Delta y_{i+1} \\
&\qquad t \leftarrow t_{initial} + k \cdot \Delta t \\
&\quad XXX
\end{aligned}
$$

For 6000 days, particle tracking in 4001st to 5000th day (process 5 described in Chapter 4) during the pumping period under homogeneous and isotropic conditions without reactions at the Meadows Pumping Center, CO.

$$
\begin{aligned}
&\textbf{Positions} := \textbf{for}\ \ i \in 0..3 \\
&\quad XXX_{1,2\cdot i+1} \leftarrow x_{i+1} \\
&\quad XXX_{1,2\cdot i+2} \leftarrow y_{i+1} \\
&\quad t \leftarrow t_{initial} \\
&\quad \textbf{for}\ \ k \in 1..1000 \\
&\qquad WSminusx_{i+1} \leftarrow WaterSurface\left(N_{wells}, XXX_{k,2\cdot i+1} - 1m, XXX_{k,2\cdot i+2}, t\right) \\
&\qquad WSplusx_{i+1} \leftarrow WaterSurface\left(N_{wells}, XXX_{k,2\cdot i+1} + 1m, XXX_{k,2\cdot i+2}, t\right) \\
&\qquad WSminusy_{i+1} \leftarrow WaterSurface\left(N_{wells}, XXX_{k,2\cdot i+1}, XXX_{k,2\cdot i+2} - 1m, t\right) \\
&\qquad WSplusy_{i+1} \leftarrow WaterSurface\left(N_{wells}, XXX_{k,2\cdot i+1}, XXX_{k,2\cdot i+2} + 1m, t\right) \\
&\qquad Gradx_{i+1} \leftarrow \frac{WSminusx_{i+1} - WSplusx_{i+1}}{2ft} \\
&\qquad Grady_{i+1} \leftarrow \frac{WSminusy_{i+1} - WSplusy_{i+1}}{2ft} \\
&\qquad \Delta x_{i+1} \leftarrow \frac{T}{32.81ft \cdot \varphi} \cdot Gradx_{i+1} \cdot \Delta t \\
&\qquad \Delta y_{i+1} \leftarrow \frac{T}{32.81ft \cdot \varphi} \cdot Grady_{i+1} \cdot \Delta t \\
&\qquad XXX_{k+1,2\cdot i+1} \leftarrow XXX_{k,2\cdot i+1} - \Delta x_{i+1} \\
&\qquad XXX_{k+1,2\cdot i+2} \leftarrow XXX_{k,2\cdot i+2} - \Delta y_{i+1} \\
&\qquad t \leftarrow t_{initial} + k \cdot \Delta t \\
&\quad XXX
\end{aligned}
$$

For 6000 days, particle tracking in 5001st to 6000th day (process 6 described in Chapter 4) during the injection period under homogeneous and isotropic conditions without reactions at the Meadows Pumping Center, CO.

$$\text{Positions} := \text{for } i \in 0..3$$
$$XXX_{1,2\cdot i+1} \leftarrow x_{i+1}$$
$$XXX_{1,2\cdot i+2} \leftarrow y_{i+1}$$
$$t \leftarrow t_{initial}$$
$$\text{for } k \in 1..1000$$
$$WSminusx_{i+1} \leftarrow \text{WaterSurface}\left(N_{wells}, XXX_{k,2\cdot i+1} - 1m, XXX_{k,2\cdot i+2}, t\right)$$
$$WSplusx_{i+1} \leftarrow \text{WaterSurface}\left(N_{wells}, XXX_{k,2\cdot i+1} + 1m, XXX_{k,2\cdot i+2}, t\right)$$
$$WSminusy_{i+1} \leftarrow \text{WaterSurface}\left(N_{wells}, XXX_{k,2\cdot i+1}, XXX_{k,2\cdot i+2} - 1m, t\right)$$
$$WSplusy_{i+1} \leftarrow \text{WaterSurface}\left(N_{wells}, XXX_{k,2\cdot i+1}, XXX_{k,2\cdot i+2} + 1m, t\right)$$
$$Gradx_{i+1} \leftarrow \frac{WSminusx_{i+1} - WSplusx_{i+1}}{2ft}$$
$$Grady_{i+1} \leftarrow \frac{WSminusy_{i+1} - WSplusy_{i+1}}{2ft}$$
$$\Delta x_{i+1} \leftarrow \frac{T}{32.81ft \cdot \varphi} \cdot Gradx_{i+1} \cdot \Delta t$$
$$\Delta y_{i+1} \leftarrow \frac{T}{32.81ft \cdot \varphi} \cdot Grady_{i+1} \cdot \Delta t$$
$$XXX_{k+1,2\cdot i+1} \leftarrow XXX_{k,2\cdot i+1} + \Delta x_{i+1}$$
$$XXX_{k+1,2\cdot i+2} \leftarrow XXX_{k,2\cdot i+2} + \Delta y_{i+1}$$
$$t \leftarrow t_{initial} + k \cdot \Delta t$$
$$XXX$$